Institut für Nutzpflanzenwissenschaften und Ressourcenschutz (INRES)

Lehrstuhl für Molekulare Phytomedizin

Effects of *Bacillus firmus* and Bacterial Secondary Metabolites on the Plant Parasitic Nematode *Heterodera schachtii*

Impact Assessment and Mechanistic Insights

Dissertation

zur Erlangung des Grades

Doktorin der Agrarwissenschaften (Dr. agr.)

der Agrar-, Ernährungs- und Ingenieurwissenschaftlichen Fakultät

der Rheinischen Friedrich-Wilhelms-Universität Bonn

von

Mengmeng Huang

aus

Zhengzhou, China

Bonn, 2025

Referent	Prof. Dr. Florian M. W. Grundler
Korreferent	Prof. Dr. Christian Borgemeister
Tag der mündlichen Prüfung	07.10.2024

Angefertigt mit Genehmigung der Agrar-, Ernährungs- und Ingenieurwissenschaftlichen Fakultät der Universität Bonn

There is only one heroism in the world: to see the world as it is, and to love it.

Romain Rolland

1866-1944

Summary

Plant-parasitic nematodes cause enormous yield losses and economic damage to a wide range of economically important crops. Although synthetic chemicals can be effective in controlling plant-parasitic nematodes, their use raises significant environmental and health concerns. In this context, bio-based control strategies, particularly those utilizing microbes and microbial compounds, have emerged as promising alternatives.

Our studies aim to explore the efficacy and mechanism of action of *Bacillus firmus* I-1582 and the bacterial secondary metabolites prodiginines and rhamnolipids as microbial control agents against the beet cyst nematode *Heterodera schachtii* using a multidisciplinary approach involving microbiology, molecular biology and bioinformatics.

Chapters 2 and 3 present a comprehensive investigation of the potential of *B. firmus* I-1582 for biological control of *H. schachtii*. We have shown that *B. firmus* I-1582 can be attracted to *Arabidopsis thaliana* root exudates and that its colonization and development at the root of the host is pH-dependent. We also show that living bacterial cells clearly protect *A. thaliana* from infestation by *H. schachtii*. In contrast, dead bacterial cells or culture supernatant show no such effect. Interestingly, the living cells of *B. firmus* I-1582 also inhibit the infection, development and reproduction of the next generation juveniles. Since bacterial colonization of the host roots is not pronounced, no bacterial biofilm is present to prevent invasion of the invading J2 infective juveniles. We hypothesize that the 2nd generation J2 are less fit and that active molecules secreted by *B. firmus* I-1582 may have an inhibitory effect on the nematodes. In another experiment, direct contact of the cell-free supernatant with *H. schachtii* juveniles was shown to have a significant nematicidal effect when formed at higher temperatures. This lethal effect can be attributed to small molecules produced by *B. firmus* I-1582 under these conditions. Their molecular weight is below ~3 kDa and they are both protease-sensitive and protease-resistant. Using genome mining tools, a biosynthetic gene cluster was identified in the genome of *B. firmus* I-1582 encoding three putative lanthipeptides that are potential compounds active against nematodes. Gene expression analysis confirms the upregulation of all three putative lanthipeptide genes in *B. firmus* I-1582 and thus their presence in the culture supernatant.

In Chapter 4, the use of prodiginines alone and together with rhamnolipids as active substances against nematodes is investigated. We observed that prodiginines remarkably inhibited parasitism of *H. schachtii* on its host plant by reducing the motility of J2 and the activity of the mouth stylet as an indicator of J2 infection activity. In addition, we investigated the synergistic effect of prodiginines and rhamnolipids for the first time and found that the application of both substances is more effective against the nematodes than the application of either substance alone.

We are convinced that this research can improve the fundamental understanding and practical implementation of microbial-based control strategies and drive the development of innovative and sustainable solutions for integrated nematode management.

Zusammenfassung

Pflanzenparasitäre Nematoden verursachen enorme Ertragseinbußen und wirtschaftliche Schäden bei einer Vielzahl von wirtschaftlich wichtigen Nutzpflanzen. Obwohl synthetische Chemikalien bei der Bekämpfung von pflanzenparasitären Nematoden durchaus wirksam sein können, wirft ihr Einsatz erhebliche Umwelt- und Gesundheitsbedenken auf. In diesem Zusammenhang haben sich biobasierte Bekämpfungsstrategien, insbesondere solche, die Mikroben und mikrobielle Verbindungen nutzen, als vielversprechende Alternativen erwiesen.

Unsere Studien zielen darauf ab, mit Hilfe eines multidisziplinären Ansatzes, der Mikrobiologie, Molekularbiologie und Bioinformatik umfasst, die Wirksamkeit und den Wirkmechanismus von *Bacillus firmus* I-1582 sowie die bakteriellen Sekundärmetabolite Prodiginine und Rhamnolipide als mikrobielle Bekämpfungsmittel gegen den Rübenzystennematoden *Heterodera schachtii* zu erforschen.

In Kapitel 2 und 3 wird eine umfassende Untersuchung des Potenzials von *B. firmus* I-1582 zur biologischen Bekämpfung von *H. schachtii* vorgestellt. Wir konnten zeigen, dass *B. firmus* I-1582 von *Arabidopsis thaliana*-Wurzelexsudaten angezogen werden kann und dass seine Besiedlung und Entwicklung an der Wurzel des Wirts pH-abhängig sind. Wir zeigen auch, dass lebende Bakterienzellen *A. thaliana* deutlich vor dem Befall mit *H. schachtii* schützen. Im Gegensatz dazu zeigen tote Bakterienzellen oder Kulturüberstand keine solche Wirkung. Interessanterweise hemmen die lebenden Zellen von *B. firmus* I-1582 auch die Infektion, Entwicklung und Vermehrung der Jungtiere der nächsten Generation. Da die bakterielle Besiedlung der Wirtswurzeln nicht ausgeprägt ist, ist auch kein bakterieller Biofilm vorhanden, der die Invasion der Invasion der J2 Infektionslarven verhindern könnte. Wir vermuten, dass die J2 der 2. Generation weniger fit sind und dass aktive Moleküle, die von *B. firmus* I-1582 abgesondert werden, möglicherweise eine hemmende Wirkung auf die Nematoden haben. In einem weiteren Versuch wurde gezeigt, dass der direkte Kontakt des zellfreien Überstands mit *H. schachtii*-Larven eine signifikant nematizide Wirkung hat, wenn dieser bei höheren Temperaturen gebildet wurde. Diese tödliche Wirkung kann auf kleine Moleküle zurückgeführt werden, die von *B. firmus* I-1582 unter diesen Bedingungen

produziert werden. Ihr Molekulargewicht liegt unter ~3 kDa und sie sind sowohl proteaseempfindlich, als auch proteaseresistent. Mit Hilfe von Genom-Mining-Tools wurde im Genom von *B. firmus* I-1582 ein biosynthetisches Gencluster identifiziert, das für drei mutmaßliche Lanthipeptide kodiert, die als gegen Nematoden wirksame Verbindungen in Frage kommen. Die Genexpressionsanalyse bestätigt die Hochregulierung aller drei mutmaßlichen Lanthipeptid-Gene in *B. firmus* I-1582 und damit ihr Vorhandensein im Kulturüberstand.

In Kapitel 4 werden Untersuchungen der Anwendung von Prodigininen allein sowie zusammen mit Rhamnolipiden als Wirkstoffe gegen Nematode

n vorgenommen. Wir konnten beobachten, dass Prodiginine den Parasitismus von *H. schachtii* an seiner Wirtspflanze durch die Verringerung der Motilität der J2 Larven und der Aktivität des Mundstachel als Indikator für die Infektionsaktivität der J2 bemerkenswert hemmen. Darüber hinaus untersuchten wir zum ersten Mal die synergistische Wirkung von Prodigininen und Rhamnolipiden und stellen fest, dass die Anwendung beider Substanzen wirksamer gegen die Nematoden ist, als die Anwendung der jeweils einzelnen Substanz.

Wir sind davon überzeugt, dass dieses Untersuchungen das grundlegende Verständnis und die praktische Umsetzung von Bekämpfungsstrategien auf mikrobieller Basis verbessern und die Entwicklung innovativer und nachhaltiger Lösungen für ein integriertes Nematodenmanagement vorantreiben kann.

Acknowledgement

I would like to express my deepest gratitude to Prof. Dr. Florian M. W. Grundler for offering me such an excellent opportunity to pursue my dream research topic in your laboratory and for providing me with invaluable scholarly insights and endless encouragement throughout my challenging academic journey.

I am thankful to my dedicated supervisor Dr. A. Sylvia S. Schleker. Your mentorship, motivation, and expertise have been indispensable in shaping the direction and outcome of my doctoral research. I admire all that you have done for me, and I hope to follow in your footsteps.

I am also indebted to the members of my doctoral committee, Prof. Dr. Karl-Heinz Südekum, Prof. Dr. Christian Borgemeister, and Prof. Dr. Janina Dierks, for your critical evaluation of my PhD work.

My sincere appreciation extends to Dr. Zoran Radakovic, Dr. Samer Habash, and Dr. Christiane Matera for sharing your scientific experience and giving your professional advice, which enabled me to quickly adapt to laboratory work in the early stage of my PhD.

Special thanks to Birgit Otte, Stefan Neumann, Ute Schlee, and Gisela Sichtermann for your ongoing technical assistance and administrative support. Many thanks to all members of the MPM group for creating a cooperative atmosphere.

A heartfelt thank you goes to my beloved family, my parents, Jian and Fang, and my husband, Yang, for your unconditional love during my doctoral studies. Your unwavering support and understanding have been a source of strength and hope for me.

I am grateful for everyone in my life that has left their mark and made their impact on me.

Table of contents

Chapter 2

Chapter 3

Chapter 4

Chapter 5

List of abbreviations

ANOVA	Analysis of variance
ARE	*A. thaliana* root exudates
BCA	Biological control agents
BGC	Biosynthetic gene clusters
CDS	Coding sequences
CFS	Cell-free supernatant
CFU	Colony-forming units
CS	Cell suspension
DBC	Dead bacterial cells
DPI	Day-post-inoculation
EC_{50}	Half maximal effective concentration
HPLC	High performance liquid chromatography
IAA	Indole-3-acetic acid
IPM	Integrated pest management
ISC	Initial syncytial cell
J2	Second-stage juveniles
LAMP	Loop-mediated isothermal amplification
LBC	Living bacterial cells
LFD	Lateral flow dipstick
MW	Molecular weight
MWCO	Molecular weight cut-off
NP	Natural products

NRP	Non-ribosomal peptides
OA	Organic acids
OD_{600}	Optical density at 600 nm
PCA	Principle component analysis
PCR	Polymerase chain reaction
PGPR	Plant growth-promoting rhizobacteria
PK	Polyketides
PPN	Plant-parasitic nematodes
PTM	Post-translational modifications
QS	Quorum sensing
RAPD	Random amplified polymorphic DNA
RFLP	Restriction fragment length polymorphism
RiPP	Ribosomally-synthesized and post-translationally modified peptides
ROS	Reactive oxygen species
RPA	Recombinase polymerase amplification
RT-qPCR	Real-time quantitative PCR
SCAR	Sequence characterized amplified regions
SE	Standard error
TSA	Tryptic soy agar
TSB	Tryptic soy broth
VOC	Volatile organic compounds

List of figures and tables

Chapter 1

Chapter 2

Chapter 3

Chapter 4

Chapter 1

Introduction

Nematodes in general

Morphology and anatomy

Nematodes, commonly known as roundworms, belong to the kingdom Animalia and the phylum Nematoda. They are multicellular invertebrates with thread-like, non-segmented, and bilaterally symmetrical bodies. To date, approximately 30,000 nematode species have been identified, but the existence of more than a million species has been estimated (Hugot et al., 2001; Kiontke and Fitch, 2013). The majority of nematodes are microscopically small, for examples, the females of *Aphelenchoides bicaudatus* can only reach up to 0.47 mm long. However, the animal parasite *Placentonema gigantissima*, has been recorded as over 8 meters in the placenta of the sperm whale (Gubanov, 1951; Gibbons, 2002).

The most best-known and most-studied nematode is *Caenorhabditis elegans*. It is a tiny (~1 mm) nematode that is commonly free-living in soil, and feeds on microbes, primarily bacteria. Since *C. elegans* is the first multicellular organism to have its whole genome sequenced, it is frequently used as a research model in molecular genetics, cell biology, and neuroscience (*C. elegans* Sequencing Consortium, 1998). Figure 1 represents a lateral anatomical diagram of an adult *C. elegans*. Similar to other nematodes, *C. elegans* consists of an outer tube and an inner tube separated by a pseudocoelom. The outer tube, also known as body wall, includes cuticle, hypodermis, excretory system, neurons, and muscles. The inner tube comprises pharynx, intestine, and, in adults, gonad. All these organs and tissues are under an internal hydrostatic pressure, regulated by an osmoregulatory system (Riddle et al., 1997). *C. elegans* has two sexes, XX hermaphrodite and XO male. Most *C. elegans* are hermaphrodites, which are structurally females and reproduce by self-fertilization, while approximately 0.1 % are males, resulting from a spontaneous loss of an X chromosome (Meyer, 1997).

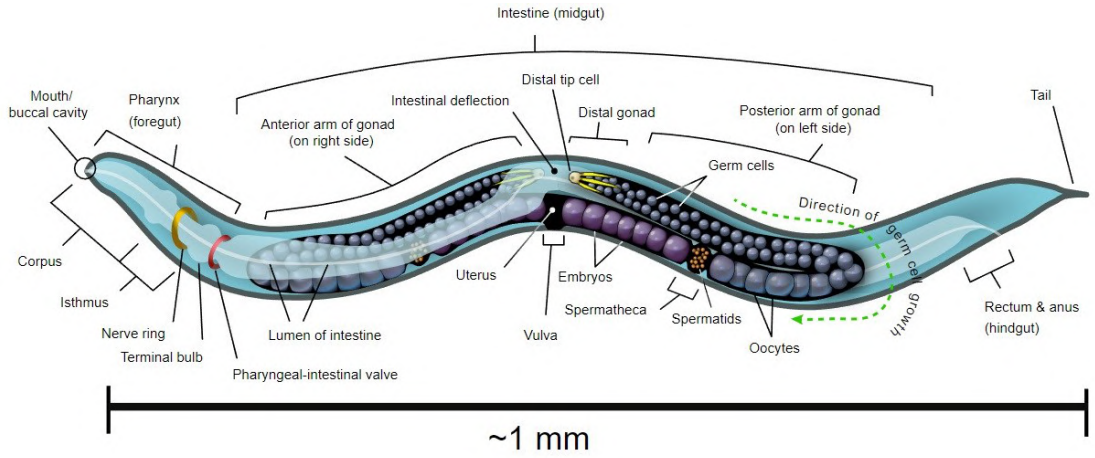

Fig. 1: Body plan of *Caenorhabditis elegans* (https://bio.libretexts.org/@go/page/5960).

Habitat and diversity

Nematodes are adaptive to almost every ecological niche on earth, ranging from terrestrial to marine environments. Although their locomotion is dependent on moisture, many of them are able to withstand adverse environmental conditions, such as cryobiosis, thermobiosis, anoxybiosis, osmobiosis, and anhydrobiosis (Decreamer and Hunt, 2006). Ecologically, nematodes are categorized into two main groups: free-living and parasitic.

Free-living nematodes are found in marine and freshwater, as well as in soils and sediments of various types of terrestrial biomes. Although most of them feed on a diverse range of food, including bacteria, fungi, algae, protozoa, small invertebrates, and even other nematodes, they all have a similar life cycle (Lee, 2002; Iqbal and Jones, 2017). These soil species make a great contribution to maintain the bio-dynamic system. For example, they improve the recycling of nutrients and minerals by releasing nitrogen and vitamins as they feed on microbes (Yadav et al., 2018). In addition, free-living nematodes can act as biological indicators of soil health and environmental pollution, as their presence in soil reflect changes in the soil microbial community, as well as the physical and chemical property of the ecological habitat (Lu et al., 2020).

Parasitic nematodes are capable of infecting various types of organisms, including plants, animals, and insects. Their survival requires frequent synchronization with the host in order to optimize the chances of successful invasion (Perry and Clarke, 1981). The synchrony is normally centered on the host-derived hatching stimuli. In some animal- and insect parasitic

nematodes, eggs are ingested by the host and the host intestine provides optimum condition for hatching. In some species of plant-parasitic nematodes (PPN), the hatching stimulus comes from the host roots (Perry, 2002). The life cycle of parasitic nematodes is usually longer than free-living nematodes. It is comprised of two phases, the pre-parasitic and parasitic. The pre-parasitic phase, which may correspond to the infective stage, emerges as a free-living form for host seeking. After locating and invading the definitive host, the parasitic phase starts (Perry and Moens, 2011).

Plant-parasitic nematodes

Economic importance in agriculture

Although only 15% of the total numbers of nematode species described are plant-parasitic nematodes, they cause tremendous yield losses and economic damage from fields to markets all around the world (Decreamer and Hunt, 2006). They can injure plants not only by direct feeding from and migration within plant tissues, but also by facilitating subsequent infestation by other secondary pathogens, such as fungi, bacteria and viruses (Powell, 1971). The global crop losses due to PPN have been estimated to US$80 billion per year (Nicol et al., 2011). However, in reality, damaged caused by PPN is likely to be underestimated by many growers due to their microscopic size, subterranean existence, and non-specific symptoms (Jones et al., 2013). General symptoms of nematode infection in crops include suppression of nutrition uptake, retardation of root growth and biomass accumulation, and decline of agricultural yield and productivity, which are often confused with abiotic (i.e. drought stress and nutrient deficiency) symptoms. Root-knot nematodes (*Meloidogyne* spp.), cyst nematodes (*Heterodera* and *Globodera* spp.), and root lesion nematodes (*Pratylenchus* spp.) rank among the top three most economically and scientifically important PPN due to the intricate relationship with their hosts, and the extent of damage caused by infection (Jones et al., 2013). Table 1 reports a comprehensive estimation of crop damages by PPN on a worldwide basis (Sasser and Freckman, 1987; Abd-Elgawad and Askary, 2015). It is estimated that 40 representative live-sustaining and economically important crops have average annual yield losses of 12.6% and 14.5%, respectively. On a monetary basis, the

worldwide crop losses are estimated to be US$215.77 million and US$142.47 million, respectively.

Tab. 1: Summary of estimated annual yield losses in life-sustaining crops and economically important crops due to damage by plant-parasitic nematodes (Sasser and Freckman, 1987; Abd-Elgawad and Askary, 2015).

Life-sustaining crops	**Annual loss (%)**	**Annual loss (US$ million)**	**Economically important crops**	**Annual loss (%)**	**Annual loss (US$ million)**
Banana	21.3	25,375.07	Aubergine	18.1	30,437.41
Barley	6.1	1,694.86	Cacao	10.5	1,161.41
Cassava	10.0	5,408.33	Citrus	14.2	564.57
Chickpea	13.7	1,247.92	Coffee	15.0	5,015.64
Coconut	20.7	24,452.76	Cotton	11.1	8,142.33
Field bean	12.5	360.00	Cowpea	15.1	7,469.97
Groundnut	14.2	17,443.89	Cucumber	18.5	69,383.17
Maize	7.9	17,013.80	Forages	9.1	-
Millet	12.0	2,405.46	Grape	14.8	5,940.79
Oat	13.5	848.69	Guava	11.9	-
Pigeonpea	13.2	155.58	Melons	15.7	1,443.36
Potato	15.1	12,914.21	Okra	21.3	11,989.08
Rice	12.8	49,697.05	Ornamentals	11.1	-
Rye	3.5	135.48	Papaya	15.1	574.07
Sorghum	7.8	1,213.06	Pepper	12.5	352.00
Soybean	13.1	17,412.69	Pineapple	14.9	3,874.82
Sugarbeet	11.8	2,273.62	Tea	8.2	3,417.38
Sugarcane	24.9	19,782.31	Tobacco	11.8	2,683.58
Sweet potato	10.2	968.38	Tomato	22.4	96,887.44
Wheat	7.0	14,966.76	Yams	17.7	7,227.04
Average loss (%)	12.6		**Average loss (%)**	14.5	
Total loss (US$ million)		215,769.92	**Total loss (US$ million)**		142,473.80

Feeding habit of plant-parasitic nematodes

PPN exhibit a wide variety of interactions with their hosts, and feed on almost all plant tissues, including roots, stems, leaves, buds and seeds (Perry and Moens, 2011). They have hollow, protrusible oral spears or stylets to pierce cell walls and withdraw nutrients from host plants. Researchers have to date mainly focused on root-infecting nematodes due to their economic and social impacts. Based on their feeding habit, PPN are classified into three

groups: ectoparasites, endoparasites, and semi-endoparasites. Ectoparasitic nematodes stay outside of the host and feed on root epidermis as an intermittent food sources. Endoparasitic nematodes entirely penetrate host roots, migrate through root tissues, induce a complex feeding structure within their host, and thereby establish a long-lasting food source. Semi-endoparasitic nematodes, unlike endoparasitic nematodes, do not entirely enter root tissues. In fact, their anterior parts stay permanently in the cortex and the posterior section extents freely into the soil.

Cyst nematodes and their life cycle

As obligate biotrophs, cyst nematodes cause considerable yield losses to a wide range of essential crops. They penetrate the host roots, migrate towards the vascular cylinder, and induce the formation of metabolic sinks from which nutrients are withdrawn. Additionally, they manipulate host plant's cellular processes to facilitate their parasitic mechanisms by producing effectors in the esophageal gland and delivering these effector proteins into host cells through their hollow stylet (Mejias et al., 2019). Eight genera, *Heterodera* (82 species), *Globodera* (12 species), *Cactodera* (13 species), *Dolichodera* (1 species), *Paradolichodera* (1 species), *Betulodera* (1 species), *Punctodera* (4 species) and *Vittatidera* (1 species) are currently identified within this nematode group (Subbotin et al., 2010). In Europe, the genera *Heterodera* and *Globodera* have been identified as the most damaging PPN to plants. Cysts are tanned cuticles of the dead female body, protecting the eggs inside from unfavorable conditions, and are able to remain viable in the soil for up to 20 years (Sukhanova et al., 2022). Cyst of both genera can be seen with the naked eye and distinguished by their shape: *Heterodera* produces lemon-shaped cysts, while *Globodera* produces spherical cysts. Among these, *Globodera rostochiensis* and *G. pallida* have a limited host range and show a high dependence on host root exudates for hatching, whereas *Heterodera schachtii* has a very wide host range and hatches under a large number of stimuli (Jones et al., 1998; Lilley et al., 2005).

Nematodes require successful host interactions throughout their life cycle to survive. The life cycle of cyst nematodes is illustrated in Figure 2. In the presence of host plants, the second-stage juveniles (J2) start to hatch from eggs, and direct themselves towards well-growing roots, which in most cases are lateral roots (Wyss and Zunke, 1986). Upon finding suitable

host roots, the juveniles pierce epidermal cells with their robust stylet at adjacent sites until starting a slit for invasion. Along with aggressive movement of stylet and secretion of cell wall degrading proteins and enzymes, the juveniles initiate the fusion of neighboring cells, and migrate towards the vascular cylinder. After reaching the vascular cylinder, stylet thrusting of juveniles becomes gentle. They probe cells one by one until a suitable cell is selected, which forms the initial syncytial cell (ISC) (Jones and Northcote, 1972; Grundler et al., 1991; Wyss and Grundler, 1992). Once ISC is established, a syncytium is formed within the vascular cylinder, and serves as the only nutrient source throughout the development of cyst nematodes (Grundler et al., 1998). Juveniles remain sedentary, commence feeding, and undergo three molting to reach adulthood, where they develop into either lemon-shaped female or vermiform male (Golinowski et al., 1996). In contrast with male, female consumes 29 times more food in its life (Müller et al., 1981). As a result, the syncytium associated with female is metabolically hyperactive and stays active for longer periods than male. With continuous feeding, the swollen female ruptures roots, and embeds the anterior part inside host roots (Williamson and Gleason, 2003). The adult male hatches from the juvenile cuticle and migrates to females for mating. After fertilizing, the female dies and turns into a brown cyst harboring hundreds of eggs. Eggs of cyst nematodes remain dormant if they do not receive any proper stimulus to hatch. Once stimuli diffused from host plants, infective juveniles within the eggs will start to hatch (Tefft and Bone, 1985; Seinhorst, 1986).

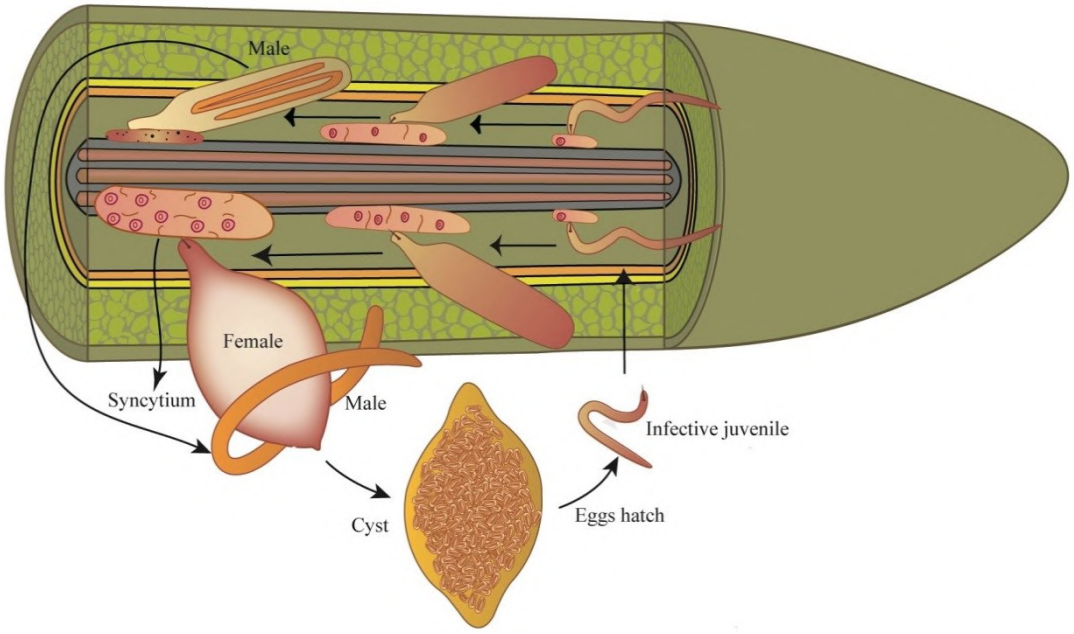

Fig. 2: Life cycle of cyst nematodes (Siddique and Grundler, 2018). Infective juvenile emerges from the cyst stimulated by root exudate; Juvenile migrates towards the vascular cylinder, initiates feeding site, and establishes multinucleate syncytium; Sex differentiation is determined by environmental condition and nutrition availability; Mature male leaves its shell and seeks female for mating; Fertilized female produces 200-300 eggs and becomes dead cyst.

Control strategies of plant-parasitic nematodes

Nematode diagnosis

A reliable and rapid nematode diagnosis is the keystone for the implementation of a successful nematode control (Shao et al., 2023). An accurate identification helps in understanding nematode diversity and designing efficient management strategies. In addition, due to the fact that symptoms on the ground usually do not appear until the infection reaches a high level, an early detection of these destructive pests is indispensable.

The traditional identification of PPN is based on morphological and anatomical characterizations, such as length of stylet and body, shape of head and stylet knob, presence and shape of spermathecal, shape of female tail terminus, shape and length gubernaculum. However, differences in some of these morphological features are subtle, subjective, and have overlapping characters or show intraspecific variation, which may lead to erroneous species identification (Hunt and Handoo, 2009). In addition, morphology-based techniques

are sophisticated, because the preparation of nematode specimens may result in artificial modifications. Specifically, specimens after being extracted, killed, fixed, and mounted under microscopic preparations, often show artifacts that make it difficult to localize external or internal structures of the diagnostic parameters, or even produce unnatural features (Carneiro et al., 2017). Furthermore, characterization of morphological evidence requires specialized and experienced nematode taxonomists, whose numbers have recently been decreasing due to a lack of interest in classical taxonomy among young researchers (Oliveira et al., 2011).

Since the development of polymerase chain reaction (PCR), DNA-based molecular diagnosis has been widely used for the detection and identification of PPN. Compared with morphological analyses, they have the following advantages: 1) they are applicable in high-throughput systems; 2) homology of genes is simpler to predict and detect than homology of morphological features; 3) DNA information can be obtained and communicated easily across laboratories without interpretation (Abebe et al., 2011). Broadly speaking, molecular-based approaches can be categorized into traditional PCR methods and isothermal amplification technologies. Traditional PCR methods include DNA barcoding, restriction fragment length polymorphism (RFLP), random amplified polymorphic DNA (RAPD), sequence characterized amplified regions (SCAR), and real-time quantitative PCR (RT-qPCR). However, all of the above methods are either time-consuming or costly, and only applicable under laboratory condition (Hebert et al., 2003; Chen et al., 2005; ; Berry et al., 2008; Blok and Powers, 2009; Chen et al., 2011). On the other hand, the advent of isothermal amplification techniques, including loop-mediated isothermal amplification (LAMP) and recombinase polymerase amplification (RPA), offers promising alternatives for nematode characterization. They are rapid, specific, sensitive, and well-suited for in-field use (Badu et al., 2018; Ahuja and Somvanshi, 2021). For example, the combination of lateral flow dipstick (LFD) with LAMP and RPA and allows amplification products to be clearly identified in the field by naked eye (Panno et al., 2020; Yao et al., 2021).

In addition to morphological identification and molecular diagnosis, protein-based biochemical detection techniques are also utilized to delineate nematode species. Unlike DNA, who possesses a redundancy of the genetic code, protein provides a reduced

vocabulary. However, the alphabet used by protein is more complicated, with typically more than 20 characters compared with the four DNA bases. Moreover, the post-translational modification of proteins increases the potential for changes in protein structures and properties (Bogale et al., 2020). Enzyme phenotypes, also known as multi-locus enzyme electrophoresis, were the first non-morphology-based methods applied in the early 1970s for the identification of several PPN, such as *Meloidogyne*, *Heterodera*, *Ditylenchus* and *Aphelenchus* spp. (Dickson et al., 1970). However, this technique has some limitations because isozyme extraction is subject to strict conditions in a specific stage of the nematode life cycle. For example, it is most applicable to root-knot nematodes, especially young females (Esbenshade and Triantaphyllou, 1985; Esbenshade and Triantaphyllou, 1990). Matrix-assisted laser desorption/ionization has been widely used in laboratories for the analysis of complex molecules, where molecules are ionized due to the loss/gain of protons and the resulting fingerprint signals enter the mass spectrometer for detection (Bizzine et al., 2010).

Nematode control

The aim of controlling plant-parasitic nematodes is to improve crop growth, quality and yield by keeping nematode populations below a certain economic threshold. The control measures should be profitable and cost effective, and the cost-benefit ratio must be calculated before control measures are taken. Generally, nematode control methods fall into three categories: cultural control, chemical control and biological control.

Cultural control

Cultural control strategies are agronomic practices employed to minimize problems caused by nematodes. A grower can achieve this by a single or combination of the following approaches: 1) selection of healthy seed material; 2) adjusting the time of planting; 3) fallowing; 4) deep summer ploughing; 5) manuring; 6) flooding; 7) trap cropping; 8) antagonistic crops; 9) removal and destruction of infected plants; 10) use of resistant varieties. In particular, the implementation of trap cropping, where susceptible crops are planted first and then removed, can help reduce nematode inoculum and henceforth nematode damage to the main crop. For instance, cowpea can be used as a cover crop in

irrigated tomato production system to suppress populations of *M. incognita*, and enhance yields of tomato (Roberts et al., 2005). In addition, planting antagonistic crops along with main crops creates an environment that is unsuitable for nematode populations. For example marigold produces the bioactive compound α-therthienyl throughout the plant from root to shoot, which is capable of repelling root-knot nematodes and lesion nematodes (Wang et al., 2007). Moreover, genetic engineering has proven a promising tool for the development of nematode resistance in crop plants. For example, several natural host resistance genes, such as *Hs1*$^{pro-1}$, *Gpa*-2, Hero A, *Cre* loci, have been cloned from some plant species and could be used to develop cyst nematode resistance in crops (Ali et al., 2017).

Chemical control

Since the late 19th century, chemical control has proven to be effective against nematode populations in soil. The use of chemically synthesized nematicides has dramatically increased the yields of several crops around the world. According to the mode of application, nematicides are classified as fumigants or non-fumigants.

Fumigant compounds are applied by soil drench or drip irrigation in gaseous form by moving through the soil pores or dissolving into the water film surrounding the soil particles to reach the target organisms. The nematicidal efficacy of fumigants is influenced by soil type, soil temperature, and soil moisture owing to their volatility. In general, they kill nematodes through multiple modes of action, such as by affecting enzymatic, nervous, and respiratory systems. Unfortunately, they also pose a potential danger to non-target organisms and humans (Rich et al., 2004). For example, aldicarb, one of the most toxic pesticides, was banned by 2015 in all global markets. The pesticide's metabolite residue (aldicarb sulfoxide) poisoned thousands of people in the United States that consumed contaminated melons at a concentration close to detection limit of 0.2 ppm (Goldman et al., 1990). Another example is methyl bromide, which is the most notable fumigant for controlling soil pests and pathogens, including plant-parasitic nematodes. It has a broad-spectrum effect and is particularly considered as a potent ozone-depleting substance. Therefore, it was phased out by 2005 under the Clean Air Act (United States General Accounting Office, 1995; Giannakou et al., 2002).

The withdrawal of broad-spectrum soil fumigants initiated the application of non-fumigants. In recent years, a small number of novel non-fumigant nematicides, with a relatively high efficacy to PPN and low toxicity to non-target organisms, have been commercialized or are in the phase of registration for use. Fluensulfone, fluopyram, and fluazaindolizine are three promising nematicides for nematode control. Since all three compounds contain trifluoromethyl (-CF3), they are known as 3F or fluorinated nematicides (Oka, 2020). For example fluensulfone exhibits effective nematicidal activity against *M. incognita* and *M. javanica* via soil injection or foliage spray, and low toxicity to vertebrates (e.g. rats) and non-target organisms (e.g. honey bees and earthworms) (Oka et al., 2012; Oka et al., 2013). However, it has been reported that the recommended doses of fluensulfone tend to cause phytotoxicity to plants, such as inhibition of seed germination and retardation of root development (Giannakou and Panopoulou, 2019).

Biological control

As most chemical nematicides are banned due to environmental hazard and human health concerns, there is an urgent demand to search for safer alternatives. Biological control, which aims at reducing nematode populations by natural enemies, has gained considerable attention in recent decades. In nature, nematode densities are stabilized by a constant series of check and balance that keep their populations between certain upper and lower limits (Stirling, 2011). Therefore, understanding the habits of diverse soil organism, including microfauna (e.g. fungi, bacteria, viruses and protozoa), mesofauna (e.g. rotifers, nematodes, tardigrades, collembolans, mites and enchytraeids) and macrofauna (e.g. earthworms, termites and millipedes), provides a better insight into the biological interactions occurring in the soil environment and facilitates a successful implementation of biological control agents (BCA) in nematode control. Nematophagous fungi, nematophagous bacteria, predatory nematodes, mites, and viruses are the five main groups used as BCA. Among these, the biocontrol potential of nematophagous fungi and bacteria against PPN has been well studied and described.

Generally, nematophagous fungi live in almost all soil types and consume one or more stages of nematodes (eggs, juveniles, vermiform adults and sedentary females) with various mechanisms (Jansson and Lopez-Llorca, 2004). According to their modes of infection, they

are classified into four groups: 1) egg- and female-parasitic fungi invading nematode eggs or female with their hyphal tips, 2) nematode-trapping fungi using adhesive or mechanical hyphal traps, 3) endoparasitic fungi infecting vermiform nematodes by their spores, 4) toxin-producing fungi immobilizing nematodes prior to penetration by secreting nematicidal or nematostatic compounds (Liu et al., 2009). For example, *Arthrobotrys oligospora*, a nematode-trapping fungus, is able to initiate predation under a nutrient-deprived condition by developing hyphal rings or adhesive hyphae. The specialized mycelial structure is able to capture nematodes, penetrate their cuticle, grow mycelia inside the prey and consume them. (Niu and Zhang, 2011). Besides its trapping strategy, *A*. *oligospora* also secretes compounds, such as linoleic acid, as a potent nematicidal weapon (Stadler et al., 1993). Recently, four fungal metabolites, linoleyl alcohol, desferriferrichrome, nonadecanamide, and citicoline, have been identified as being abundantly produced in *Arthrobotrys* spp. during the predatory stage (Kuo et al., 2020). Among them, linoleyl alcohol is the substrate for the production of linoleic acid. Through oxidation, large amounts of linoleyl alcohol might produce linoleic acid, which acts as a potential nematicide.

Another effective group of natural enemies of nematodes are nematophagous bacteria. They affect PPN by the following mechanisms: parasitism; production of toxins, antibiotics, or enzymes; interference with nematode-host plant recognition; competition for space and nutrients; induction of systemic resistance in plants; and promotion of plant health (Siddiqui and Mahmood, 1999). The nematophagous bacteria can be categorized into parasitic bacteria and non-parasitic bacteria. Parasitic group, such as the genus *Pasteuria*, eliminates nematodes through their parasitic behavior, while non-parasitic rhizobacteria, such as *Agrobacterium* spp., *Alcaligenes* spp., *Bacillus* spp., *Clostridium* spp., *Desulfovibrio* spp., *Pseudomonas* spp., *Serratia* spp., and *Streptomyces* spp., reduce nematode populations by colonizing the rhizosphere of the host plant. In soil, endospores of *Pasteuria penetrans* remain dormant until they attach to the cuticle of J2 migrating through the soil. Once contact occurs, germ tubes emerge from the spores, penetrate the cuticle, and then form microcolonies that proliferate within the developing female. The microcolonies then begin to sporulate, filling the body of the nematode with spores and preventing it from reproducing (Sayre and Wergin, 1977). To ensure successful infection of J2, a minimum of five spores per nematode is required (Davies et al., 1988). Rhizobacteria, on the other hand,

suppress nematode reproduction, egg hatching and juvenile mobility by secreting secondary metabolites, interfering with nematode-host plant identification, and inducing systemic resistance, rather than by parasitizing (Tian et al., 2007). *Bacillus* spp. and *Pseudomonas* spp. are the two dominant nematode-antagonistic rhizobacteria in the rhizosphere. They exhibit diverse pathogenic mechanisms upon interaction with nematodes, including the genera *Meloidogyne*, *Heterodera* and *Rotylenchulus* (Kloepper et al., 1992; Jayakumar et al., 2003; Siddiqui et al., 2005). Some of these, known as plant growth-promoting rhizobacteria (PGPR), have shown beneficial effect on stimulating plant development and yield by aggressively colonizing the rhizosphere (Kloepper et al., 1980). They provide plants with compounds synthesized by them, such as phytohormones, or assist in the uptake of certain nutritious substances from the environment (Idris et al., 2007; Liu et al., 2012).

Crosstalk between plants and their microbiome in the rhizosphere

Rhizosphere, the narrow region of soil in the vicinity of the roots, is considered as a hotspot for a variety of microbial activities and is represented by one of the most complex and dynamic ecosystems (Hiltner, 1904). This high density ecological niche allows plants to interact with associated microorganisms through chemical signals and metabolites carried by root exudates, which in turn activates many regulatory mechanisms. The quantity and quality of root exudates depend on plant species, growth stage, nutrition status, and external factors like biotic and abiotic stressors. Due to their distinct metabolic profiles, root exudates are usually divided into two classes: 1) low-molecular weight compounds, such as monosaccharides, amino acids, and organic acids, which account for the diversity of root exudates; 2) high-molecular weight compounds such as polysaccharides, proteins, and lipids, which are less diverse but account for a large proportion of root exudates by mass (Badri and Vivanco, 2009).

The plant-microbe interactions can be either beneficial or detrimental, depending on the interaction of colonizing microorganisms on the host plants. Beneficial interactions include symbiotic and associative interactions with beneficial microbes, such as ecto- and endo-mycorrhiza, nitrogen-fixing bacteria, and plant growth-promoting rhizobacteria, which help

plant get access to otherwise unavailable soil nutrients through solubilisation and mobilisation, enhance tolerance to abiotic stresses, defend against pests and pathogens, and promote plant growth. Detrimental interactions include associations with parasitic plants, pathogenic bacteria, fungi, oomycetes, nematodes, and invertebrate herbivores, resulting in negative consequences such as host plant necrosis and crop yield loss (Jamil et al., 2022).

An increasing amount of evidence suggests that different signalling mechanisms are involved in plant-microbe interactions. In particular, quorum sensing (QS) is a cell-to-cell communication process that allows bacteria to regulate gene expression in a population-dependent manner through constant synthesis, excretion, detection, and response of extracellular signalling molecules (Rutherford and Bassler, 2012). Common categories of these signalling molecules include acyl-homoserine lactone in Gram-negative bacteria, autoinducer peptides in Gram-positive bacteria, and autoinducers 2 in both Gram-negative and Gram-positive bacteria (Fuqua et al., 2001; Kleerebezem et al., 1997; Chen et al., 2002). Gram-positive and Gram-negative bacteria use QS communication networks to regulate a wide range of physiological activities, including symbiosis, virulence, competence, conjugation, motility, sporulation, antibiotic production, and biofilm formation (Miller and Bassler, 2001). Another signalling mechanism is through the production of volatile organic compounds (VOC). Microbial VOC are low-molecular weight lipophilic compounds and belong to different chemical classes such as alkenes, alcohols, ketones, terpenes, benzenoids, pyrazines, acids, and esters (Tyc et al., 2015). Due to their ability to travel through the air, soil, and water, VOC are ideal signalling molecules for mediating both short- and long-distance intercellular and interkingdom interactions (Bitas et al., 2013). For example, *Bacillus nematocida* B16 is able to lure *C. elegans* by releasing a mixture of VOC. Once bacteria colonize the intestinal tract of nematodes, they secrete two extracellular proteases that primarily target intestinal proteins, resulting in nematode death (Niu et al., 2010).

A plant-nematode model system for studying biological control agents

Interaction of *Arabidopsis thaliana*, *Heterodera schachtii*, and *Bacillus* spp.

Arabidopsis thaliana, which is a member of the *Brassicaceae* family, has become the model organism in plant genetic research since the 1980s. There are several advantages of using *A. thaliana*, including 1) a rapid life cycle from seed germination to maturation; 2) an easy cultivation under laboratory and greenhouse conditions; 3) a relatively small, genetically tractable genome; 4) a large number of mutant lines and genomic resources (Gepstein and Horwitz, 1995). Since *A. thaliana* can be parasitized by a variety of pathogens including insects, bacteria, fungi, viruses, and nematodes, it provides an alternative system to commonly used crop plants for the study of plant physiology and development at the molecular level (Pang et al., 1987; Meinke et al., 1998). Root exudates comprising amino acids, organic acids, sugars, phenolics, polysaccharides, and proteins not only provide a carbon-rich environment for microorganisms, but also act as chemical signals to facilitate contact between bacteria and the host root surface by initiating chemotaxis (Bais et al., 2006; Strehmel et al., 2014). L-malic acid secreted by *A. thaliana* roots has been proven to be one of the active compounds that attract beneficial bacteria in a dose-dependent manner (Rudrappa et al., 2008). Interestingly, the composition of *A. thaliana* root exudate varies over the course of plant development. In fact, principle component analysis (PCA) shows that the secretion of sugars and sugar alcohols from *A. thaliana* roots reaches the greatest abundance at an early development stage, while the quantity of secreted amino acids and organic acids accumulates during the same period and rises at later developmental time points of the plant (Chaparro et al., 2013).

In the present study, we focus on the beet cyst nematodes *H. schachtii*, which was first discovered by Hermann Schacht in 1859, and later named and described by Adolf Schmidt in 1871 (Schacht, 1859; Schmidt, 1871). *H. schachtii* appeared in Western Europe soon after the introduction of sugar beet (*Beta vulgaris*) and is considered as a major problem on sugar beet industry. It is widely distributed in most growing regions with a long history of sugar beet cultivation. After infestation by *H. schachtii*, sugar beets show symptoms such as root

stunting and leaf wilting, which ultimately leads to yield reduction. *H. schachtii* has an extensive host range, being capable of infecting more than 200 plant species from 23 different plant families (Steele, 1965). Among these hosts, *H. schachtii* is mainly parasitic on members of the families *Amaranthaceae* and *Brassicaceae* (Franklin, 1972), which creates possibilities to use *A*. *thaliana* as a model host for the study of plant-nematode interaction. In 1991 it was first documented that the sedentary cyst nematodes *H. schachtii*, *H. trifolii*, and *H. cajani*, the root-knot nematodes *Meloidogyne incognita* and *M. arenaria*, and the migratory nematode *Pratylenchus penetrans* can complete their life cycles in *Arabidopsis* roots under monoxenic conditions. Among these, *H. schachtii* is the most rapidly developing one (Sijmons et al., 1991). Therefore, the system of *A. thaliana* and *H. schachtii* provides an ideal model to observe plant responses and nematode behaviour (Grundler et al., 1994). Figure 3 demonstrates a successful establishment of *H. schachtii* at *A. thaliana* 14 days after inoculation.

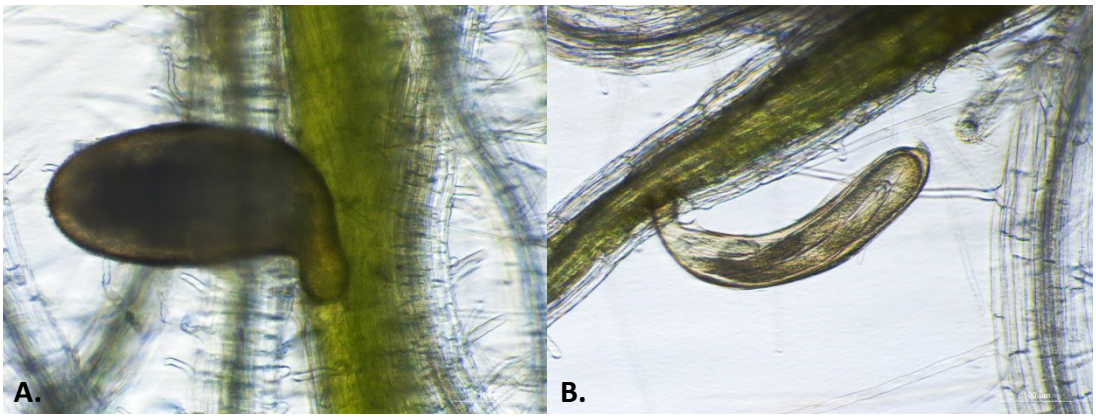

Fig. 3: Schematic representation of beet cyst nematode *Heterodera schachtii* parasitism at *Arabidopsis thaliana* root. A. Adult female at 14 day-post-inoculation; B. Adult male at 14 day-post-inoculation.

Previous studies have suggested that microorganisms in the rhizosphere require a successful root surface colonization to suppress soil pathogens and protect host plants (Weller, 1988; Chin-A-Woeng et al., 2000). It was reported that *Bacillus subtilis* evolving on *A. thaliana* shows a rapid increase in root colonization (Nordgaard et al., 2022). After a successful attachment by *B*. *subtilis*, *A. thaliana* is protected from pathogen infection, such as *Pseudomonas syringae* (Massalha et al., 2017). However, in order to initiate an effective colonization, chemotactic response of rhizobacteria towards host roots is considered as a

prerequisite (Broek and Vanderleyden, 1995; Turnbull et al., 2001). Sequencing revealed that the rhizosphere of *A. thaliana* roots is rich in diverse microbial communities, and high performance liquid chromatography (HPLC) suggests that microbial assemblages could be highly dependent on root exudation patterns of their host - *A. thaliana* (Micallef et al., 2009; Lundberg et al., 2012). According to Allard-Massicotte et al. (2016), *A. thaliana* root exudates actively recruit *B*. *subtilis,* which can sense plant compounds through chemotaxis receptors like McpB, McpC, and TlpC, which subsequently facilitates colonization. The rhizobacterium *Bacillus amyloliquefaciens* is another example. It is able to beneficially interact with *A*. *thaliana* through root colonization, thus promoting plant growth and development (Asari et al., 2017).

Biocontrol potential of rhizobacterium *Bacillus firmus* I-1582 and microbial prodiginines and rhamnolipids

B. firmus is an aerobic, alkaliphilic, and endospore-forming bacterium, that has been proven to possess great potentials not only for promoting the growth of host plants, such as tomato and cotton, but also for controlling several PPN, such as *M*. *incognita*, *Heterodera glycines*, *Radopholus similis*, and *Ditylenchus dipsaci* (Mendoza et al., 2008; Terefe et al., 2009; Castillo et al., 2013; Beeman and Tylka, 2018). For example, pot experiments have shown that the application of *B. firmus* YBF-10 results in decreased gall index, egg mass and final population of *M. incognita*, as well as increased shoot height and root length of tomato plants (Xiong et al., 2015). The strain *B*. *firmus* I-1582, which was originally isolated from soil obtained from the central plain area in Israel, is commercially available as a seed treatment product (VOTiVO®) or as a soil drench product (Nortica®) for PPN management in crops (Wilson and Jackson, 2013). It is able to grow in solid and liquid media between 15 and 45°C, with an optimal temperature of 35°C for bacterial growth and biofilm formation. Therefore, it is best to apply this strain in summer for nematode management in soil. The split-root experiment showed that *B*. *firmus* I-1582 induces systemic resistance against *M. incognita* in tomato but not in cucumber, suggesting this control effect is dependent on the plant species (Ghahremani et al., 2020). Since the control effect achieved by *B*. *firmus* I-1582 can be difficult to predict in general, a more thorough understanding of this strain and its

interaction with nematodes and plants in standard control system is a prerequisite for further advancing nematode control research.

Prodiginines are a family of red-pigmented, tripyrrolic molecules produced by Gram-negative bacteria, such as *Pseudomonas*, *Serratia*, *Hahella*, and *Vibrio*, and Gram-positive bacteria, such as Streptomyces. As bacterial secondary metabolites, prodiginines exhibit a variety of biological activities, and are widely used as natural food colorants in food industry and as anticancer and antimicrobial agents in drug research (Williamson et al., 2007; Darshan and Manonmani, 2015). According to Habash et al. (2020), the single application of prodigiosin or its 12-ring derivative effectively inhibits nematode infection and development at *A. thaliana* without causing harmful effect on the host plant. Rhamnolipids are surface-active glycolipids that can be produced by many bacterial species. *Pseudomonas* spp. and *Burkholderia* spp. are the two main producers that have been investigated intensively. It has been reported several times that the amphiphilic compounds can exert synergistic effect with various antibiotics (Sotirova et al., 2012; Magalhães and Nitschke, 2013; Das et al., 2014). Due to their surfactant properties, they not only increase the solubility of drugs and facilitate their access to target cells, but also increase the permeability of cell membranes by interfering with phospholipid bilayers (Beal and Bells, 2000; Ortiz et al., 2006). Recently, the efficacy of di-rhamnolipids against PPN has been described, which affects nematode parasitism at *A. thaliana* during early events (Bredenbruch et al., 2023). However, as a potential drug synergist, its nematicidal activity of combined application has never been studied.

Aims of this study

This study investigates novel biocontrol strategies against plant-parasitic nematodes by utilizing the plant - nematode model system *A. thaliana* - *H. schachtii*. To achieve this goal, the following work is done:

In chapter 2, a ternary *in vitro* system is developed to understand the behaviour of the rhizobacterium *B. firmus* I-1582 that help to explore its potential against two generations of *H. schachtii*.

In chapter 3, the nematicidal activity of *B. firmus* I-1582 is evaluated and the putative microbial secondary metabolites are predicted, suggesting that *B. firmus* I-1582 could function as a natural antagonist through the production of specialized metabolites.

In chapter 4, the bioactivity of microbe-derived prodiginines alone and in combination with rhamnolipids on *H. schachtii* is investigated, which offers a promising start for the development of a potential multicomponent antinematodal agent.

In all chapters, the mode of action against *H. schachtii* by using microbes and microbe-derived compounds is elucidated.

References

Abd-Elgawad MMM, Askary TH. 2015. Impact of phytonematodes on agriculture economy. In: Askary TH, Martinelli, PRP, eds. Biocontrol Agents of Phytonematodes. CAB International, 3-49.

Abebe E, Mekete T, Thomas WK. 2011. A critique of current methods in nematode taxonomy. African Journal of Biotechnology. 10, 312-323.

Ahuja A, Somvanshi VS. 2021. Diagnosis of plant-parasitic nematodes using loop-mediated isothermal amplification (LAMP): A review. Crop Protection. 147, 105459.

Ali MA, Azeem F, Abbas A, Joyia FA, Li H, Dababat AA. 2017. Transgenic strategies for enhancement of nematode resistance in plants. Frontiers in plant science. 8, 750.

Allard-Massicotte R, Tessier L, Lécuyer F, Lakshmanan V, Lucier JF, Garneau D, Caudwell L, Vlamakis H, Bais HP, Beauregard PB. 2016. *Bacillus subtilis* early colonization of *Arabidopsis thaliana* roots involves multiple chemotaxis receptors. mBio. 7, e01664-16.

Asari S, Tarkowská D, Rolčík J, Novák O, Palmero DV, Bejai S, Meijer J. 2017. Analysis of plant growth-promoting properties of *Bacillus amyloliquefaciens* UCMB5113 using *Arabidopsis thaliana* as host plant. Planta. 245, 15-30.

Babu B, Ochoa-Corona FM, Paret ML. 2018. Recombinase polymerase amplification applied to plant virus detection and potential implications. Analytical biochemistry. 546, 72-77.

Badri DV, Vivanco JM. 2009. Regulation and function of root exudates. Plant, Cell and Environment. 32, 666-681

Bais HP, Weir TL, Perry LG, Gilroy S, Vivanco JM. 2006. The role of root exudates in rhizosphere interactions with plants and other organisms. Annual Review of Plant Biology. 57, 233-266.

Beal R, Betts WB. 2000. Role of rhamnolipid biosurfactants in the uptake and mineralization of hexadecane in *Pseudomonas aeruginosa*. Journal of Applied Microbiology. 89, 158-168.

Beeman AQ, Tylka GL. 2018. Assessing the effects of ILeVO and VOTiVO seed treatments on reproduction, hatching, motility, and root penetration of the soybean cyst nematode, *Heterodera glycines*. Plant Disease. 102, 107-113.

Berry SD, Fargette M, Spaull VW, Morand S, Cadet P. 2008. Detection and quantification of root-knot nematode (*Meloidogyne javanica*), lesion nematode (*Pratylenchus zeae*) and dagger nematode (*Xiphinema elongatum*) parasites of sugarcane using real-time PCR. Molecular and Cellular Probes. 22, 168-76.

Bitas V, Kim HS, Bennett JW, Kang S. 2013. Sniffing on microbes: diverse roles of microbial volatile organic compounds in plant health. Molecular Plant-Microbe Interactions. 26, 835-843.

Bizzini A, Durussel C, Bille J, Greub G, Prod'hom G. 2010. Performance of matrix-assisted laser desorption ionization-time of flight mass spectrometry for identification of bacterial strains routinely isolated in a clinical microbiology laboratory. Journal of Clinical Microbiology. 48, 1549-1554.

Blok VC, Powers TO. 2009. Biochemical and molecular identification. In: Perry RN, Moens M, Starr JL, eds. Root-Knot Nematodes. CAB International, 98-118.

Bogale M, Baniya A, DiGennaro P. 2020. Nematode identification techniques and recent advances. Plants (Basel). 9, 1260.

Bredenbruch S, Mueller C, Atemnkeng H, Schroeder L, Tiso T, Blank LM, Grundler FMW, Schleker ASS. 2023. The biological activity of bacterial rhamnolipids is linked to their molecular structure. bioRxiv.

Broek AV, Vanderleyden J. 1995. The role of bacterial motility, chemotaxis, and attachment in bacteria-plant interactions. Molecular Plant-Microbe Interactions. 8, 800-810.

C. elegans Sequencing Consortium. 1998. Genome sequence of the nematode *C. elegans*: a platform for investigating biology. Science. 282, 2012-2018.

Carneiro RMDG, Lima FS de O, Correia VR. 2017. Methods and tools currently used for the identification of plant parasitic nematodes. In: Shah MM, Mahamood M, eds. Nematology - Concepts, Diagnosis and Control. IntechOpen, 19-35.

Castillo JD, Lawrence KS, Kloepper JW. 2013. Biocontrol of the reniform nematode by *Bacillus firmus* GB-126 and *Paecilomyces lilacinus* 251 on cotton. Plant Disease. 97, 967-976.

Chaparro JM, Badri DV, Bakker MG, Sugiyama A, Manter DK, Vivanco JM. 2013. Root exudation of phytochemicals in *Arabidopsis* follows specific patterns that are developmentally programmed and correlate with soil microbial functions. PLoS One. 8, e55731.

Chen FM, Negi S, Ye JR. 2011. A SCAR molecular marker to distinguish *Bursaphelenchus mucronatus* from the pinewood nematode, *B. xylophilus*. Forest Pathology. 41, 376-381.

Chen FM, Ye JR, Tang J, Wu XQ. 2005. A study on detection technique of *Bursaphelenchus xylophilus* and *B. mucronatus* by RAPD. Journal of Nanjing Forestry University. 48, 25-28.

Chen X, Schauder S, Potier N, Van Dorsselaer A, Pelczer I, Bassler BL, Hughson FM. 2002. Structural identification of a bacterial quorum-sensing signal containing boron. Nature. 415, 545-549.

Chin-A-Woeng TFC, Bloemberg GV, Mulders IHM, Dekkers LC, Lugtenberg BJJ. 2000. Root colonization by phenazine-1-carboxamide-producing bacterium *Pseudomonas chlororaphis* PCL1391 is essential for biocontrol of tomato foot and root rot. Molecular Plant-Microbe Interactions. 13, 1340-1345.

Darshan N, Manonmani HK. 2015. Prodigiosin and its potential applications. Journal of Food Science and Technology. 52, 5393-5407.

Das P, Yang XP, Ma LZ. 2014. Analysis of biosurfactants from industrially viable *Pseudomonas* strain isolated from crude oil suggests how rhamnolipids congeners affect emulsification property and antimicrobial activity. Frontiers in Microbiology. 5, 696.

Davies KG, Kerry BR, Flynn CA. 1988. Observations on the pathogenicity of *Pasteuria penetrans*, a parasite of root-knot nematodes. Annals of Applied Biology. 112, 491-501.

Decreamer W, Hunt DJ. 2006. Structure and classification. In: Perry RN, Moens M, eds. Plant Nematology. CAB International, 3-39.

Dickson DW, Sasser JN, Huisingh D. 1970. Comparative disc-electrophoretic protein analyses of selected *Meloidogyne*, *Ditylenchus*, *Heterodera* and *Aphelenchus* spp. Journal of nematology. 2, 286-293.

Esbenshade PR, Triantaphyllou AC. 1985. Use of enzyme phenotypes for identification of *Meloidogyne* species. Journal of nematology. 17, 6-20.

Esbenshade PR, Triantaphyllou AC. 1990. Isozyme phenotypes for the identification of *Meloidogyne* species. Journal of nematology. 22, 10-15.

Franklin MT. 1972. *Heterodera schachtii*. In: Willmott S, ed. C.I.H. Descriptions of Plant-Parasitic Nematodes. Commonwealth Institute of Helminthology.

Fuqua C, Parsek MR, Greenberg EP. 2001. Regulation of gene expression by cell-to-cell communication: acyl-homoserine lactone quorum sensing. Annual Review of Genetics. 35, 439-468.

Gepstein S, Horwitz BA. 1995. The impact of *Arabidopsis* research on plant biotechnology. Biotechnology Advances. 13, 403-414.

Ghahremani Z, Escudero N, Beltrán-Anadón D, Saus E, Cunquero M, Andilla J, Loza-Alvarez P, Gabaldón T, Sorribas FJ. 2020. *Bacillus firmus* strain I-1582, a nematode antagonist by itself and through the plant. Frontiers in Plant Science. 11, 796.

Giannakou IO, Panopoulou S. 2019. The use of fluensulfone for the control of root-knot nematodes in greenhouse cultivated crops: efficacy and phytotoxicity effects. Cogent Food & Agriculture. 5, 1643819.

Giannakou IO, Sidiropoulos A, Prophetou-Athanasiadou D. 2002. Chemical alternatives to methyl bromide for the control of root-knot nematodes in greenhouses. Pest Management Science. 58, 290-296.

Gibbons LM. 2002. General organisation. In: Lee DL, ed. The Biology of nematodes. CRC Press, 59-140.

Goldman LR, Beller M, Jackson RJ. 1990. Aldicarb food poisonings in California, 1985–1988: toxicity estimates for humans. Archives of Environmental Health. 45, 141-147.

Golinowski W, Grundler FMW, Sobczak M. 1996. Changes in the structure of *Arabidopsis thaliana* during female development of the plant-parasitic nematode *Heterodera schachtii*. Protoplasma. 194, 103-116.

Grundler F, Schnibbe L, Wyss U. 1991. *In vitro* studies on the behaviour of second-stage juveniles of *Heterodera schachtii* (Nematoda: Heteroderidae) in response to host plant root exudates. Parasitology. 103, 149-155.

Grundler FMW, Böckenhoff A, Schmidt KP, Sobczak M, Golinowski W, Wyss U. 1994. Arabidopsis thaliana and Heterodera schachtii: a versatile model to characterize the interaction between host plants and cyst nematodes. In: Lamberti F, De Giorgi C, Bird DM, eds. Advances in Molecular Plant Nematology. Springer, 171-180.

Grundler FMW, Sobczak M, Golinowski W. 1998. Formation of wall openings in root cells of *Arabidopsis thaliana* following infection by the plant-parasitic nematode *Heterodera schachtii*. European Journal of Plant Pathology. 104, 545-551.

Gubanov NM. 1951. A giant nematode from the placenta of cetaceans *Placenttnema gigantissima* nov. gen., nov. sp. Doklady Akademii Nauk SSSR. 77, 1123-1125.

Habash SS, Brass HUC, Klein AS, Klebl DP, Weber TM, Classen T, Pietruszka J, Grundler FMW, Schleker ASS. 2020. Novel prodiginine derivatives demonstrate bioactivities on plants, nematodes, and fungi. Frontiers in Plant Science. 11, 579807.

Hebert PDN, Cywinska A, Ball SL, deWaard JR. 2003. Biological identifications through DNA barcodes. Proceedings of the Royal Society B: Biological Sciences. 270, 313-321.

Hiltner L. 1904. Über neuere Erfahrungen und Probleme auf dem Gebiete der Bodenbakteriologie unter besonderer Berücksichtigung der Gründüngung und Brache. Arbeiten der Deutschen Landwirtschaftlichen Gesellschaft. 98, 59-78.

Hugot JP, Baujard P, Morand S. 2001. Biodiversity in helminths nematodes as a field study: an overview. Nematology. 3, 199-208.

Hunt D, Handoo Z. 2009. Taxonomy, identification and principal species. In: Perry RN, Moens M, Starr JL, eds. Root-Knot Nematodes. CAB International, 55-97.

Idris EE, Iglesias DJ, Talon M, Borriss R. 2007. Tryptophan-dependent production of indole-3-acetic acid (IAA) affects level of plant growth promotion by *Bacillus amyloliquefaciens* FZB42. Molecular Plant-Microbe Interactions. 20, 619-626.

Iqbal S, Jones MGK. 2017. Nematodes. In: Thomas B, Murray BG, Murphy DJ, eds. Encyclopedia of Applied Plant Sciences. Elsevier Academic Press, 113-119.

Jamil F, Mukhtar H, Fouillaud M, Dufossé L. 2022. Rhizosphere signaling: insights into plant-rhizomicrobiome interactions for sustainable agronomy. Microorganisms. 10, 899.

Jansson HB, Lopez-Llorca LV. 2004. Control of nematodes by fungi. In: Aroa DK, ed. Fungal Biotechnology in Agricultural, Food, and Environmental Applications. Marcel Dekker Inc, 205-215.

Jayakumar J, Ramakrishnan S, Rajendran G. 2003. Effect of *Pseudomonas fluorescens* strain on reniform nematode, *Rotylenchulus reniformis* penetration in cotton. Current Nematology. 14, 43-45.

Jones JT, Haegeman A, Danchin EG, Gaur HS, Helder J, Jones MG, Kikuchi T, Manzanilla-López R, Palomares-Rius JE, Wesemael WM, Perry RN. 2013. Top 10 plant-parasitic nematodes in molecular plant pathology. Molecular Plant Pathology. 14, 946-961.

Jones MGK, Northcote DH. 1972. Nematode-induced syncytium - a multinucleate transfer cell. Journal of Cell Science. 10, 789-809.

Jones PW, Tylka GL, Perry RN. 1998. Hatching. In: Perry RN, Wright DJ, eds. The Physiology and Biochemistry of Free-Living and Plant-Parasitic Nematodes. CAB International, 181-212.

Kiontke K, Fitch DH. 2013. Nematodes. Current Biology. 23, 862-864.

Kleerebezem M, Quadri LEN, Kuipers OP, deVos WM. 1997. Quorum sensing by peptide pheromones and two-component signal-transduction systems in Gram-positive bacteria. Molecular Microbiology. 24, 895-904.

Kloepper JW, Rodriguez-Kabana R, Mcinroy JA, Young RW. 1992. Rhizosphere bacteria antagonistic to soybean cyst (*Heterodera glycines*) and root-knot (*Meloidogyne incognita*) nematodes: identification by fatty acid analysis and frequency of biological control activity. Plant and Soil. 139, 75-84.

Kloepper JW, Schroth MN, Miller TD. 1980. Effects of rhizosphere colonization by plant growth-promoting rhizobacteria on potato plant development and yield. Phytopathology. 70, 1078-1082.

Kuo TH, Yang CT, Chang HY, Hsueh YP, Hsu CC. 2020. Nematode-trapping fungi produce diverse metabolites during predator-prey interaction. Metabolites. 10, 117.

Lee DL. 2002. Life cycles. In: Lee DL, ed. The Biology of nematodes. CRC Press, 141-161.

Lilley CJ, Atkinson HJ, Urwin PE. 2005. Molecular aspects of cyst nematodes. Molecular Plant Pathology. 6, 577-588.

Liu F, Xing S, Ma H, Du Z, Ma B. 2013. Plant growth-promoting rhizobacteria affect the growth and nutrient uptake of *Fraxinus americana* container seedlings. Applied Microbiology and Biotechnology. 97, 4617-4625.

Liu X, Xiang M, Che Y. 2009. The living strategy of nematophagous fungi. Mycoscience. 50, 20-25.

Lu Q, Liu T, Wang N, Dou Z, Wang K, Zuo Y. 2020. A review of soil nematodes as biological indicators for the assessment of soil health. Frontiers of Agricultural Science and Engineering. 7, 275-281.

Lundberg DS, Lebeis SL, Paredes SH, Yourstone S, Gehring J, Malfatti S, Tremblay J, Engelbrektson A, Kunin V, Del Rio TG, Edgar RC, Eickhorst T, Ley RE, Hugenholtz P, Tringe SG, Dangl JL. 2012. Defining the core *Arabidopsis thaliana* root microbiome. Nature. 488, 86-90.

Magalhães L, Nitschke M. 2013. Antimicrobial activity of rhamnolipids against *Listeria monocytogenes* and their synergistic interaction with nisin. Food Control. 29, 138-142.

Massalha H, Korenblum E, Malitsky S, Shapiro OH, Aharoni A. 2017. Live imaging of root-bacteria interactions in a microfluidics setup. Proceedings of the National Academy of Sciences of the United States of America. 114, 4549-4554.

Meinke WD, Cherry MJ, Dean C, Rounsley DS, Koornneef M. 1998. *Arabidopsis thaliana*: A model plant for genome analysis. Science. 282, 662-682.

Mejias J, Truong NM, Abad P, Favery B, Quentin M. 2019. Plant proteins and processes targeted by parasitic nematode effectors. Frontiers in Plant Science. 10, 970.

Mendoza AR, Kiewnick S, Sikora RA. 2008. *In vitro* activity of *Bacillus firmus* against the burrowing nematode *Radopholus similis*, the root-knot nematode *Meloidogyne incognita* and the stem nematode *Ditylenchus dipsaci*. Biocontrol Science and Technology. 18, 377-389.

Meyer BJ. 1997. Chapter 9. Sex determination and X chromosome dosage compensation. II Sexual dimorphism. In. Riddle DL, Blumenthal T, Meyer BJ, Priess JR, eds. *C. elegans* II, 2nd edition. Cold Spring Harbor Laboratory Press.

Micallef SA, Shiaris MP, Colón-Carmona A. 2009. Influence of *Arabidopsis thaliana* accessions on rhizobacterial communities and natural variation in root exudates. Journal of Experimental Botany. 60, 1729-1742.

Miller MB, Bassler BL. 2001. Quorum sensing in bacteria. Annual Review of Microbiology. 55, 165-199.

Müller J, Rehbock K, Wyss U. 1981. Growth of *Heterodera schachtii* with remarks on amounts of food consumed. Revue Nématol. 4, 227-234.

Nicol JM, Turner SJ, Coyne DL, den Nijs L, Hockland S, Tahna Maafi Z. 2011. Current nematode threats to world agriculture. In: Jones J, Gheysen G, Fenoll C, eds. Genomics and Molecular Genetics of Plant-Nematode Interactions. Springer, 21-44.

Niu Q, Huang X, Zhang L, Xu J, Yang D, Wei K, Niu X, An Z, Bennett JW, Zou C, Yang J, Zhang KQ. 2010. A Trojan horse mechanism of bacterial pathogenesis against nematodes. Proceedings of the National Academy of Sciences of the United States of America. 107, 16631-16636.

Niu XM, Zhang KQ. 2011. *Arthrobotrys oligospora*: a model organism for understanding the interaction between fungi and nematodes. Mycology. 2, 59-78.

Nordgaard M, Blake C, Maróti G, Hu G, Wang Y, Strube ML, Kovács ÁT. 2022. Experimental evolution of *Bacillus subtilis* on *Arabidopsis thaliana* roots reveals fast adaptation and improved root colonization. iScience. 25, 104406.

Oka Y, Shuker S, Tkachi N. 2012. Systemic nematicidal activity of fluensulfone against the root-knot nematode *Meloidogyne incognita* on pepper. Pest Management Science. 68, 268-275.

Oka Y, Shuker S, Tkachi N. 2013. Influence of soil environments on nematicidal activity of fluensulfone against *Meloidogyne javanica*. Pest Management Science. 69, 1225-1234.

Oka Y. 2020. From old-generation to next-generation nematicides. Agronomy. 10, 1387.

Oliveira CMG de, Monteiro AR, Blok VC. 2011. Morphological and molecular diagnostics for plant-parasitic nematodes: working together to get the identification done. Tropical Plant Pathology. 36, 65-73.

Ortiz A, Teruel JA, Espuny MJ, Marqués A, Manresa A, Aranda FJ. 2006. Effects of dirhamnolipid on the structural properties of phosphatidylcholine membranes. International Journal of Pharmaceutics. 325, 99-107.

Pang PP, Meyerowitz ME. 1987. *Arabidopsis thaliana*: a model system for plant molecular biology. Nature Biotechnology. 5, 1177-1181.

Panno S, Matić S, Tiberini A, Caruso AG, Bella P, Torta L, Stassi R, Davino AS. 2020. Loop mediated isothermal amplification: principles and applications in plant virology. Plants (Basel). 9, 461.

Perry RN, Clarke AJ. 1981. Hatching mechanisms of nematodes. Parasitology. 83, 435-449.

Perry RN, Moens M. 2011. Introduction to plant-parasitic nematodes; modes of parasitism. In: Jones J, Gheysen G, Fenoll C, eds. Genomics and Molecular Genetics of Plant-Nematode Interactions. Springer, 3-20.

Perry RN, Moens M. 2011. Survival of parasitic nematodes outside the host. In: Perry RN, Wharton DA, eds. Molecular and Physiological Basis of Nematode Survival. CAB International, 1-27.

Perry RN. 2002. Hatching. In: Lee DL, ed. The Biology of nematodes. CRC Press, 294-337.

Powell NT. 1971. Interaction of plant parasitic nematodes with other disease-causing agents. In: Zuckerman BM, Mai WF, Rohde RA, eds. Plant Parasitic Nematodes. Academic Press, 119-136.

Rich JR, Dunn RA, Noling JW. 2004. Nematicides: past and present uses. In: Chen ZX, Chen SY, Dickson DW, eds. Nematode Management and Utilization. CAB International, 1179-1200.

Riddle DL, Blumenthal T, Meyer BJ, Priess JR. 1997. Chapter 1. Introduction to *C. elegans*. IV Anatomy. In. Riddle DL, Blumenthal T, Meyer BJ, Priess JR, eds. *C. elegans* II, 2nd edition. Cold Spring Harbor Laboratory Press.

Roberts PA, Matthews Jr WC, Ehlers JD. 2005. Root-knot nematode resistant cowpea cover crops in tomato production systems. Agronomy Journal. 97, 1626-1635.

Rudrappa T, Czymmek KJ, Paré PW, Bais HP. 2008. Root-secreted malic acid recruits beneficial soil bacteria. Plant Physiology. 148, 1547-1556.

Rutherford ST, Bassler BL. 2012. Bacterial quorum sensing: its role in virulence and possibilities for its control. Cold Spring Harbor Perspectives in Medicine. 2, a012427.

Sasser JN, Freckman DW. 1987. A world perspective on nematology: the role of the society. In: Veech JA, Dickson DW, eds. Vistas on Nematology. Society of Nematologists, 7-14.

Sayre RM, Wergin WP. 1977. Bacterial parasite of a plant nematode: morphology and ultrastructure. Journal of Bacteriology. 129, 1091-1101.

Schacht H. 1859. Über einige Feinde der Rübenfelder. Zeitschrift des Vereins für die Rübenzuckerindustrie im Zollverein. 9, 175-179.

Schmidt A. 1871. Über den Rüben-Nematoden (*Heterodera schachtii* A.S.). Zeitschrift des Vereins für die Rübenzuckerindustrie im Zollverein. 21, 1-19.

Seinhorst JW. 1986. The development of individuals and populations of cyst nematodes on plants. In: Lamberti F, Taylor CE, eds. Cyst Nematodes. Springer, 101-117.

Shao H, Zhang P, Peng D, Huang W, Kong LA, Li C, Liu E, Peng H. 2023. Current advances in the identification of plant nematode diseases: from lab assays to in-field diagnostics. Frontiers in plant science. 14, 1106784.

Siddiqui IA, Haas D, Heeb S. 2005. Extracellular protease of *Pseudomonas fluorescens* CHA0, a biocontrol factor with activity against the root-knot nematode *Meloidogyne incognita*. Applied and Environmental Microbiology. 71, 5646-5649.

Siddiqui ZA, Mahmood I. 1999. Role of bacteria in the management of plant parasitic nematodes: A review. Bioresource Technology. 69, 167-179.

Sijmons CP, Grundler FMW, von Mende N, Burrows RP, Wyss U. 1991. *Arabidopsis thaliana* as a new model host for plant-parasitic nematodes. The Plant Journal. 1, 245-254.

Sotirova A, Avramova T, Stoitsova S, Lazarkevich I, Lubenets V, Karpenko E, Galabova D. 2012. The importance of rhamnolipid-biosurfactant-induced changes in bacterial membrane lipids of *Bacillus subtilis* for the antimicrobial activity of thiosulfonates. Current Microbiology. 65, 534-541.

Stadler M, Anke H, Sterner O. 1993. Linoleic acid - the nematicidal principle of several nematophagous fungi and its production in trap-forming submerged cultures. Archives of Microbiology. 160, 401-405.

Steele AE. 1965. The host range of the sugar beet nematode, *Heterodera schachtii* Schmidt. Journal of Sugarbeet Research. 13, 573-603.

Stirling GR. 2011. Biological control of plant-parasitic nematodes: an ecological perspective, a review of progress and opportunities for further research. In: Davies K, Spiegel Y, eds. Biological Control of Plant-parasitic Nematodes: Building Coherence between Microbial Ecology and Molecular Mechanisms. Springer, 1-38.

Strehmel N, Böttcher C, Schmidt S, Scheel D. 2014. Profiling of secondary metabolites in root exudates of *Arabidopsis thaliana*. Phytochemistry. 108, 35-46.

Subbotin SA, Mundo-Ocampo M, Baldwin JG. 2010. Systematics of cyst nematodes (Nematoda: Heteroderinae). In: Hunt DJ, Perry RN, eds. Nematology Monographs and Perspectives. Brill, 351.

Sukhanova AA, Boyandin AN, Ertiletskaya NL. 2022. Potato cyst nematode management strategies: current situation and promising approaches. ACS Agricultural Science and Technology. 2, 415-425

Tefft PM, Bone LW. 1985. Plant-induced hatching of eggs of the soybean cyst nematode *Heterodera glycines*. Journal of Nematology. 17, 275-279.

Terefe M, Tefera T, Sakhuja PK. 2009. Effect of a formulation of *Bacillus firmus* on root-knot nematode *Meloidogyne incognita* infestation and the growth of tomato plants in the greenhouse and nursery. Journal of Invertebrate Pathology. 100, 94-99.

Tian B, Yang J, Zhang KG. 2007. Bacteria used in the biological control of plant parasitic nematodes: populations, mechanisms of action and future prospects. FEMS Microbiology Ecology. 61, 197-213.

Turnbull GA, Morgan JA, Whipps JM, Saunders JR. 2001. The role of motility in the *in vitro* attachment of *Pseudomonas putida* PaW8 to wheat roots. FEMS Microbiology Ecology. 35, 57-65.

Tyc O, Zweers H, de Boer W, Garbeva P. 2015. Volatiles in inter-specific bacterial interactions. Frontiers in Microbiology. 6, 1412.

United States General Accounting Office. 1995. Pesticides: The phaseout of methyl bromide in the United States. GAO/RCED-96-16.

Wang KH, Hooks CR, Ploeg A. 2007. Protecting crops from nematode pests: using marigold as an alternative to chemical nematicides. University of Hawaii. Plant Disease, PD-35.

Weller DM. 1988. Biological control of soilborne plant pathogens in the rhizosphere with bacteria. Annual Review of Phytopathology. 26, 379-407.

Williamson NR, Fineran PC, Gristwood T, Chawrai SR, Leeper FJ, Salmond GP. 2007. Anticancer and immunosuppressive properties of bacterial prodiginines. Future Microbiology. 2, 605-618.

Williamson VM, Gleason CA. 2003. Plant-nematode interactions. Current Opinion in Plant Biology. 6, 327-333.

Wilson MJ, Jackson TA. 2013. Progress in the commercialisation of bionematicides. BioControl. 58, 715-722.

Wyss U, Grundler FMW. 1992. Feeding behavior of sedentary plant parasitic nematodes. Netherlands Journal of Plant Pathology. 98, 165-173.

Wyss U, Zunke U. 1986. Observations on the behavior of second stage juveniles of *Heterodera schachtii* inside host roots. Revue Nématol. 9, 153-165.

Xiong J, Zhou Q, Luo H, Xia L, Li L, Sun M, Yu Z. 2015. Systemic nematicidal activity and biocontrol efficacy of *Bacillus firmus* against the root-knot nematode *Meloidogyne incognita*. World Journal of Microbiology and Biotechnology. 31, 661-667.

Yadav S, Patil J, Kanwar RS. 2018. The role of free living nematode population in the organic matter recycling. International Journal of Current Microbiology and Applied Sciences. 7, 2726-2734.

Yao K, Peng D, Jiang C, Zhao W, Li G, Huang W, Kong L, Gao H, Zheng J, Peng H. 2021. Rapid and visual detection of *Heterodera schachtii* using recombinase polymerase amplification combined with Cas12a-mediated technology. International Journal of Molecular Sciences. 22, 12577.

Chapter 2

scientific reports

Check for updates

OPEN

Bacillus firmus I-1582 promotes plant growth and impairs infection and development of the cyst nematode *Heterodera schachtii* over two generations

Mengmeng Huang, Aylin Bulut, Bidhya Shrestha, Christiane Matera, Florian M. W. Grundler & A. Sylvia S. Schleker✉

Plant-parasitic nematodes wreak havoc on crops by root parasitism worldwide. An approach to combat nematode root parasitism is the application of antagonistic microbes like the rhizobacterium *Bacillus firmus* I-1582 which is promoted as biological control agent. Although *B. firmus* is a known nematode antagonist in general, the underlying mechanisms about its interaction with nematodes and plants have not yet been elucidated. Therefore, we explored the influence of *B. firmus* I-1582 as well as its extracellular and secreted molecules on plant–nematode interaction utilizing the plant–pathogen system *Arabidopsis thaliana–Heterodera schachtii*. We demonstrated that *B. firmus* I-1582 is attracted by *A. thaliana* root exudates, particularly by those of young plants. The bacterium colonized the root and showed a strictly pH-dependent development and plant growth promotion effect. Our results revealed that root colonization by *B. firmus* I-1582 significantly protected *A. thaliana* from infestation by the beet cyst nematode whereas dead bacterial cells or the culture supernatant were not effective. The bacterium also negatively affected nematode reproduction as well as pathogenicity and development of next generation nematodes. The obtained results highlight *B. firmus* I-1582 as a promising biocontrol agent that is well suited as an element of integrated control management strategies in sustainable agriculture.

Plant-parasitic nematodes (PPNs) cause severe losses in almost all kind of crops. PPNs mostly inhabit the soil and primarily attack underground parts of the plants. Therefore, it is often very difficult to diagnose, identify and control PPNs[1]. Nematode infestation affects plants on the one hand directly leading to growth reduction and lower crop yield, on the other hand, some PPN species are vectors of plant viruses or are associated with specific microbial root pathogens[2,3]. Over the past few decades, the most common approach of PPN management has been the application of synthetic nematicides. However, many synthetic products cause major safety concerns due to their general toxicity and their effects on non-target organisms, resulting in severe restrictions or complete banning[4]. Therefore, there is an urgent demand for the development and implementation of alternatives to control PPNs that provide effective and sustainable management while minimizing negative consequences for human health and environmental safety.

The rhizosphere is teeming with microscopic life forms including bacteria, fungi, and protozoa, thus creating possibilities of using specific organisms as biocontrol agents against soil-borne pathogens[5–7]. Among the range of soil organisms, the plant growth-promoting rhizobacteria (PGPR) were found to have promising potentials. PGPR are bacteria which have the ability to colonize the roots thereby stimulating plant growth and/or suppressing plant diseases[8,9]. For example, the application of *Pseudomonas* strains has shown the favourable effect of increasing yield of potato, sugar beet, and radish[10–12]. Certain *Bacillus* strains have also been announced to have antagonistic activity against soil-borne pathogens[6,13–15]. According to the mode of action, PGPR are divided into two groups that show either direct or indirect mechanisms. Direct contribution includes secreting phytohormones, facilitating nutrition acquisition, and producing volatile organic compounds, while indirect benefit

INRES-Department of Molecular Phytomedicine, Rheinische Friedrich-Wilhelms-University of Bonn, 53115 Bonn, Germany. ✉email: sylvia.schleker@uni-bonn.de

consists of restraining deleterious rhizosphere microorganisms through antibiosis, competition for space and nutrients, and parasitism of pathogenic agents, and/or inducing systemic resistance[16–18].

Previous studies have found that PGPR usually require efficient root surface colonization to exert their beneficial effects on plants[9,19,20]. However, to achieve successful colonization, chemotaxis of PGPR towards the root system is considered as a prerequisite[21,22]. Chemotaxis enables bacteria to sense a wide range of signals, and guides them to an appropriate environment for survival. Accumulative evidence suggests that root exudates are active in initiating and regulating this chemotactic response in the rhizosphere[23–26]. Root exudates, consisting of amino acids, organic acids (OAs), sugars, phenolics, polysaccharides, and proteins, provide nutrition for PGPR and act as signals to attract or repel microorganisms[27,28]. The composition of root exudates may vary over the course of plant development. For example, secretion of sugars from *A. thaliana* roots reaches the greatest abundance at an early development stage, while the quantity of secreted amino acids and OAs increases during development[29].

Bacillus firmus, which was first reported in 1933, is an aerobic, alkaliphilic, Gram-positive, and endospore-forming bacterium[30]. *B. firmus* has been shown to possess a great potential in promoting the growth of host plants, such as tomato, cotton, and Bermudagrass[31–33]. It has also been well characterized in a series of laboratory, greenhouse and field studies for its nematicidal property against a wide range of nematodes, such as the root-knot nematode *Meloidogyne incognita*[33–36], the soybean cyst nematode *Heterodera glycines*[37,38], the burrowing nematode *Radopholus similis*[34,39], and the stem nematode *Ditylenchus dipsaci*[34]. Greenhouse experiments demonstrated that the application of *B. firmus* on tomato plants not only efficiently reduce gall index, egg masses and final populations of *M. incognita*, but also significantly increase plant height, plant biomass, fruit number, and fruit weight[33,36,40].

The strain *Bacillus firmus* I-1582 was originally isolated from soil obtained from the central plain area in Israel. *B. firmus* I-1582 is easy to formulate and is commercially available as a seed treatment or as a wettable powder for the bio-control of PPNs[41]. The spores are able to persist durably in fields. Despite its appealing traits, the effects accomplished by *B. firmus* I-1582 is often unpredictable. The main reason for this is a lack of knowledge of the complex biology of the control system. Deeper understanding of *B. firmus* I-1582 and its overall interactions with nematodes and plants is a pre-requisite for improving biocontrol.

In the present study, we approached this by (i) examining the attractiveness of *A. thaliana* root exudates for *B. firmus* I-1582, (ii) determining the optimal pH for *B. firmus* I-1582 colonization of *A. thaliana* roots and its impact on plant development; (iii) establishing a robust ternary in vitro test system for the evaluation of nematode parasitism at *A. thaliana* in the presence of *B. firmus* I-1582. Utilizing this sophisticated agar-based gnotobiotic system enabled us to analyse the plant-promoting effect and nematode-antagonistic activity of *B. firmus* I-1582, and facilitated us to explore these interspecies interactions in detail.

Results

Chemotactic response of *B. firmus* I-1582 towards *A. thaliana* root exudates and components. To understand the initiation of root colonization by *B. firmus* I-1582, its chemotactic response to root exudates of *A. thaliana* Col-0 was investigated. It has been reported that bacteria are more motile and more strongly chemotactic in the late exponential phase[42]. Thus, we first determined *B. firmus* I-1582 development under defined growth conditions. In order to standardize the procedure, the main culture was always inoculated with a fresh overnight culture to obtain an initial OD_{600} of 0.1 (Suppl. Fig. 1). After an initial lag phase of about 2 h, the growth rate increased sharply between 2.5 and 5 h, and began to taper off until reaching stationary phase at about an OD_{600} of 3. Accordingly, the OD_{600} between 2.0 and 2.5 was determined as *B. firmus* I-1582 late exponential phase, and chemotaxis assays were performed using bacteria in this growth phase.

In order to obtain a qualitative indication whether and how effective the bacterium is attracted by root exudates, *B. firmus* I-1582 was exposed to *A. thaliana* root exudates (AREs) harvested from plants of three different developmental stages (Fig. 1a–d, Suppl. Fig. 2). The turbid ring surrounding the centre of the Petri dish indicated that bacterial cells aggregated around the concentrated AREs placed there. In contrast to the control, the size of the chemotactic ring increased with increasing volume of root exudate. Moreover, bacterial cells were attracted to all the AREs of plants from different development stages. The strongest chemotactic ring appeared when using AREs from 7-day-old plants. This qualitative test showed that *B. firmus* I-1582 is attracted by *A. thaliana* root exudates, particularly by those of young plants.

Subsequently, the chemotactic response of *B. firmus* I-1582 towards AREs freshly extracted from 7-day-old *A. thaliana* plants, and malic acid previously identified in the AREs was validated in a quantitative assay[43]. The concentrated AREs as well as DL-malic acid and L-malic acid at 50 and/or 100 µM caused a positive chemotactic response to *B. firmus* I-1582 (Fig. 1e). Thus, the capillary assay further supports the observations of the qualitative drop assay.

Establishment of a ternary in vitro test system. Since *B. firmus* I-1582 is an alkaliphilic bacterium, the pH of the surrounding environment might be a crucial factor for successful root colonization and bacterial development. Therefore, the behaviour of *B. firmus* I-1582, *H. schachtii*, and *A. thaliana* at different pH levels was studied.

We observed that attachment and development of *B. firmus* I-1582 at *A. thaliana* roots are strongly pH-dependent (Fig. 2a). Twelve days after inoculation, 1.7×10^3 CFUs and 4.4×10^3 CFUs per 1 cm root piece were detected at pH 6.4 and pH 7, respectively. Bacterial counts significantly increased by 80–90% to 2.7×10^4 and 2.0×10^4 CFUs at pH 7.5 and pH 8, respectively.

As pH has a tremendous impact on *B. firmus* development at the root, it was analysed whether parasitic success of *H. schachtii* at *A. thaliana* is influenced by the pH levels applied. It was confirmed that there was no significant difference in the average number of developed females, males, and total nematodes as well as the

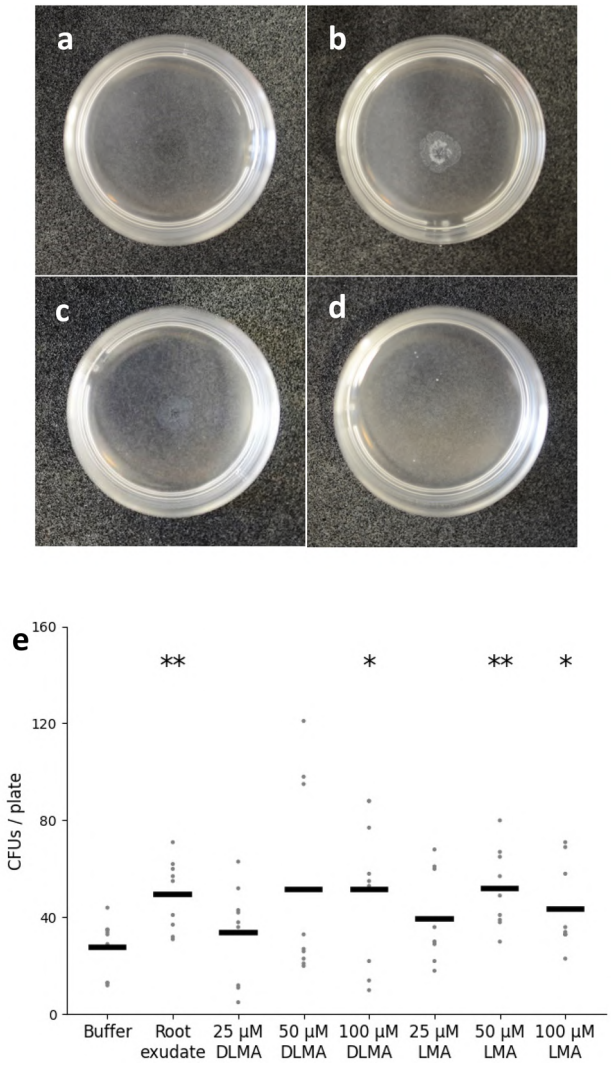

Figure 1. Chemotactic response of *Bacillus firmus* I-1582 towards *Arabidopsis thaliana* root exudates (AREs) (**a**–**e**) and organic acids (OAs) (**e**). Upper row: A drop of the test substance was placed in the centre of a 35 mm diameter Petri dish containing *B. firmus* I-1582. A turbid ring indicated the aggregation of bacteria. 10 µl of chemotaxis buffer (A); 10 µl of AREs extracted from 7- (**b**), 21- (**c**), and 28- (**d**) day-old *A. thaliana* plants. Photographs are representative examples taken after incubation for 30 s at room temperature. Bottom graph (**e**): Chemotactic response of *B. firmus* I-1582 towards AREs of 7-day-old seedlings and OAs in a capillary assay. *DLMA* DL-malic acid, *LMA* L-malic acid, *AREs A. thaliana* root exudates, *OAs* organic acids. Results are expressed as the mean ± standard error of three independent biological replicates (n = 9). Data are statistically analysed using Student's *t* test. Asterisk (*) indicate statistically significant differences compared with the control (*$p < 0.05$, **$p < 0.01$).

average size of females at the four different medium pH values (Fig. 2b and Suppl. Fig. 3). To avoid overgrowth of bacteria in the test system, the growth medium did not contain sucrose. Based on Hofmann et al.[44], limited carbohydrate supply can affect sexual differentiation leading to a reduced number of females and a shift towards male development. This can also be observed in our experiments.

Next, we investigated the impact of pH and the bacterium on plant phenotype (Fig. 3). Plants without bacterial treatment grown at different pH exhibited no differences for all aboveground and belowground parameters. Inoculation with *B. firmus* I-1582 resulted in a significant increase of shoot fresh weight at pH 7.5. The leaf number also showed an increasing trend when the root is exposed to the bacterium. All belowground parameters (root length, root surface and root tips) of the variants with bacterium at pH 7 and pH 7.5 had significantly higher values compared with the bacteria-free ones. Taken together, pH 7.5 is the optimal pH of the growth medium for testing the impact of *B. firmus* on *H. schachtii* in our gnotobiotic *A. thaliana* test system.

Impact of *B. firmus* I-1582 on *H. schachtii* parasitism at *A. thaliana*. In order to determine nematode susceptibility to *B. firmus* I-1582 and to get an indication for the mechanism, infection assays were performed in the presence of living bacterial cells (LBC), dead bacterial cells (DBC) or cell-free supernatant (CFS).

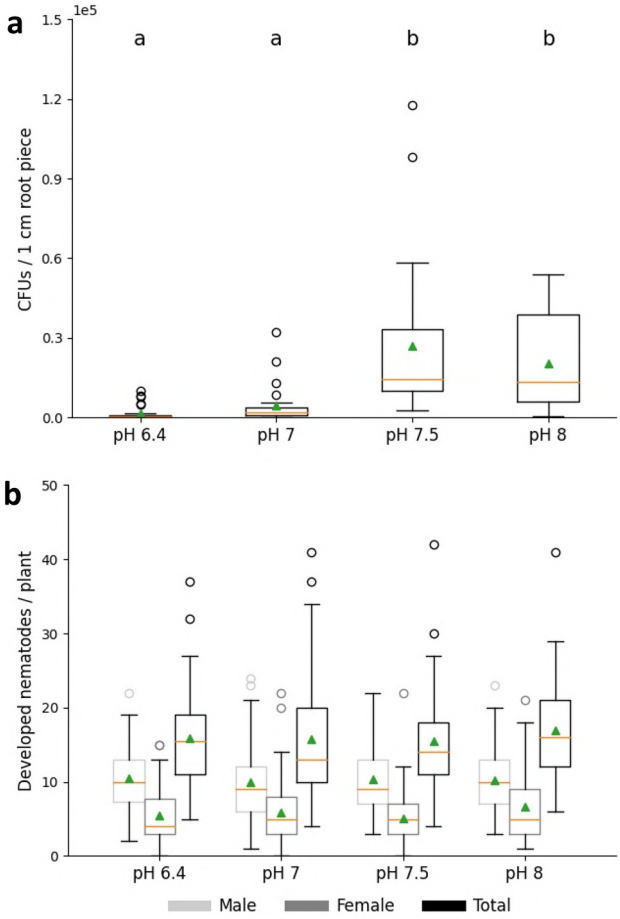

Figure 2. Impact of pH on colonization of *Bacillus firmus* I-1582 (**a**) and infection of *Heterodera schachtii* (**b**) at *Arabidopsis thaliana* roots. Results are expressed as the mean (orange line) and median (green triangle) ± standard error of three independent biological replicates [n ≥ 22 (**a**); n ≥ 50 (**b**)]. Different letters indicate statistically significant differences among treatments according to Dunn's Method ($p < 0.05$). No significant differences were observed for (**b**).

Three parameters (nematode number, female size and syncytium size) indicating the parasitic success of nematodes were evaluated. Treatment with LBC, DBC or CFS was differently efficient against *H. schachtii*. The presence of living cells caused a significant reduction of the number of developed males, females and total nematodes at 14 dpi, with an average decrease of 17.7%, 26%, and 20.6% compared with the control, respectively (Fig. 4a). Inoculation with DBC only reduced male number by 19.1%, while CFS did not have any suppressive impact on nematode parasitism (Fig. 4b,c).

In addition, we found that the direct contact of the female nematode to living bacteria is a key factor to stunt nematode development. At 28 dpi, the females surrounded by bacteria (w LBC) were significantly smaller in size (18.6%) compared with those of the control, while the females developed at the bacterium-treated plants that were not colonized by bacteria (w/o LBC) were not different in size compared with the females at the control plants (Fig. 5a). DBC and CFS treatment did not influence female development (Fig. 5b,c). None of the treatments had an impact on the female-associated feeding site (Fig. 5).

Since *B. firmus* I-1582 living cells had a considerable impact on *H. schachtii* parasitism, we decided to study nematode interaction with plant and bacteria in more detail. For this purpose, the early events after nematode inoculation were investigated. It was observed that *H. schachtii* started to invade the root at 1 dpi but penetrated at a decreased rate at 1, 2 and 3 dpi when exposed to LBC (Fig. 6a). In addition, at 3 dpi nematode size was significantly reduced in the bacteria-treated variant (13.8%) compared with the control (Fig. 6b). As expected, CFS treatment neither influenced nematode penetration nor nematode development (Fig. 6c,d).

Impact of *B. firmus* I-1582 on *H. schachtii* progeny. As *B. firmus* I-1582 living cells play a vital role in preventing nematode parasitism at *A. thaliana* roots, the influence of *B. firmus* application on the amount and infectivity of the next generation juveniles as well as their development at the host plant was investigated. Therefore, cysts from bacteria-inoculated plants were separated into two groups: those with microscopically visual attachment of bacterial (w LBC) and those obviously not in contact with bacteria (w/o LBC). Cysts from plates without bacterial inoculation served as control. Juveniles hatching from cysts of the 3 different groups

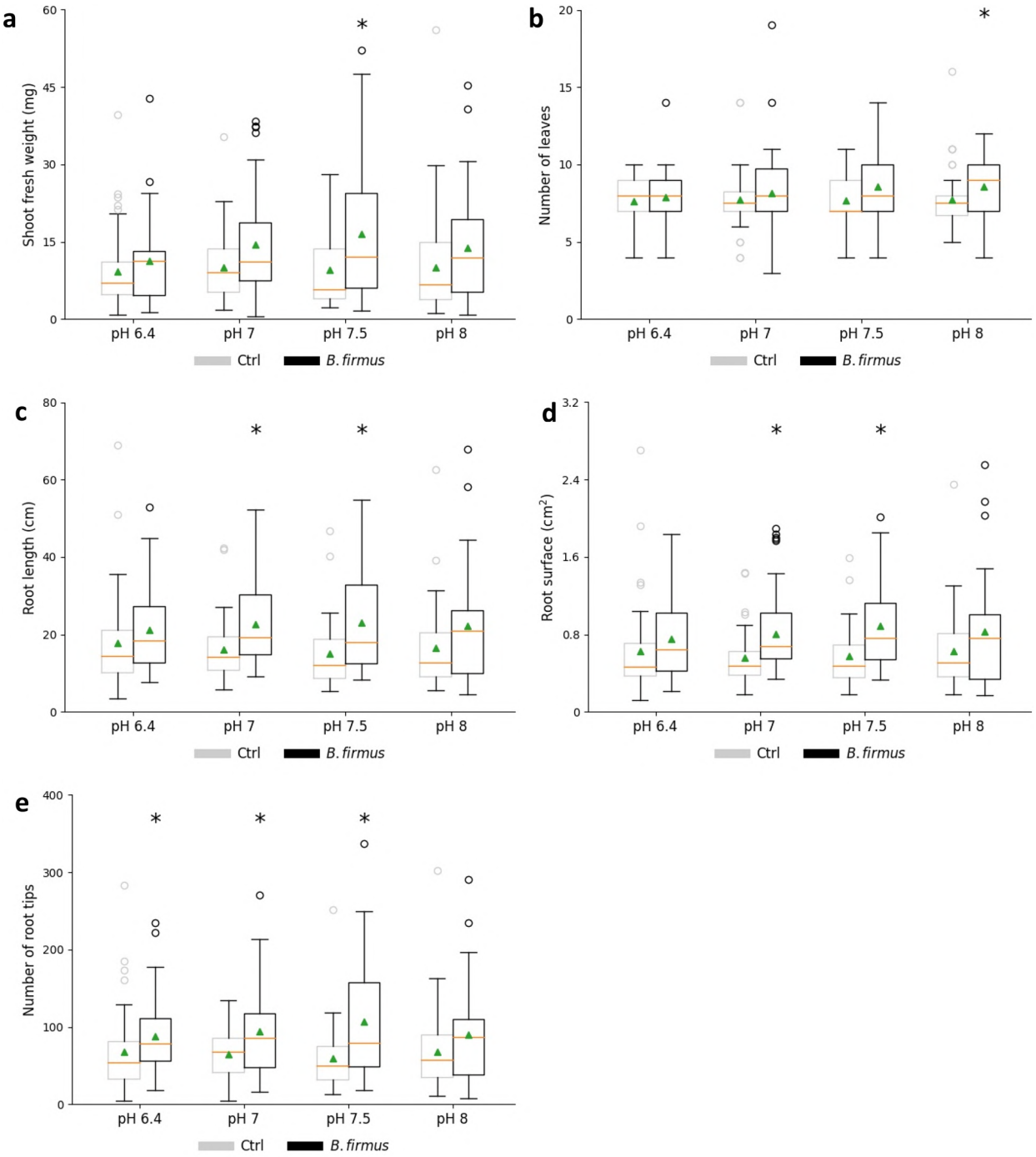

Figure 3. Impact of pH and *Bacillus firmus* I-1582 inoculation on *Arabidopsis thaliana* development. Average shoot fresh weight (**a**), average number of leaves (**b**), average total root length (**c**), average root surface (**d**), average number of root tips (**e**) per plant. Results are expressed as the mean (orange line) and median (green triangle) ± standard error of three independent biological replicates ($n \geq 31$). *Ctr* control. Data are statistically analysed using Dunn's Method. Asterisk (*) indicate statistically significant differences compared with the control ($p < 0.05$).

were used to inoculate *A. thaliana* and to investigate parasitic parameters. The cysts that developed at the end of these 2nd generation infection assays were analysed for presence of bacteria. Although the attachment of bacteria in the 'w/o LBC' group of the 1st generation cysts was not visible under the microscope, the amount of bacteria attached to the 2nd generation cysts was quantifiable (Suppl. Fig. 5). On average 8 and 5 CFUs could be determined on the 2nd generation cysts that developed from juveniles that hatched from the 1st generation cysts of the 'w LBC' group and the 'w/o LBC' group, respectively. Thus, we concluded that the two groups represent 1st

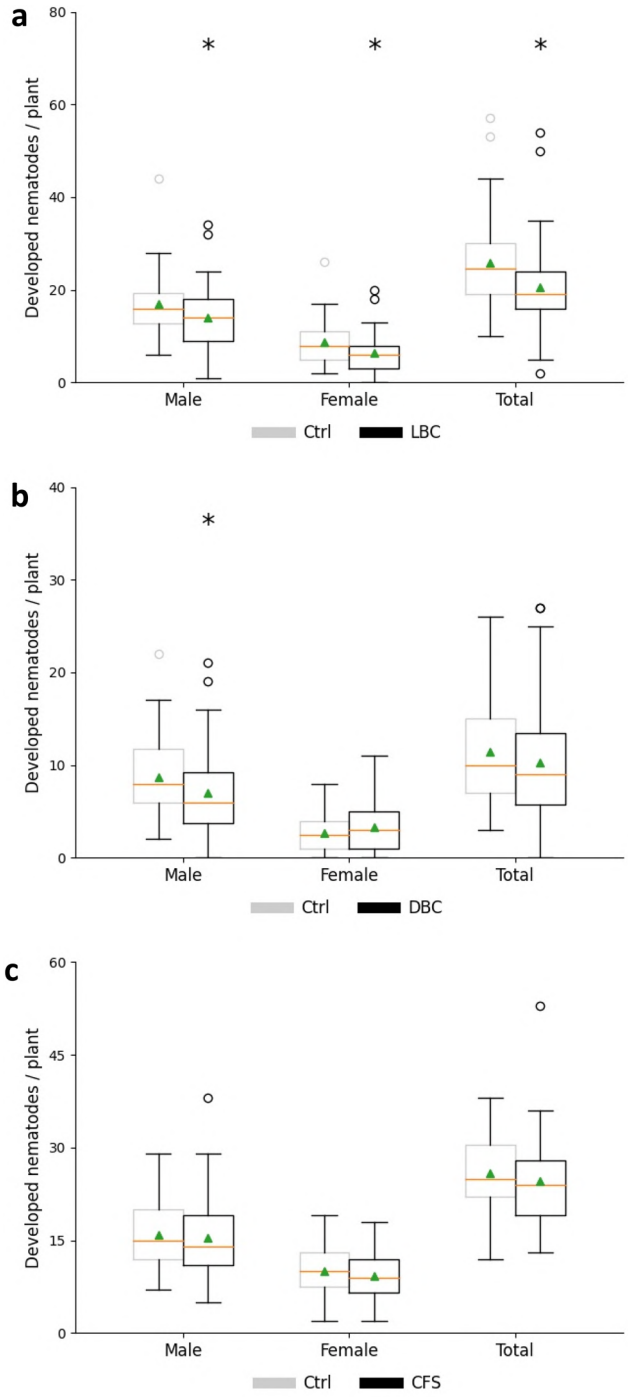

Figure 4. Infection assay of *Heterodera schachtii* at *Arabidopsis thaliana* roots. Average number of nematodes per plant at 14 dpi (days post inoculation) in the presence of LBC (**a**), DBC (**b**) or CFS (**c**). *LBC* living bacterial cells, *DBC* dead bacterial cells, *CFS* cell-free supernatant. Results are expressed as the mean (orange line) and median (green triangle) ± standard error of three independent biological replicates ($n \geq 40$). Data are statistically analysed using Dunn's Method. Asterisk (*) indicate statistically significant differences compared with the control ($p < 0.05$).

generation cysts with a different bacterial load and are subsequently referred to as 'w hLBC' (with high number of LBC) and 'w lLBC' (with low number of LBC).

Egg counts revealed that *B. firmus* reduced the number of offspring. First generation cysts of the 'w lLBC' group harboured a significantly lower number of offspring in comparison to those of the untreated control. The average egg numbers of cysts of the 'w hLBC' group was considerably lower compared with the control though

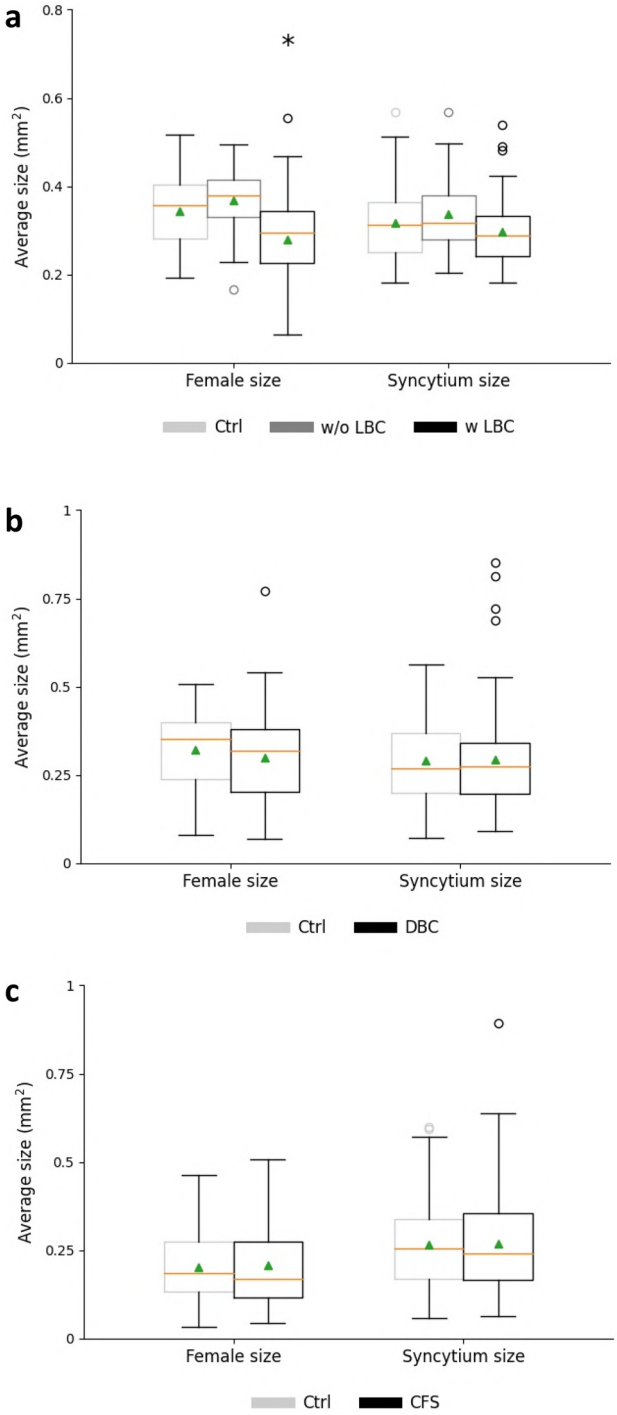

Figure 5. Development of *Heterodera schachtii* at *Arabidopsis thaliana* roots. Average size of female and syncytium at 28 dpi (days post inoculation) in the presence of LBC (**a**), DBC (**b**) or CFS (**c**). *LBC* living bacterial cells, *DBC* dead bacterial cells, *CFS* cell-free supernatant. Results are expressed as the mean (orange line) and median (green triangle) ± standard error of three independent biological replicates ($n \geq 53$). Data are statistically analysed using Dunn's Method. Asterisk (*) indicate statistically significant differences compared with the control ($p < 0.05$).

not significantly different to the control or the 'w lLBC' group (Fig. 7). The CFS treatment had no influence on nematode reproduction (Suppl. Fig. 6).

The virulence of hatched juveniles from control cysts and those with bacterial colonization was assessed by evaluating nematode invasion, infection and reproduction. As illustrated in Fig. 8 A, nematode penetration

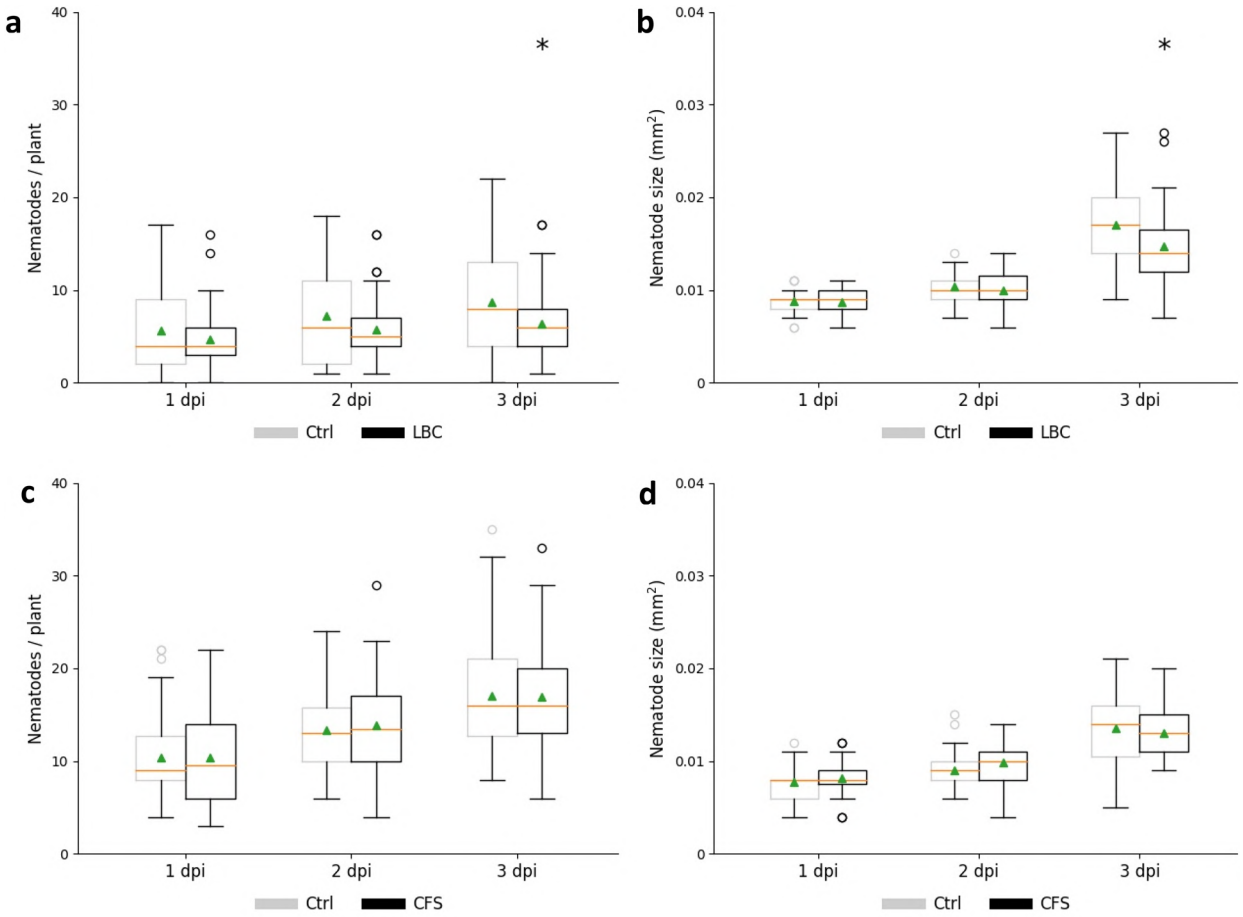

Figure 6. Invasion assay of *Heterodera schachtii* at *Arabidopsis thaliana* roots. Average number of nematodes per plant in the presence of LBC (**a**) or CFS (**c**); Average size of nematodes in the presence of LBC (**b**) or CFS (**d**). *LBC* living bacterial cells, *CFS* cell-free supernatant, *dpi* days post inoculation. Results are expressed as the mean (orange line) and median (green triangle) ± standard error of three independent biological replicates ($n \geq 37$). Data are statistically analysed using Dunn's or Holm–Sidak Method. Asterisk (*) indicate statistically significant differences compared with the control ($p < 0.05$).

number (at 1 dpi) and adult number (at 14 dpi) were significantly decreased by 25.5% and 17.8%, respectively for the 'w lLBC' variant, while higher bacterial load caused a larger reduction of nematode invasion and establishment by 43.4% and 31.5%, respectively. The development of females and syncytia was also significantly suppressed by high (17.7% and 26.4%, respectively) or low (11.5% and 13%, respectively) bacterial amounts on the cysts of the previous generation (Fig. 8b). Second generation cysts originating from juveniles of the 'w lLBC' and the 'w hLBC' 1st generation cyst groups contained significantly fewer eggs compared with those of the untreated control group, with a reduction of 24.7% and 32.2%, respectively (Fig. 8c).

Discussion

PGPR are commercially applied for biofertilization, phytoremediation, phytostimulation or biocontrol of soil-borne plant diseases[17]. Gaining insights into the interaction between plant and PGPR will contribute to improve effective application of these organisms in agriculture. Here, *B. firmus* I-1582 is investigated for its associations with *A. thaliana* and its efficiency to combat *H. schachtii* over 2 nematode generations.

Successful colonization of the root system by PGPR is an important factor for effective biological control[45]. Prior to root colonization, chemotaxis of PGPR towards root exudates is regarded to be a "sine qua non"[21]. Zhang et al.[46] reported that *Bacillus subtilis* N11 was able to colonize banana root and prevent fungal infection by forming biofilms along the root. Subsequently, it was proved that the tested strain, isolated from banana rhizosphere, showed a stronger chemotactic response towards banana root exudates than to cucumber root exudates[47]. We observed that *B. firmus* I-1582 is attracted by AREs from differently aged *A. thaliana* plants. GC–MS analysis pointed out that AREs released from early development stage contain high level of sugars[29]. A high level of available carbon sources might be an explanation why we observe the strongest chemotactic response of *B. firmus* I-1582 to AREs extracted from young plants. During aging plants release a higher proportion of amino acids and phenolics resulting in a higher antimicrobial activity[48]. In fact, our data confirmed that the accumulation of bacterial cells was lowered by using AREs from older plants. Besides, an attraction assay was carried out utilizing AREs and two OAs. Result indicated that the chemotactic mobility of *B. firmus* I-1582 to DL-malic acid and

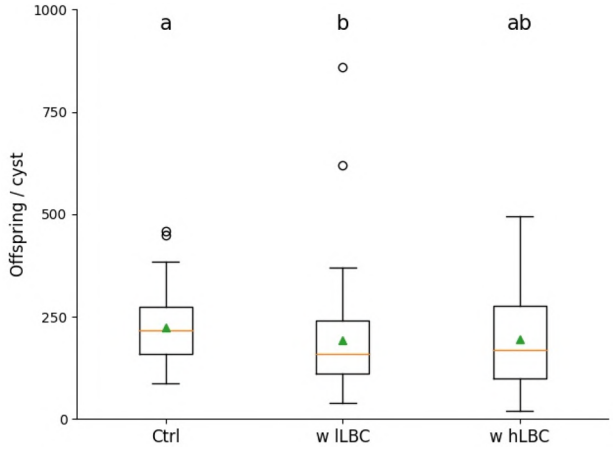

Figure 7. Reproduction assay of *Heterodera schachtii* at *Arabidopsis thaliana* roots. Average number of eggs and juveniles per cyst at 35 dpi in the presence of LBC. *w hLBC* with high number of living bacterial cells, *w lLBC* with low number of living bacterial cells. Results are expressed as the mean (orange line) and median (green triangle) ± standard error of three independent biological replicates ($n \geq 49$). Different letters indicate statistically significant differences among treatments according to Dunn's Method ($p < 0.05$).

L-malic acid were comparable to AREs. DL-Malic acid and L-malic acid are known to effectively recruit *B. subtilis* and stimulate biofilm formation of *B. subtilis* via a KinD-Spo0A pathway[43,49]. Based on our study, malic acid from AREs in fact seems to play an essential role in the chemoattraction of *B. firmus* I-1582.

Plenty of evidence demonstrated the antagonistic action of *B. firmus* species towards plant-parasitic nematodes. However, there is only little information about its interaction with and morphological impact on host plants. Consequently, the role bacteria–plant interaction plays in combating nematode infestation is not well studied but is essential as it may help us understand the interplay of the three organisms: the host plant, *B. firmus* and PPNs. Since *Bacillus* species are alkaliphiles[50], we expected that colonization of *B. firmus* I-1582 at *A. thaliana* roots is pH-dependent. In fact, propagation of *B. firmus* I-1582 was remarkably enhanced in plant-growth medium at pH 7.5 and 8. In accordance, the tested strain also had a positive impact on the growth of *A. thaliana* in a pH-dependent manner. Shoot weight was significantly increased at pH 7.5. The belowground biometrical parameters of *A. thaliana* significantly increased after inoculation with *B. firmus* I-1582 in our axenic system at pH 7 and 7.5. In particular, attention should be payed to the expansion of the root system mirrored by the total root length, the root surface area and the number of root tips. An increase in root surface area indicates an increase of root hair formation. Root hairs facilitate plants in nutrient uptake and microbe interactions[51].

PGPR can promote plant growth by biosynthesis of phytohormones[52]. Indole-3-acetic acid (IAA) secreted by *Bacillus amyloliquefaciens* UCMB5113 has been reported for its ability to induce *A. thaliana* plant cell division, and stimulate the development of lateral roots and root hairs[53]. Some other *Bacillus* strains, such as *Bacillus cereus*, *Bacillus flexus*, *Bacillus licheniformis*, *Bacillus megaterium*, *B. subtilis*, and *Bacillus thuringiensis*, were also able to synthesize IAA and could be considered as possible growth promoters of plant[54–57]. In addition, the increase of aboveground parameters of treated plants could be attributed to volatile organic compounds (VOCs) produced by PGPR strains[18]. The extracted bacterial volatiles from two *Bacillus* strains, *B. subtilis* GB03, *B. amyloliquefaciens* IN937a, significantly increase total leaf surface area of *A. thaliana*[58]. 2,3-Butanediol, a bacterial compound detected from volatile blends by GC analysis, was found to be released from both *Bacillus* strains and involved in the cytokinin-signaling pathway to activate plant growth. Regarding the biometrical response of *A. thaliana* seedlings, *B. firmus* I-1582 most probably impacts plant growth by releasing IAA and/or VOCs.

In our study, we validated that *H. schachtii* is susceptible to the presence of LBC as the bacterium significantly reduced the number of developed females and males, female size, and reproduction. Additionally, we proved that the LBC protects the host plant from J2 invasion and interferes with the nematodes' development at the early sedentary phase. In contrast, the CFS as well as the DBC was not effective. Possible explanations for the observed characteristics are as follows.

(a) Microscopic observations during the reported study showed that the bacterium colonizes the root system building layers of bacterial cells along the root. This is in accordance with a recent study documenting *B. firmus* biofilm formation and colonization of tomato and cucumber roots[59]. Thus, it might be that the bacterium constitutes a physical barrier protecting the plant from nematode invasion.
(b) Generally, PPNs locate their preferred host by perceiving root exudate signals[60]. Strigolactones, which are a class of phytohormones exuded by Arabidopsis roots, were proven to play an active role in host attraction during beet cyst nematode parasitism[61]. Moreover, AREs were demonstrated to stimulate stylet thrusting of PPNs[62,63]. Simultaneously, root exudates also act as an attractant to and/or a rich source of nutrients for rhizobacteria[64,65]. Thus, it might be that the presence of *B. firmus* changes composition of root ARE in a way that roots become less attractive to the nematodes thus leading to a lower number of infection events.

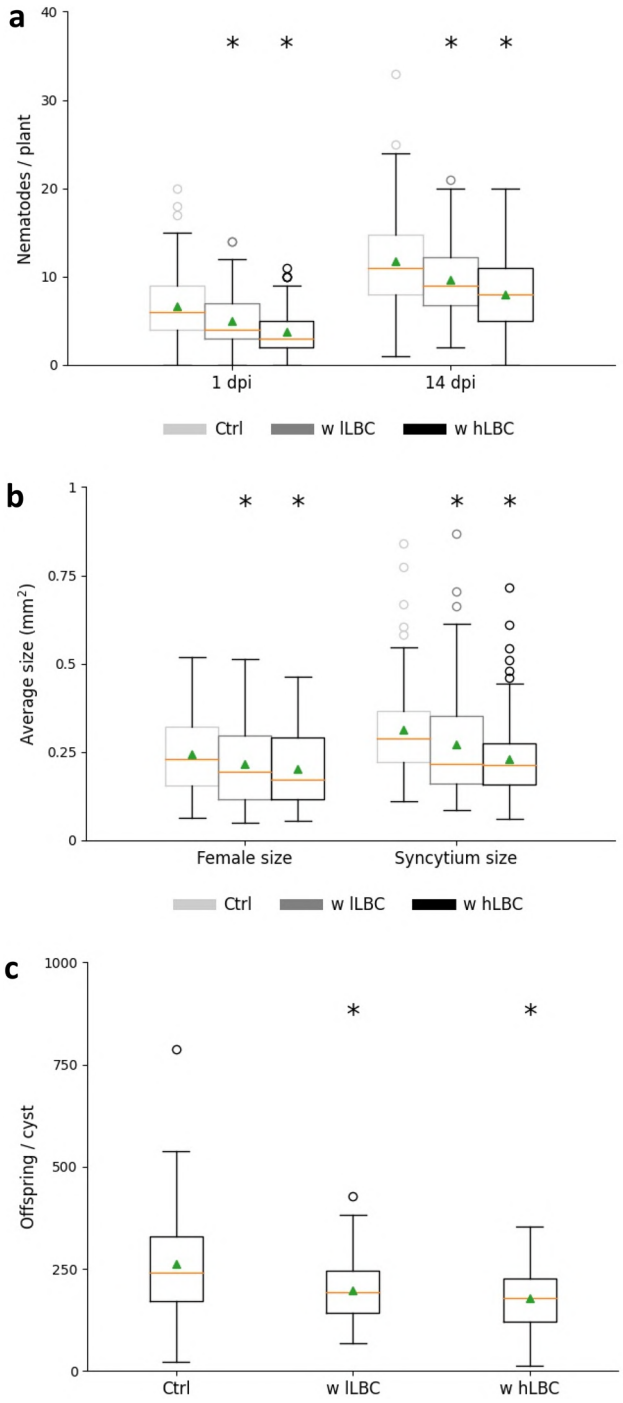

Figure 8. *Arabidopsis thaliana* root parasitism of *Heterodera schachtii* 2nd generation nematodes originating from *Bacillus firmus* colonized cysts. Average number of nematodes per plant at 1 dpi and 14 dpi (**a**); Average size of female and syncytium at 28 dpi (**b**); Average number of eggs and juveniles per cyst at 35 dpi (**c**). *w hLBC* with high number of living bacterial cells; *w lLBC* with low number of living bacterial cells; *dpi* days post inoculation Results are expressed as the mean (orange line) and median (green triangle) ± standard error of three independent biological replicates ($n \geq 97$). Data are statistically analysed using Dunn's Method. Asterisk (*) indicate statistically significant differences compared with the control ($p < 0.05$).

(c) *Bacillus sphaericus* strain B43 was shown to stimulate induced systemic resistance against potato cyst nematode *Globodera pallida* juveniles in a split-root-trial[66]. *B. firmus* I-1582 is reported to induce systemic resistance in tomato active against *M. incognita* but not in cucumber[58]. Moreover, *Bacillus pumilus* T4 was capable to induce resistance in transgenic NahG Arabidopsis against two *Pseudomonas syringae* strains by

activating SA-independent pathway[67]. Therefore, one possibility is that *B. firmus* I-1582 elicits plant defence responses effective against *H. schachtii*.

(d) There is a possibility that molecules secreted by *B. firmus* I-1582 are directly antagonistic against PPNs. According to Geng et al.[68], *B. firmus* DS-1 isolated from marine sediment of the coast of the South China Sea has toxicity against *M. incognita* and *H. glycines*. They unravelled that a novel nematicidal virulence factor, Serine Protease 1 (Sep1), plays a role in nematode control by its serine protease activity. Sep1 was shown to target and degrade intestinal and cuticular proteins of *M. incognita*. In our study, we observed that CFS is not effective in inhibiting *H. schachtii* parasitism. Therefore, it is possible that the concentration of putative molecules involved in the nematicidal activity is too low in the CFS or/and that these virulence factors are secreted upon contact with the nematode.

(e) Based on our finding, virulence of the 2nd generation nematodes towards the host plant was decreased after exposure of 1st generation females to *B. firmus* I-1582 living cells. Since there are no bacteria established at the root, invasion of the 2nd generation juveniles cannot be influenced by a bacterial barrier along the roots or behavioural changes due to an altered root exudate composition. Thus, *B. firmus* I-1582 might reduce fitness of the 2nd generation juveniles before they hatch or bacterial attachment to the 2nd generation J2s directly influences the nematodes' virulence. Alternatively/additionally, the J2-attached bacteria could trigger plant defence responses effective against the nematode.

Studies usually only consider the impact of an agent on one generation of nematodes on the host. However, *H. schachtii*—like other PPNs—has several generations within one vegetation period. Additionally, the juveniles remain viable inside the cysts for several years ready to hatch once the soil reaches appropriate temperature and moisture, and a suitable host plant is present. Therefore, we also examined the impact of *B. firmus* I-1582 living cells on the virulence of *H. schachtii* progeny inside the bacteria-colonized cysts. Intriguingly, J2s hatching from these cysts were significantly impaired in their development and reproduction at the host plant. The bacterial load of the developing 2nd generation cysts was with an average of about 8 CFU per cyst fairly low. Our results demonstrate that a single root application of *B. firmus* I-1582 not only reduces the plant's infestation with the attacking nematode and the nematode's reproduction but is also efficient in suppressing infection, development, and reproduction of the emerging 2nd nematode generation on a new host plant that was not treated with *B. firmus* I-1582 before. Future studies will reveal how strong the effects of *B. firmus* I-1582 against *H. schachtii* that we observed in our controlled in vitro studies will be in pot and field experiments. In conclusion, *B. firmus* I-1582 is a biological nematode control agent with high potential and sustainability that can be worth to integrate in PPN management strategies.

Materials and methods

Bacterial strain and culture conditions. *B. firmus* I-1582 was obtained from Bayer AG, Monheim and routinely stored in Tryptic soy broth (TSB) with 25% glycerol at − 80 °C. The strain was grown at 28 °C in liquid TSB with an overnight orbital shaking at 200 rpm. The main culture was inoculated with the overnight culture to obtain an initial optical density at 600 nm (OD_{600}) of 0.1. The main culture was grown at 28 °C at 200 rpm for different time periods depending on the subsequent applications.

Plant material and growth conditions. *A. thaliana* Columbia (Col-0) seeds were first surface-sterilized in 0.7% sodium hypochlorite for 5 min, then submerged in 70% ethanol for 1 min, and finally rinsed with sterile distilled water 5 times. Subsequently, the seeds were dried at room temperature for 4 h and stored at 4 °C until use. Surface-sterilized seeds were germinated in either normal Knop medium at pH 6.4 or modified Knop medium as described in the relevant sections, and kept in a climate chamber under a red/blue light with a 16-h/8-h light/dark photoperiod at 24 °C[69].

All experiments involving plants were performed with *A. thaliana* Col-0. *Sinapis alba* was used for nematode propagation. All local, national or international guidelines and legislation were adhered to in the study.

Nematode preparation. Approximately 300 cysts of *H. schachtii* were harvested from mustard (*Sinapis alba*) roots grown aseptically, and submerged with sterile 3 mM $ZnCl_2$ in the Baermann funnel. After 7 days, the freshly hatched second-stage juveniles (J2s) were collected for subsequent analyses[61].

Chemotactic response of *B. firmus* I-1582 towards *A. thaliana* root exudates. *Bacteria preparation.* The OD_{600} of the main culture was measured every 30 min in triplicate to determine the growth rate of *B. firmus* I-1582 strain. Bacterial cells which reached the late exponential growth phase (OD_{600} of 2.0–2.5) were harvested by centrifugation [Eppendorf, Germany] at 4000 rpm for 10 min, washed with chemotaxis buffer (100 mM potassium phosphate [pH 7.0], 20 µM EDTA), and re-suspended in 16 ml of chemotaxis solution (12 ml of chemotaxis buffer and 4 ml of 1% hydroxypropylmethylcellulose). The resulting cell suspension was applied to two chemotaxis assays immediately after preparation.

Root exudates collection. AREs were collected from 7-, 21-, and 28-day-old seedlings. Seedlings were washed with sterile water, and incubated in sterile water for 3 days with orbital shaking at 100 rpm in a climate chamber under a red/blue light with a 16-h/8-h light/dark photoperiod at 24 °C. The collected AREs were filtrated through a 0.2 µm pore size syringe filter, and concentrated by lyophilisation [Thermo Scientific, USA] at − 104 °C until the volume reduced to 0.5 ml. The resulting AREs were stored at − 80 °C until further analyses.

Chemotaxis assays. The chemotactic response of *B. firmus* I-1582 towards the chemo-attractants (AREs and individual exudate components) was qualitatively examined by drop assay and quantitatively evaluated by capillary assay.

In the drop assay, the concentrated AREs (10 µl and 20 µl), which were collected from different development stages (7-, 21-, and 28-day), were dropped into the centre of a 35-mm-diameter Petri dish which contained 2 ml of bacterial cell suspension. A ring of turbidity near the centre of each petri dish would appear after 30 s of incubation at room temperature, if the chemotactic response of bacterial cells was triggered. Chemotaxis solution alone served as control. Each treatment was performed in triplicate.

In the capillary assay, a sealed disposable 200 µl pipette tip was used as the chemotaxis chamber for loading 100 µl of bacterial cell suspension. A disposable needle was used as the chemotaxis capillary and was attached to a 1 ml tuberculin syringe [B. Braun, Germany]. The needle-syringe capillary was filled with 100 µl of concentrated AREs of 7-day-old seedlings, or one of the two tested malic acid (DL-malic acid and L-malic acid), and tightly fitted into the sealed tips containing bacterial cell suspension. After 1 h of incubation at 28 °C, the content from each syringe was diluted 1000 times with liquid TSB and then plated onto TSA plates (3 plates for each chemo-attractant). The colony-forming units (CFUs) were determined by first plating on TSA plates and then incubated at 28 °C for 48 h. Chemotaxis solution alone served as control. Each treatment was performed in triplicate.

Establishment of an in vitro agar system to investigate the interaction of *B. firmus* I-1582, *A. thaliana*, and *H. schachtii* at different pH levels. *B. firmus I-1582 colonization at A. thaliana roots.* Colonization by *B. firmus* I-1582 at *A. thaliana* roots was performed in a modified in vitro agar system as described below. First, 90-mm-diameter Petri dishes were filled with Knop medium (− sucrose) with pH 6.4, 7, 7.5 or 8, and then two droplets of Knop medium (+ sucrose) with pH 6.4 were added. Two sterilized *A. thaliana* seeds were placed on the sucrose-containing Knop droplets. The whole agar system was held at an angle of 60° to facilitate surface growth of the roots, and cultivated as described above. At 8 days post seeding, each seedling was inoculated with 10 µl of bacterial suspension ($OD_{600} = 0.1$) prepared from the 3-day-old bacterial culture. Seedlings inoculated with TSB alone served as control. After colonization for 12 days, a 1 cm root piece below the bacterial inoculation point was removed from the main roots and shaken vigorously in 1 ml of sterile water. A serial dilution of the suspension was plated on TSA. The CFUs were determined after incubating the plates for 48 h at 28 °C. Each treatment was performed in triplicate.

A. thaliana development colonized by B. firmus I-1582 living cells. 10 µl of bacterial suspension ($OD_{600} = 0.1$) was inoculated to 8-day-old seedlings grown at pH 6.4, 7, 7.5 or 8 as described above. Seedlings inoculated with TSB alone served as control. After colonization for 12 days, aboveground-related parameters (shoot fresh weight and leaf number) were evaluated, underground-related parameters (root length, root surface and root tips) were measured using Epson Perfection V700 Photo scanner [Epson, Japan] equipped with WinRHIZO software. Each treatment was performed in triplicate.

Impact of *B. firmus* I-1582 on *H. schachtii* parasitism at *A. thaliana*. *Living bacterial cells (LBC), dead bacterial cells (DBC) and cell-free supernatant (CFS) preparation.* To investigate the impact of *B. firmus* I-1582 on *H. schachtii* parasitism at *A. thaliana*, LBC, DBC, and CFS were applied separately. The main culture was cultivated at 28 °C for 72 h. LBC were pelleted by centrifugation at 4000 rpm for 10 min, washed by sterile water, and re-suspended in 50% TSB by adjusting OD_{600} to 0.1. DBC were subsequently produced by autoclaving at 121 °C for 20 min at 1.2×10^5 Pa pressure. Bacterial supernatant was withdrawn and filtrated through a 0.2 µm filter. LBC, DBC and CFS were used freshly after preparation. As *B. firmus* is a spore-forming bacterium and as we only wanted to work with vegetative cells, we analysed whether spores could be found in the LBC preparation. Therefore, the cells were incubated at 80 °C for 10 min, a condition which spores survive but vegetative cells not. The heated cells and fresh LBC were spread onto TSA and incubated for 72 h at 28 °C. No colonies developed on the heated variant thus proving that the culture contains vegetative cells only.

Nematode infection and invasion assays. *A. thaliana* was grown on sucrose-free Knop plates with sucrose-containing Knop (pH 6.4) droplets as described above. At 8 days post seeding, each seedling was inoculated with 10 µl of prepared living cells or dead cells suspension ($OD_{600} = 0.1$). Seedlings inoculated with 50% TSB served as control. At 20 days post seeding, each plant was inoculated with 60–70 surface-sterilized *H. schachtii* J2s.

For the in vitro test system treated with CFS, two seeds were grown on the upper half plate filled with sucrose-containing Knop (pH 6.4). The plate was held at an angle of 60° and cultivated as described above. At 8 days post seeding, the CFS mixed with Knop medium was applied to the lower half plate. TSB mixed with Knop medium served as control. At 14 days post seeding, each plant was inoculated with 60–70 surface-sterilized *H. schachtii* J2s.

The infection assay was carried out to analyse nematode parasitism at *A. thaliana* plant by counting the number of males and females at 14 day-post-inoculation (dpi) under a Stereo Microscope [Leica, Germany], and measuring the size of female and syncytium at 28 dpi under a digital Stereo Microscope [Leica, Germany] equipped with Leica Application Suite (LAS) software. Each treatment was performed in triplicate.

Nematode invasion was quantified by evaluating the number and size of nematodes at 1, 2, and 3 dpi to examine the penetration ability of nematodes and their early development. Each treatment was performed in triplicate.

Impact of *B. firmus* I-1582 on *H. schachtii* progeny at *A. thaliana*. To investigate the effect of *B. firmus* I-1582 on *H. schachtii* progeny, two assays were performed by using analogous experiment with LBC and TSB control as described above. First, cysts were collected at 35 dpi in 3 groups:

(a) 'Ctrl': cysts without bacteria colonization from TSB control plates,
(b) 'w/o LBC': cysts where colonization with *B. firmus* I-1582 is not visible under a microscope, and
(c) 'w LBC': cysts where colonization with *B. firmus* I-1582 is visible under a microscope.

The number of eggs of cysts of these 3 separate groups was evaluated for each individual plant. Each treatment was performed in triplicate.

In the second assay, the parasitism of juveniles that hatched from cysts of the described 3 groups was determined by inoculating *A. thaliana*. Therefore, cysts were collected separately at 84 dpi and incubated in 3 mM $ZnCl_2$. After 7 days, 60–70 freshly hatched juveniles were inoculated to each 20-day-old plant. The invasion assay, infection assay, and reproduction assay were assessed at 1 dpi, at 14 dpi and 28 dpi, and at 35 dpi, respectively. Each treatment was performed in triplicate.

Statistical analysis. All data are expressed as mean and median ± standard error (SE). Statistical analysis was performed by using Student's *t*-test ($p < 0.05$ and $p < 0.01$) or one-way analysis of variance (ANOVA) ($p < 0.05$).

Data availability

All data generated or analysed during this study are included in this published article and the supplementary material. More details are available from the corresponding author on reasonable request.

Received: 5 March 2021; Accepted: 25 June 2021
Published online: 08 July 2021

References

1. Stirling, G. R., Nicol, J. & Reay, F. *Advisory Services for Nematode Pests* (Rural Industries Research and Development Cooperation, 1999).
2. Lucas, G. B., Campbell, C. L. & Lucas, L. T. *Causes of Plant Diseases in Introduction to Plant Diseases: Identification and Management* 9–14 (Springer, 1992).
3. Worner, S. P., Venette, R. C., Braithwaite, M. & Dobesberger, E. The importance of core biological disciplines in plant biosecurity. In *The Handbook of Plant Biosecurity: Principles and Practices for the Identification, Containment and Control of Organisms that Threaten Agriculture and the Environment Globally* (eds Gordh, G. & McKirdy, S.) 73–117 (Springer Netherlands, 2014).
4. Nico, A. I., Jiménez-Díaz, R. M. & Castillo, P. Control of root-knot nematodes by composted agro-industrial wastes in potting mixtures. *Crop Prot.* **23**, 581–587. https://doi.org/10.1016/j.cropro.2003.11.005 (2004).
5. Handelsman, J. & Stabb, E. V. Biocontrol of soilborne plant pathogens. *Plant Cell* **8**, 1855–1869. https://doi.org/10.1105/tpc.8.10.1855 (1996).
6. Koeberl, M. *et al. Bacillus* and *Streptomyces* were selected as broad-spectrum antagonists against soilborne pathogens from arid areas in Egypt. *FEMS Microbiol. Lett.* **342**, 168–178. https://doi.org/10.1111/1574-6968.12089 (2013).
7. Raaijmakers, J. M., Paulitz, T. C., Steinberg, C., Alabouvette, C. & Moënne-Loccoz, Y. The rhizosphere: A playground and battlefield for soilborne pathogens and beneficial microorganisms. *Plant Soil* **321**, 341–361. https://doi.org/10.1007/s11104-008-9568-6 (2008).
8. Kloepper, J. W. Plant growth-promoting rhizobacteria on radishes. In *Proceedings of the 4th International Conference on Plant Pathogenic Bacteria, Station de Pathologie Vegetale et Phytobacteriologie. INRA, Angers, France, 1978*, Vol. 2, 879–882 (1978).
9. Weller, D. M. Biological control of soilborne plant pathogens in the rhizosphere with bacteria. *Annu. Rev. Phytopathol.* **26**, 379–407. https://doi.org/10.1146/annurev.py.26.090188.002115 (1988).
10. Kloepper, J. W., Schroth, M. N. & Miller, T. D. Effects of rhizosphere colonization by plant growth-promoting Rhizobacteria [*Pseudomonas* spp.] on potato plant development and yield. *Phytopathology* **70**, 1078–1082 (1980).
11. Schroth, M. N. & Hancock, J. G. Disease-suppressive soil and root-colonizing bacteria. *Science* **216**, 1376–1381. https://doi.org/10.1126/science.216.4553.1376 (1982).
12. Suslow, T. V. & Schroth, M. N. Rhizobacteria of sugarbeets: Effects of seed application and root colonization on yield [Fungal and bacterial phytopathogens]. *Phytopathology* **72**, 199–206 (1982).
13. Broadbent, P., Baker, K. F. & Waterworth, Y. Bacteria and actinomycetes antagonistic to fungal root pathogens in Australian soils. *Aust. J. Biol. Sci.* **24**, 925–944. https://doi.org/10.1071/bi9710925 (1971).
14. Yuan, J. *et al.* Production of bacillomycin- and macrolactin-type antibiotics by *Bacillus amyloliquefaciens* NJN-6 for suppressing soilborne plant pathogens. *J. Agric. Food Chem.* **60**, 2976–2981. https://doi.org/10.1021/jf204868z (2012).
15. Yuen, G. Y., Schroth, M. N. & McCain, A. H. Reduction of Fusarium wilt of carnation with suppressive soils and antagonistic bacteria. *Plant Dis.* **69**, 1071–1075 (1985).
16. Glick, B. R. Plant growth-promoting bacteria: Mechanisms and applications. *Scientifica (Cairo)* **963401**, 2012. https://doi.org/10.6064/2012/963401 (2012).
17. Lugtenberg, B. & Kamilova, F. Plant-growth-promoting rhizobacteria. *Annu. Rev. Microbiol.* **63**, 541–556. https://doi.org/10.1146/annurev.micro.62.081307.162918 (2009).
18. Podile, A. R. & Kishore, G. K. Plant growth-promoting rhizobacteria. In *Plant-Associated Bacteria* (ed. Gnanamanickam, S. S.) 195–230 (Springer Netherlands, 2006).
19. Bull, C. T., Weller, D. M. & Thomashow, L. S. Relationship between root colonization and suppression of *Gaeumannomyces graminis* var. *tritici* by *Pseudomonas fluorescens* strain 2-79. *Phytopathology* **81**, 954–959. https://doi.org/10.1094/Phyto-81-954 (1991).
20. Chin-A-Woeng, T. F., Bloemberg, G. V., Mulders, I. H., Dekkers, L. C. & Lugtenberg, B. J. Root colonization by phenazine-1-carboxamide-producing bacterium *Pseudomonas chlororaphis* PCL1391 is essential for biocontrol of tomato foot and root rot. *Mol. Plant Microbe Interact.* **13**, 1340–1345. https://doi.org/10.1094/MPMI.2000.13.12.1340 (2000).
21. Sood, G. S. Chemotactic response of plant-growth-promoting bacteria towards roots of vesicular-arbuscular mycorrhizal tomato plants. *FEMS Microbiol. Ecol.* **45**, 219–227. https://doi.org/10.1016/s0168-6496(03)00155-7 (2003).
22. Turnbull, G. A., Morgan, J. A., Whipps, J. M. & Saunders, J. R. The role of motility in the in vitro attachment of *Pseudomonas putida* PaW8 to wheat roots. *FEMS Microbiol. Ecol.* **35**, 57–65. https://doi.org/10.1111/j.1574-6941.2001.tb00788.x (2001).
23. Bacilio-Jiménez, M. *et al.* Chemical characterization of root exudates from rice (*Oryza sativa*) and their effects on the chemotactic response of endophytic bacteria. *Plant Soil* **249**, 271–277. https://doi.org/10.1023/A:1022888900465 (2003).
24. Bais, H. P., Park, S. W., Weir, T. L., Callaway, R. M. & Vivanco, J. M. How plants communicate using the underground information superhighway. *Trends Plant Sci.* **9**, 26–32. https://doi.org/10.1016/j.tplants.2003.11.008 (2004).

25. de Weert, S. *et al.* Flagella-driven chemotaxis towards exudate components is an important trait for tomato root colonization by *Pseudomonas fluorescens*. *Mol. Plant Microbe Interact.* **15**, 1173–1180. https://doi.org/10.1094/MPMI.2002.15.11.1173 (2002).
26. Zheng, X. Y. & Sinclair, J. B. Chemotactic response of *Bacillus megaterium* strain B153-2-2 to soybean root and seed exudates. *Physiol. Mol. Plant Pathol.* **48**, 21–35. https://doi.org/10.1006/pmpp.1996.0003 (1996).
27. Badri, D. V. & Vivanco, J. M. Regulation and function of root exudates. *Plant Cell Environ.* **32**, 666–681. https://doi.org/10.1111/j.1365-3040.2008.01926.x (2009).
28. Bais, H. P., Weir, T. L., Perry, L. G., Gilroy, S. & Vivanco, J. M. The role of root exudates in rhizosphere interactions with plants and other organisms. *Annu. Rev. Plant Biol.* **57**, 233–266. https://doi.org/10.1146/annurev.arplant.57.032905.105159 (2006).
29. Chaparro, J. M. *et al.* Root exudation of phytochemicals in *Arabidopsis* follows specific patterns that are developmentally programmed and correlate with soil microbial functions. *PLoS One* **8**, e55731. https://doi.org/10.1371/journal.pone.0055731 (2013).
30. Werner, W. E. G. Botanische Beschreibung häufiger am Buttersäureabbau beteiligter sporenbildender Bakterienspezies. *Zentralblatt Bakteriol. Parasitenkd. Infekt. Hyg.* **87**, 446–475 (1933).
31. Castillo, J. D., Lawrence, K. S. & Kloepper, J. W. Biocontrol of the reniform nematode by *Bacillus firmus* GB-126 and *Paecilomyces lilacinus* 251 on Cotton. *Plant Dis.* **97**, 967–976. https://doi.org/10.1094/PDIS-10-12-0978-RE (2013).
32. Crow, W. T. Effects of a commercial formulation of *Bacillus firmus* I-1582 on golf course bermudagrass infested with *Belonolaimus longicaudatus*. *J. Nematol.* **46**, 331–335 (2014).
33. Terefe, M., Tefera, T. & Sakhuja, P. K. Effect of a formulation of Bacillus firmus on root-knot nematode *Meloidogyne incognita* infestation and the growth of tomato plants in the greenhouse and nursery. *J. Invertebr. Pathol.* **100**, 94–99. https://doi.org/10.1016/j.jip.2008.11.004 (2009).
34. Mendoza, A. R., Kiewnick, S. & Sikora, R. A. In vitro activity of *Bacillus firmus* against the burrowing nematode *Radopholus similis*, the root-knot nematode *Meloidogyne incognita* and the stem nematode *Ditylenchus dipsaci*. *Biocontrol Sci. Technol.* **18**, 377–389. https://doi.org/10.1080/09583150801952143 (2008).
35. Xiang, N. *et al.* Biological control of *Meloidogyne incognita* by spore-forming plant growth-promoting rhizobacteria on cotton. *Plant Dis.* **101**, 774–784. https://doi.org/10.1094/PDIS-09-16-1369-RE (2017).
36. Xiong, J. *et al.* Systemic nematicidal activity and biocontrol efficacy of *Bacillus firmus* against the root-knot nematode *Meloidogyne incognita*. *World J. Microbiol. Biotechnol.* **31**, 661–667. https://doi.org/10.1007/s11274-015-1820-7 (2015).
37. Schrimsher, D. W. The studies of plant host resistance to the reniform nematode in upland cotton and the effects of *Bacillus firmus* GB-126 on plant-parasitic nematodes. *Master thesis, Auburn University* (2013).
38. Xiang, N., Lawrence, K. S., Kloepper, J. W., Donald, P. A. & McInroy, J. A. Biological control of *Heterodera glycines* by spore-forming plant growth-promoting rhizobacteria (PGPR) on soybean. *PLoS One* **12**, e0181201. https://doi.org/10.1371/journal.pone.0181201 (2017).
39. Mendoza, A. R. & Sikora, R. A. Biological control of *Radopholus similis* in banana by combined application of the mutualistic endophyte *Fusarium oxysporum* strain 162, the egg pathogen *Paecilomyces lilacinus* strain 251 and the antagonistic bacteria *Bacillus firmus*. *Biocontrol* **54**, 263–272. https://doi.org/10.1007/s10526-008-9181-x (2009).
40. d'Errico, G. *et al.* Integrated management strategies of *Meloidogyne incognita* and *Pseudopyrenochaeta lycopersici* on tomato using a *Bacillus firmus*-based product and two synthetic nematicides in two consecutive crop cycles in greenhouse. *Crop Prot.* **122**, 159–164. https://doi.org/10.1016/j.cropro.2019.05.004 (2019).
41. Wilson, M. J. & Jackson, T. A. Progress in the commercialisation of bionematicides. *Biocontrol* **58**, 715–722. https://doi.org/10.1007/s10526-013-9511-5 (2013).
42. Makinoshima, H. *et al.* Growth phase-coupled alterations in cell structure and function of *Escherichia coli*. *J. Bacteriol.* **185**, 1338–1345. https://doi.org/10.1128/jb.185.4.1338-1345.2003 (2003).
43. Rudrappa, T., Czymmek, K. J., Pare, P. W. & Bais, H. P. Root-secreted malic acid recruits beneficial soil bacteria. *Plant Physiol.* **148**, 1547–1556. https://doi.org/10.1104/pp.108.127613 (2008).
44. Hofmann, J., Wieczorek, K., Blöchl, A. & Grundler, F. M. W. Sucrose supply to nematode-induced syncytia depends on the apoplasmic and symplasmic pathways. *J. Exp. Bot.* **58**, 1591–1601. https://doi.org/10.1093/jxb/erl285 (2007).
45. Lugtenberg, B. J., Dekkers, L. & Bloemberg, G. V. Molecular determinants of rhizosphere colonization by *Pseudomonas*. *Annu. Rev. Phytopathol.* **39**, 461–490. https://doi.org/10.1146/annurev.phyto.39.1.461 (2001).
46. Zhang, N. *et al.* A new bioorganic fertilizer can effectively control banana wilt by strong colonization with *Bacillus subtilis* N11. *Plant Soil* **344**, 87–97. https://doi.org/10.1007/s11104-011-0729-7 (2011).
47. Zhang, N. *et al.* Effects of different plant root exudates and their organic acid components on chemotaxis, biofilm formation and colonization by beneficial rhizosphere-associated bacterial strains. *Plant Soil* **374**, 689–700. https://doi.org/10.1007/s11104-013-1915-6 (2014).
48. Chaparro, J. M., Badri, D. V. & Vivanco, J. M. Rhizosphere microbiome assemblage is affected by plant development. *ISME J.* **8**, 790–803. https://doi.org/10.1038/ismej.2013.196 (2014).
49. Chen, Y. *et al.* A *Bacillus subtilis* sensor kinase involved in triggering biofilm formation on the roots of tomato plants. *Mol. Microbiol.* **85**, 418–430. https://doi.org/10.1111/j.1365-2958.2012.08109.x (2012).
50. Fritze, D., Flossdorf, J. & Claus, D. Taxonomy of alkaliphilic *Bacillus* strains. *Int. J. Syst. Bacteriol.* **40**, 92–97. https://doi.org/10.1099/00207713-40-1-92 (1990).
51. Grierson, C. & Schiefelbein, J. Root hairs. *Arabidopsis Book* **1**, e0060. https://doi.org/10.1199/tab.0060 (2002).
52. Idris, E. E., Iglesias, D. J., Talon, M. & Borriss, R. Tryptophan-dependent production of indole-3-acetic acid (IAA) affects level of plant growth promotion by *Bacillus amyloliquefaciens* FZB42. *Mol. Plant Microbe Interact.* **20**, 619–626. https://doi.org/10.1094/MPMI-20-6-0619 (2007).
53. Asari, S. *et al.* Analysis of plant growth-promoting properties of *Bacillus amyloliquefaciens* UCMB5113 using *Arabidopsis thaliana* as host plant. *Planta* **245**, 15–30. https://doi.org/10.1007/s00425-016-2580-9 (2017).
54. Ahmed, A. & Hasnain, S. Auxin-producing *Bacillus* sp.: Auxin quantification and effect on the growth of *Solanum tuberosum*. *Pure Appl. Chem.* **82**, 313–319. https://doi.org/10.1351/PAC-CON-09-02-06 (2010).
55. Chagas Junior, A. F. *et al.* Production of indole-3-acetic acid by bacillus isolated from different soils. *Bulg. J. Agric. Sci.* **21**, 282–287 (2015).
56. Lim, J.-H. & Kim, S.-D. Synergistic plant growth promotion by the indigenous auxins-producing PGPR *Bacillus subtilis* AH18 and *Bacillus licheniforims* K11. *J. Korean Soc. Appl. Biol. Chem.* **52**, 531–538. https://doi.org/10.3839/jksabc.2009.090 (2009).
57. Xu, L., Xu, W., Jiang, Y., Hu, F. & Li, H. Effects of interactions of auxin-producing bacteria and bacterial-feeding nematodes on regulation of peanut growths. *PLoS One* **10**, e0124361. https://doi.org/10.1371/journal.pone.0124361 (2015).
58. Ryu, C. M. *et al.* Bacterial volatiles promote growth in *Arabidopsis*. *Proc. Natl. Acad. Sci. U.S.A.* **100**, 4927–4932. https://doi.org/10.1073/pnas.0730845100 (2003).
59. Ghahremani, Z. *et al.* *Bacillus firmus* strain I-1582, a nematode antagonist by itself and through the plant. *Front. Plant Sci.* **11**, 796. https://doi.org/10.3389/fpls.2020.00796 (2020).
60. Bird, D. M. Signaling between nematodes and plants. *Curr. Opin. Plant Biol.* **7**, 372–376. https://doi.org/10.1016/j.pbi.2004.05.005 (2004).
61. Escudero Martinez, C. M. *et al.* Distinct roles for strigolactones in cyst nematode parasitism of *Arabidopsis* roots. *Eur. J. Plant Pathol.* **154**, 129–140. https://doi.org/10.1007/s10658-019-01691-5 (2019).

62. Grundler, F., Schnibbe, L. & Wyss, U. *In vitro* studies on the behaviour of second-stage juveniles of *Heterodera schachtii* (Nematoda: Heteroderidae) in response to host plant root exudates. *Parasitology* **103**, 149–155. https://doi.org/10.1017/s0031182000059394 (1991).
63. Teillet, A. *et al.* Transcriptional changes of the root-knot nematode *Meloidogyne incognita* in response to *Arabidopsis thaliana* root signals. *PLoS One* **8**, e61259. https://doi.org/10.1371/journal.pone.0061259 (2013).
64. Haichar, F. Z., Santaella, C., Heulin, T. & Achouak, W. Root exudates mediated interactions belowground. *Soil Biol. Biochem.* **77**, 69–80. https://doi.org/10.1016/j.soilbio.2014.06.017 (2014).
65. Sasse, J., Martinoia, E. & Northen, T. Feed your friends: Do plant exudates shape the root microbiome?. *Trends Plant Sci.* **23**, 25–41. https://doi.org/10.1016/j.tplants.2017.09.003 (2018).
66. Hasky-Gunther, K., Hoffmann-Hergarten, S. & Sikora, R. A. Resistance against the potato cyst nematode *Globodera pallida* systemically induced by the rhizobacteria *Agrobacterium radiobacter* (G12) and *Bacillus sphaericus* (B43). *Fundam. Appl. Nematol.* **21**, 511–517 (1998).
67. Ryu, C.-M., Hu, C.-H., Reddy, M. S. & Kloepper, J. W. Different signaling pathways of induced resistance by rhizobacteria in *Arabidopsis thaliana* against two pathovars of *Pseudomonas syringae*. *New Phytol.* **160**, 413–420. https://doi.org/10.1046/j.1469-8137.2003.00883.x (2003).
68. Geng, C. *et al.* A novel serine protease, Sep1, from *Bacillus firmus* DS-1 has nematicidal activity and degrades multiple intestinal-associated nematode proteins. *Sci. Rep.* **6**, 25012. https://doi.org/10.1038/srep25012 (2016).
69. Sijmons, P. C., Grundler, F. M. W., von Mende, N., Burrows, P. R. & Wyss, U. *Arabidopsis thaliana* as a new model host for plant-parasitic nematodes. *Plant J.* **1**, 245–254. https://doi.org/10.1111/j.1365-313X.1991.00245.x (1991).

Acknowledgements

We thank Ute Schlee for excellent technical and experimental support.

Author contributions

A.S.S.S. and F.M.W.G. conceived the research concept and designed the study; M.H., A.B., B.S., and C.M. performed the experiments; M.H., A.B., B.S., C.M., F.M.W.G., and A.S.S.S. interpreted the results; M.H. and A.S.S.S. analysed the data and wrote the manuscript; all authors reviewed and approved the manuscript.

Funding

Open Access funding enabled and organized by Projekt DEAL. The study was partially financed by Bayer AG, Monheim, Germany. The company had no influence on the experimental work and the collection, analysis, and interpretation of data.

Competing interests

The authors declare no competing interests.

Additional information

Supplementary Information The online version contains supplementary material available at https://doi.org/10.1038/s41598-021-93567-0.

Correspondence and requests for materials should be addressed to A.S.S.S.

Reprints and permissions information is available at www.nature.com/reprints.

Publisher's note Springer Nature remains neutral with regard to jurisdictional claims in published maps and institutional affiliations.

Chapter 3

Small molecules contribute to the nematicidal activity of *Bacillus firmus* in a temperature-dependent manner

Mengmeng Huang, Volkan Cevik, Florian M. W. Grundler, A. Sylvia S. Schleker*

INRES-Department of Molecular Phytomedicine, Rheinische Friedrich-Wilhelms-University of Bonn, 53115 Bonn, Germany

*Correspondence: A. Sylvia S. Schleker, sylvia.schleker@uni-bonn.de

Manuscript in preparation

Abstract

Plant-parasitic nematodes cause considerable yield losses and pose a significant economic burden on agriculture. Historically, synthetic chemicals have been the method of choice for combating these soil-borne pests. However, concerns on human health and environmental safety lead to the demand for developing biocontrol strategies. The use of beneficial rhizobacteria that have antagonistic effects on nematodes is one of the promising approaches. The aim of this study was to explore the nematicidal potential of compounds produced by *Bacillus firmus* I-1582. We observed that the nematicidal activity of cell-free supernatant from *B. firmus* I-1582 is highly temperature-dependent. The active compounds have a molecular weight below 3 kDa and are resistant to heat and partially sensitive to proteolytic enzymes. Towards shedding light on these molecules, we sequenced the genome of *B. firmus* I-1582 and employed genome-mining tools leading to the identification of a lanthipeptide gene cluster coding for three putative lanthipeptides. Gene expression analysis further confirmed that these putative lanthipeptides are upregulated in *B. firmus* I-1582. In conclusion, *in vitro* and *in silico* analyses provided evidence that lanthipeptides secreted by *B. firmus* I-1582 might contribute to the bacterium's nematicidal activity under specific temperature conditions. Our study suggests that small molecules identified from *B. firmus* I-1582 could serve as potential active ingredients for the development of novel nematode control agents.

Introduction

Plant-parasitic nematodes (PPN) wreak havoc on crops through root parasitism and cause serious economic damage worldwide. On the one hand, they directly reduce crop growth and lower crop yield. On the other hand, many of them vector plant viruses or other root pathogens subsequently (Powell, 1971). Since nematodes are microscopic and subterranean, it is very difficult to diagnose, identify, and control them in fields. Depending on the region, old-generation synthetic nematicides are still used to manage PPN. However, they target a wide range of non-target organisms and cause a threat to humans and the environment. The discovery of eco-friendly nematicidal products is an area of intensive investigations. The rhizosphere is teeming with microorganisms, which creates possibilities to use these beneficial species and their metabolites as biological control agents (BCA) or bio-based means against nematodes (Migunova & Sasanelli, 2021). The plant growth-promoting rhizobacteria (PGPR), including *Agrobacterium* spp., *Arthrobacter* spp., *Azospirillum* spp., *Azotobacter* spp., *Bacillus* spp., *Chromobacterium* spp., *Clostridium* spp., *Corynebacterium* spp., *Desulfovibrio* spp., *Pasteuria* spp., *Serratia* spp., and Streptomyces spp., were reported for their biocontrol potential in field application (Weller, 1988).

Over the past few decades, a plethora of natural products (NP) including microbial secondary metabolites have been employed in agriculture, medicine, and food industry (Firn, 2010). Unlike primary metabolites, which participate in growth, development and reproduction of the microorganisms, the microbial NP are associated with ecological functions, and inter- and intraspecies interactions (Sanchez et al., 2012). Although the majority of NP originates from a few common biosynthetic pathways, the resulting intermediates tailored by numerous enzyme-catalyzed reactions lead to products with various chemical structures. Based on their biosynthetic origins, NP are classified as alkaloids, terpenoids, polyketides (PK), non-ribosomal peptides (NRP), and ribosomally-synthesized and post-translationally modified peptides (RiPP) (Clardy & Walsh, 2004; Kloosterman, 2020). The microbial-derived NP exhibits diverse biological activities, such as exerting antibiotic, antifungal, antitumor, anti-inflammatory, immunosuppressive, and anti-parasitic effects (Demain, 1983; Sanchez et al., 2012).

A variety of strategies have been recommended for the discovery of microbial NP since the 1940s. The conventional approach to explore NP involves the isolation and identification of potential producers with subsequent detection and characterization of active compounds. However, this procedure suffers from a high rediscovery rate and often a low production rate in the natural producer (Scherlach & Hertweck, 2009; Katz & Baltz, 2016). Alternative solutions nowadays utilize genetically engineered microbes to facilitate the synthesis of target compounds and potent derivatives (Pham et al., 2019). In the early 2000s, advances in genomics, transcriptomics, proteomics, and metabolomics elicited new interests in NP discovery and development. In fact, many microorganisms were found to harbour biosynthetic gene clusters (BGC) encoding specialized NP that remain silent under standard laboratory conditions. Such silent gene loci are referred to as “cryptic” pathways for NP biosynthesis. To obtain potential bioactive NP from underexplored resources, the investigation of microbial metabolomes is in demand (Rutledge & Challis, 2015). The application of genome-based tools makes these resources accessible. For example, the genome-mining strategy combined with bioinformatics tools is utilized to prioritize the relevant BGC from genomes/metagenomes, predict the structures of their chemical products, and optimize cluster expression in native or heterologous hosts for the production of cognate NP (Zhang et al., 2017).

In nature, microbial NP can serve as virulence factors in mediating pathogenic interactions among different organisms. Understanding the cryptic metabolome secreted by microorganisms enables scientists to not only gain insights into pathogenicity mechanisms, but also create new possibilities for disease control (Scherlach & Hertweck, 2021). For example, lanthipeptides, which are first synthesized by ribosomes as linear precursor peptides and subsequently undergo post-translational modifications (PTM), display potent antimicrobial activity against a broad range of pathogens, in particular certain antibiotic-resistant strains (Zhao & Kuipers, 2021). A very well-known lanthipeptide is nisin, which has been widely used as a safe food preservative for nearly 70 years (Hirsch, 1951). Previous studies found that nisin has a dual mode-of-action for its antimicrobial activity. Nisin can block cell wall biosynthesis on the one hand, and facilitate pore formation in the cytoplasmic membrane by binding to the pyrophosphate moiety of lipid II - an essential

bactoprenol-bound cell wall precursor – on the other hand (Brötz et al., 1998; Wiedemann et al., 2001; Hsu et al., 2004).

The genus *Bacillus* consists of a large number of aerobic Gram-positive bacteria, which are capable of forming endospores persisting durably under unfavourable environmental conditions. They are attractive industrial microorganisms for the production of diverse NP, such as enzymes, antibiotics, insecticides, bacteriocins, and biosurfactants (Perez et al., 2017). Using genome-mining prediction tools, a multitude of novel putative antimicrobial compounds from Bacillales species have been identified and characterized. These active NP include peptides that are either NRP (e.g. lipopeptides) or RiPP (e.g. lanthipeptides), as well as non-peptidic compounds such as PK (Zhao & Kuipers, 2016). Among the genus *Bacillus*, the rhizobacterium *Bacillus firmus* has been shown to be a promising BCA and has a great potential in PPN management (Mendoza et al., 2008; Terefe et al., 2009; Xiang et al., 2017; Huang et al., 2021). Based on bioinformatics investigations the mode-of-action of *B. firmus* against PPN was concluded to be related to the production of putative secondary metabolites and/or virulence factors (Geng et al., 2016; Susič et al., 2020). In the present study, we integrate wet lab experimental data with *in silico* genomic analyses with the aim to further contribute to deciphering the mode-of-action of *B. firmus* against sugar beet cyst nematode *Heterodera schachtii*. This interdisciplinary approach enabled us to uncover potentially novel NP secreted by *B. firmus* I-1582, and facilitates a deeper mechanistic understanding of the bacterium's nematicidal activity.

Materials and Methods

Bacterial strain

B. firmus strain I-1582 was obtained from Bayer AG, Monheim. 0.1 g of spore powder of *B. firmus* I-1582 was homogenized in 100 ml of 0.1 % TWEEN 20 and heat-inactivated at 80 °C in a water bath for 10 minutes. The homogeneous solution was serial diluted and spread onto Tryptic soy agar (TSA). After 72-hour-incubation at 28 °C, colonies were used for further assays.

Preparation of *B. firmus* I-1582 inoculum

Bacterial colonies formed on TSA plate were picked and cultivated in Tryptic soy broth (TSB) with an overnight orbital shaking at 200 rpm at 28 °C. The optical density at 600 nm (OD_{600}) of the overnight culture was determined by a NanoDrop 2000c spectrophotometer [Thermo Fisher Scientific, USA]. The overnight culture was adjusted to an initial OD_{600} of 0.1 by TSB with a total volume of 30 ml and grown in 300 ml Erlenmeyer flask with orbital shaking at 200 rpm at 28 °C for 72 hours. Then the 72-hour-old bacterial culture was centrifuged at 4000 rpm at 4 °C for 10 minutes to harvest bacterial cells and supernatant. Cell suspension (CS) was obtained by suspending bacterial cells in 30 ml of TSB. Cell-free supernatant (CFS) was obtained by passing the supernatant through a 0.2 µm pore size syringe filter [Sarstedt, Germany]. The prepared CS and CFS were freshly used in the liquid lethality assay.

Preparation of *H. schachtii* inoculum

H. schachtii was routinely maintained in the Department of Molecular Phytomedicine, University of Bonn. Cysts of *H. schachtii* were harvested from mustard (*Sinapsis alaba*) roots, and submerged with sterile 3 mM $ZnCl_2$ in the Baermann funnel at room temperature. The hatched second-stage juveniles (J2) were obtained after 120 hours and freshly used in the liquid lethality assay.

Determination of temperature-dependent nematicidal activity

In order to determine the temperature-dependent nematicidal efficacy, an *in vitro* liquid lethality assay of *B. firmus* I-1582 against *H. schachtii* J2 was set up in a 96-well microtiter

plate. Approximately 30 nematodes were added into each single well with a volume of 50 µl of the tested CS or CFS. TSB served as control. A minimum of three replications were set for each treatment. The plate was covered with gas-permeable sealing film and incubated at 22 °C, 27 °C, 32 °C, and 37 °C, respectively. After 72-h-incubation, 20 µl of 1 M NaOH was applied to distinguish between live/mobile and dead/immobile nematodes (Schleker et al., 2023). The number of live and dead J2 was recorded under an inverted microscope [Leica, Germany], and the mortality was calculated according to Mortality (%) = number of dead J2 / [(number of live J2 + number of dead J2)] x 100. This assay was performed in three biological replications.

Determination of sensitivity of nematicidal compounds to heat and proteolytic enzymes

The sensitivity of nematicidal compounds secreted by *B. firmus* I-1582 towards heat and proteinase K were tested. To evaluate thermo-stability, CFS was incubated for 30 minutes at 99 °C in a ThermoMixer [Eppendorf, Germany]. To analyse enzyme sensitivity, CFS was incubated with 0.1 volume of proteinase K (20 mg/ml) at 37 °C for 2 hours and subsequently at 99 °C for 30 minutes to terminate enzymatic activity. 50 µl of heat-treated or proteinase K-treated CFS was employed to perform a liquid lethality assay as described above. TSB served as control. This assay was performed in three biological replications.

Estimation of molecular weight of nematicidal compounds and its sensitivity to proteolytic enzymes

To estimate the molecular weight (MW) of CFS and its sensitivity to two proteolytic enzymes, CFS was dialyzed through an Amicon® Ultrafiltration Membrane [Merck, Germany] with a molecular weight cut-off (MWCO) of 3 KDa. The retentate fraction (> 3 KDa) and filtrate fraction (< 3 KDa) were subsequently treated with 0.1 volume of proteinase K (20 mg/ml) or pronase (20 mg/ml). 50 µl of CFS > 3 kDa or CFS < 3 kDa treated with two proteases was employed to perform a liquid lethality assay as described above. Tap water and TSB served as parallel controls. This assay was performed in three biological replications.

Genomic DNA extraction and purification

B. firmus I-1582 was cultivated in TSB at 28 °C with orbital shaking until it reached the exponential growth phase. Total genomic DNA was isolated using NucleoSpin® Microbial

DNA Kit [MACHEREY-NAGEL, Germany] and purified using NucleoSpin® Plasmid Clean-up Kit [MACHEREY-NAGEL, Germany] according to the manufacturer's instructions. The integrity of extracted DNA was determined on a 0.8% agarose gel electrophoresis, while the purity and concentration of the received DNA were estimated by a NanoDrop2000c spectrophotometer.

Genome sequencing, assembly and annotation

The sequence capture library was sequenced via Genome Sequencer Illumina HiSeq on a NovaSeq 6000 S2 [Illumina, USA]. The raw sequencing datasets were trimmed with Trimmomatic (v0.39). The sequence reads were mapped to a reference genome from NCBI (Whole Genome Shotgun accession number: VDEM01) using Burrows-Wheeler Aligner (BWA v0.7.17) with default parameters and BWA-MEM algorithm (Li, 2013). All reference genomic sequences were collected from NCBI (September 2020; WGS accession numbers: apvl: GCF_000565285.1, bcuy: GCF_001591465.1, jabvdd: GCF_013345775.1, ldwq: GCF_001038755.1, qnsf: GCF_003315495.1, uftc: GCF_900445365.1, vdem: GCF_009849605.1). BWA-MEM mapper had default settings of penalty 4 for a mismatch, gap open penalties 6, and 6 for deletion/insertion. The mapping efficiency depends on the accuracy of the reference genome and the quality of sequence reads. The variant calling (SNP, Insertion, and Deletion calling) and subsequent building of a consensus sequence is done using BCFtools (v1.9) (Danecek et al., 2021). An alternative genome was built using the tool GFinisher (v1.4) (Guizelini et al., 2016). To get the best results, our sequence reads were mapped against all six available *B. firmus* reference genomes obtained from NCBI and a consensus genome sequence was created using BCFtools. The subsequently created consensus genomes were used as alternative assembly for GFinisher. In our last step we used Mauve (v2.4.0) with algorithm progressiveMauve (Darling et al., 2010) to reorganize the contigs in our newly generated genome (Fig. 1). The resulting final genome sequence of *B. firmus* I-1582 (July 2021) was used for further analysis. The quality of the reference-based assembled genome was assessed using the Benchmarking Universal Single-Copy Orthologs (BUSCO) tool (v.5.2.2) (Manni et al., 2021).

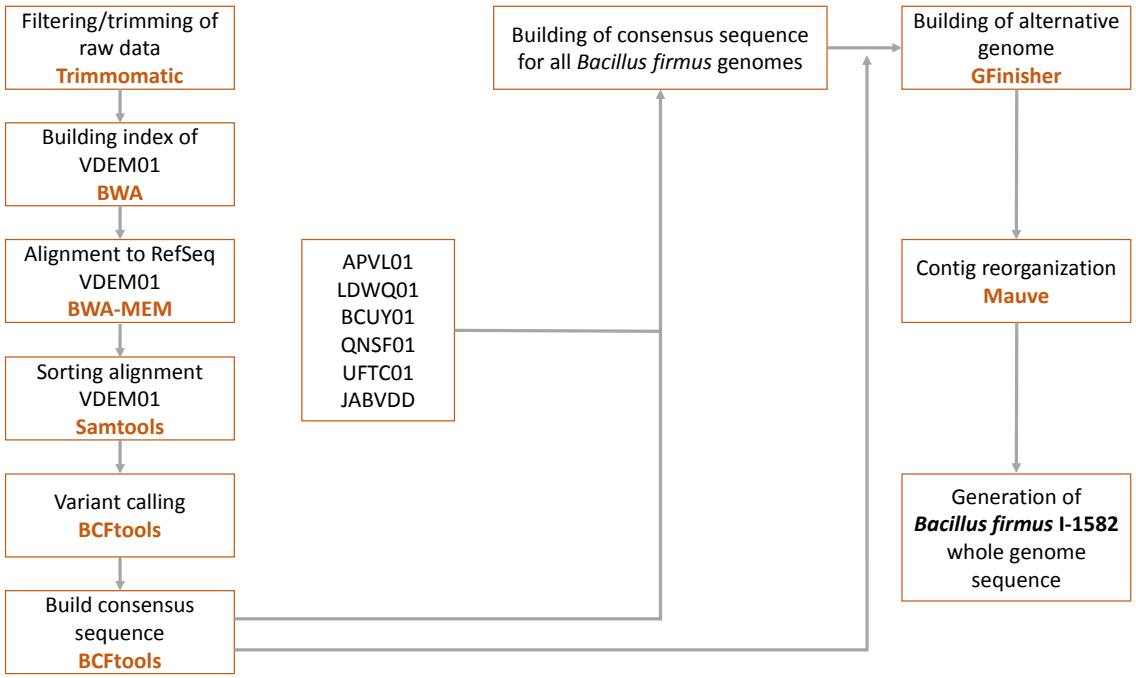

Fig. 1: The pipeline of *Bacillus firmus* I-1582 genome sequencing, assembly and annotation. Sequence reads were trimmed with trimmomatic. An index was built with BWA for the subsequent alignment to a reference genome. Sorting was performed with Samtools and variant calling was done with BCFtools. A consensus sequence was built based on the reference genome by BCFtools. Multiple consensus sequences were built in this manner based on different reference genomes. An alternative genome was built by GFinisher with VDEM01 consensus sequence, reference genome VDEM01 and six alternative assemblies based on the other reference genomes. Contigs were reorganized and *B. firmus* I-1582 genome was used for further analysis. Whole Genome Shotgun accession numbers are based on NCBI project accession of *B. firmus* whole genome sequences (https://www.ncbi.nlm.nih.gov/genome/browse/#!/prokaryotes/17454/).

Identification and characterization of predicted lanthipeptide gene cluster

For the identification of lanthipeptide gene clusters, our *B. firmus* I-1582 whole genome sequence was subjected to antiSMASH (Blin et al., 2019) 5.0 as well as BAGEL4 (van Heel et al., 2018). The predicted lanthipeptide sequences were visualized using Illustrator for Biological Sequence (IBS v1.0.3) (Liu et al., 2015).

The class, cleavage, crosslink and chemical structure of putative lanthipeptides were predicted by RiPPMiner (Agrawal et al., 2017). The tool ‘‘RiPP Cleavage & Crosslinks Prediction’’ was used with the amino acid sequence of each putative lanthipeptide gene as input.

The amino acid sequences of core peptide of putative lanthipeptides were subjected to *in silico* hydrolysis program ExPASy PeptideCutter (Gasteiger et al., 2005). The potential cleavage sites cleaved by enzymes or chemicals were predicted to indicate peptide stability.

RNA extraction and cDNA synthesis

B. firmus I-1582 was cultivated in TSB at 28 °C with orbital shaking for 72 hours. Total RNA was extracted using PureLink™ RNA Mini-Kit [Invitrogen™, Thermo Fisher Scientific, USA] and purified using TURBO DNA-free™ Kit [Invitrogen™, Thermo Fisher Scientific, USA] according to the manufacturer's instructions. The quality and quantity of the received RNA were estimated by a NanoDrop2000c spectrophotometer. The first strand cDNA synthesis was performed using High-Capacity cDNA Reverse Transcription Kit [Applied Biosystems™, Thermo Fisher Scientific, USA] according to the manufacturer's instructions. The obtained cDNA was prepared by 10-fold dilution with nuclease-free water for the subsequent RT-qPCR analysis.

Primer design and RT-qPCR analysis

Primers were designed using Primer3Plus software based on the obtained whole genome sequence of *B. firmus* I-1582. Primer information is listed in Supplementary Tab. 1. The real-time quantitative PCR (RT-qPCR) was performed at an initial denaturation of 95 °C for 20 seconds, followed by 40 amplification cycles of 95 °C for 3 seconds and 60 °C for 30 seconds using a StepOnePlus™ Real-Time PCR System [Applied Biosystems™, Thermo Fisher Scientific, USA]. Each reaction was prepared in a final volume of 20 µl, including 10 µl of Fast SYBR™ Green Master Mix [Applied Biosystems™, Thermo Fisher Scientific, USA], 9 µl of primer mix, and 1 µl of cDNA. 16S ribosomal RNA was used as an internal control for normalizing the expression results obtained in the experimental groups. This assay was performed in two biological replications.

Statistical analysis

All data are expressed as mean ± standard error (SE). Statistical analysis was performed using one-way analysis of variance (ANOVA) followed by a suitable post-hoc test ($p<0.05$).

Results

Nematicidal activity of *B. firmus* I-1582 molecules

Being originally isolated from soil in Israel, *B. firmus* I-1582 might be adapted to relatively high temperatures. Thus, in order to determine whether temperature is a key factor of the nematicidal activity of *B. firmus* I-1582, *H. schachtii* J2 were incubated with *B. firmus* I-1582 cell-free supernatant (CFS) or the respective cell suspension (CS) at different temperatures. The result revealed a strong temperature-dependent effect (Fig. 2a). Particularly, mortality of J2 increased considerably from 22 to 37 °C when incubated in CFS. J2 mortality in CFS at 37 °C was 58 %, about 10 fold higher compared to the mock control.

In order to further describe the chemical nature of the active compound(s) present in *B. firmus* I-1582 CFS, the CFS was first treated with heat or proteinase K before being added to J2. After 72 hours incubation at 37 °C the result clearly showed that the nematicidal activity of CFS is not impaired by heat but partially by proteinase K (Fig. 2b). Subsequently, molecules in the CFS were divided into two fractions by size-exclusion filtration using a 3 kDa cut-off ultrafiltration membrane. The CFS fraction > 3 kDa (retentate fraction) and the fraction < 3 kDa (filtrate fraction) were treated with two proteases, proteinase K and pronase. The treated fractions were then tested for their lethal activity on J2. It turned out that significant nematicidal activity could only be detected in the fraction containing molecules < 3 kDa (Fig. 2c). The non-treated CFS fraction < 3 kDa resulted in a J2 mortality of 93 %. In addition, the activity of CFS fraction < 3 kDa, if treated with either proteinase K or pronase, against juveniles was reduced by approximately 20 %, compared to the non-treated CFS fraction < 3 kDa. Thus, the CFS fraction < 3 kDa contains the active compound(s) responsible for the nematicidal activity. To the best of our knowledge, this is the first report that small molecules produced by *B. firmus* contribute to the nematicidal activity, since all virulence factors against nematodes secreted by *Bacillus* spp. have molecular size > 30 kDa (Niu et al., 2007; Tian et al., 2007; Zhang et al., 2012; Geng et al., 2016).

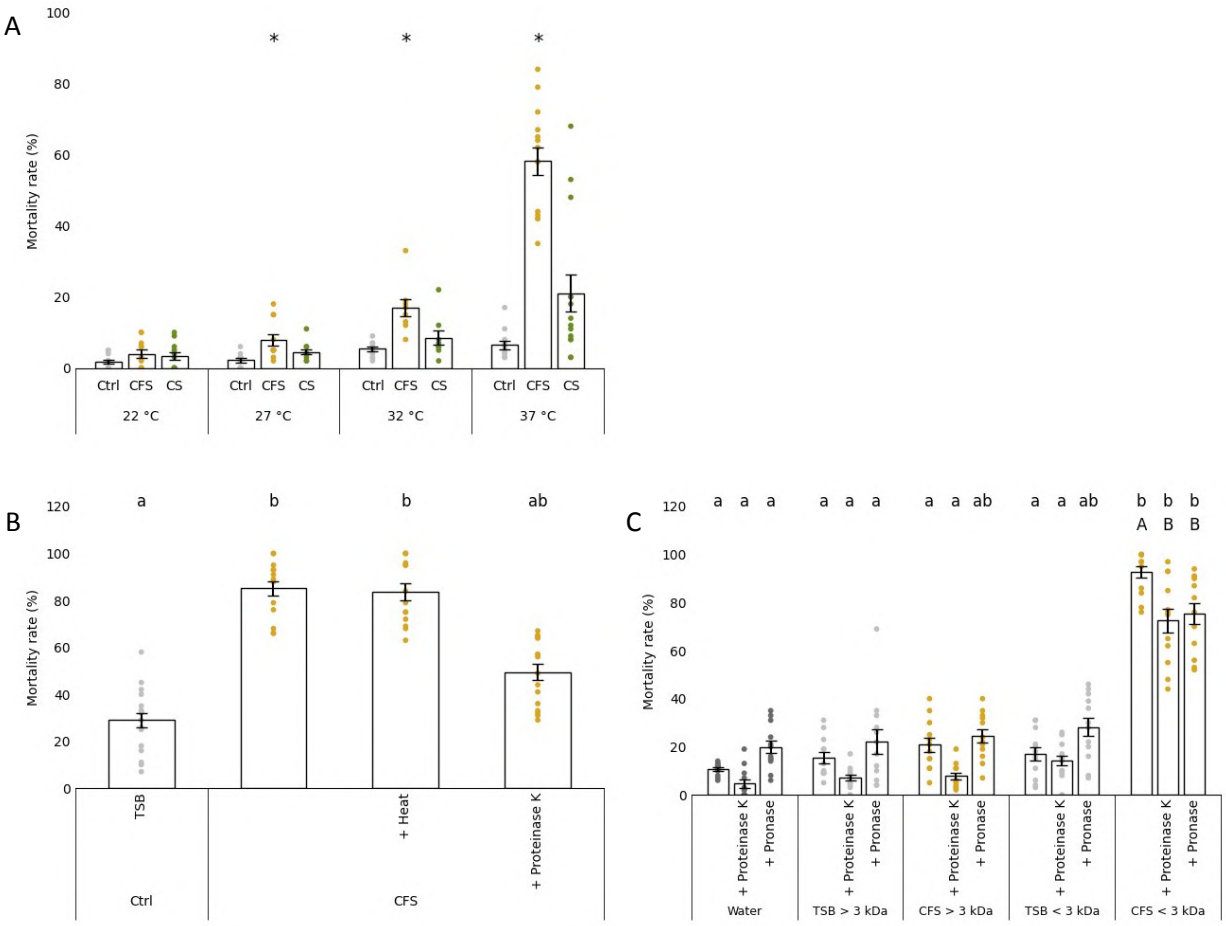

Fig. 2: *In vitro* nematicidal activity of *Bacillus firmus* I-1582 cell-free supernatant (CFS) and cell suspension (CS). (A) *Heterodera schachtii* second stage juveniles (J2) were exposed to CFS, CS, or tryptic soy broth (TSB) as negative control (Ctrl) at 22 °C, 27 °C, 32 °C, and 37 °C for 72 h. (B) CFS was treated by heat (99 °C for 30 min) or proteinase K prior to J2 exposure at 37 °C for 72 h. (C) CFS was divided into two fractions containing molecules > 3 kDa or < 3kDa. The fractions were treated with two different proteases prior to exposure to J2 at 37 °C for 72 h. Values are the mean ± standard error of three independent biological replicates (n ≥ 8 (A); n ≥ 12 (B, C)). Asterisks (*) indicate statistically significant differences compared to the control and different letters indicate statistically significant differences between all treatments (small letters) or between treatments of the same fraction (capital letters) according to Dunn's method ($p < 0.05$).

Genome sequencing of *B. firmus* I-1582

Genomic information can help to elucidate putative molecules that are responsible for the above observed activity. As the genome of *B. firmus* I-1582 was not available at the time this study was performed, sequencing was done. The assembly of the *B. firmus* I-1582 genome was based on 10,806,900 paired reads. The genomic characteristics are summarized in Table

1. The estimated size of the *B. firmus* I-1582 genome is approximately 4.95 Mb with a G+C content of 42.89 %. A total of 5,039 coding sequences (CDS) were predicted. The sequenced genome consists of 70 contigs with an N50 length of 168,292 bp (50 % of the genome is covered by contigs longer or equal to the N50 length) with the longest contig being 453,866 bp. Quality assessment with BUSCO revealed that out of the total 450 conserved single-copy orthologs searched within the genome, BUSCO analysis identified 449 complete BUSCOs, representing 99.8% completeness. Additionally, one BUSCO was detected as fragmented (0.2%), while no BUSCOs were classified as missing. These results indicate a high level of completeness and quality in the assembly, suggesting successful reconstruction of the majority of the conserved genes within the genome. This Whole Genome Shotgun project has been deposited at DDBJ/ENA/GenBank under the accession JBBPHO000000000. The version described in this paper is version JBBPHO010000000.

Tab. 1: Genomic features of *Bacillus firmus* I-1582.

Strain	Genome size (Mb)	G+C content (%)	No. of CDS	No. of contigs	N50 contig size (bp)	Coverage (x times)
B. firmus I-1582	~4.95	42.89	5,039	70	168,292	~580.9

Prediction of putative lanthipeptides in *B. firmus* I-1582 genome

As the mortality assay highlighted small protease-sensitive and heat-stable molecules to partially mediate *B. firmus* I-1582 nematicidal activity, genome-mining tools were utilized to predict putative secondary metabolite gene clusters. AntiSMASH uncovered, that *B. firmus* I-1582 harbours four BGC encoding putative secondary metabolites - one siderophore gene cluster, one lanthipeptide gene cluster, one terpene gene cluster, and one Type III PKS (T3PKS) gene cluster. As lanthipeptides are known to be heat-stable and – depending on the structure – can be digested by proteases, we focused on this class of molecules (Suda et al., 2010; Xin et al., 2015). Figure 3 illustrates the *in silico* identification of lanthipeptide BGC in *B. firmus* I-1582 using two genome-mining tools, antiSMASH and BAGEL. The combination of the two lanthipeptide gene clusters predicted by BAGEL (Fig. 3b and 3c) constitutes the

single lanthipeptide gene cluster predicted by antiSMASH (Fig. 3a), which strongly indicates the existence of a lanthipeptide BGC in the *B. firmus* I-1582 genome.

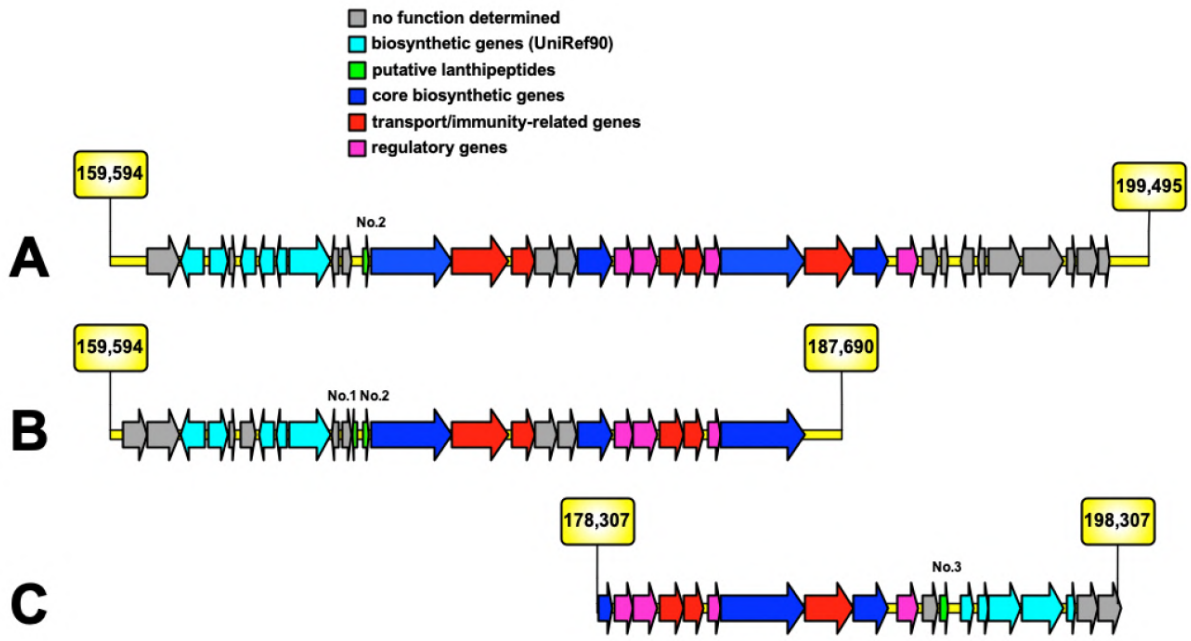

Fig. 3: Schematic representation of putative lanthipeptide gene clusters predicted in the *Bacillus firmus* I-1582 genome. (**A**) antiSMASH prediction of lanthipeptide gene cluster; (**B**) BAGEL prediction of lanthipeptide gene cluster #1; (**C**) BAGEL prediction of lanthipeptide gene cluster #2. The arrows indicate the gene loci, which are color-coded based on the functions.

Based on the predictions of antiSMASH and BAGEL, sequences of three putative lanthipeptides (No. 1, 2 and 3) were extracted. Table 2 shows the features of these three lanthipeptides, including lanthipeptide class, and no. of amino acids in core peptides, cleavage sites, and cross-links. The core peptides of lanthipeptide No. 1, No. 2, and No. 3, comprise 36, 25, and 21 amino acids, respectively. To gain insight into the proteolytic stability of the lanthipeptides, protease K-specific cleavage sites within the core peptides were determined by ExPASy PeptideCutter, revealing that proteinase K is able to digest all three lanthipeptides at multiple sites (Supplementary Tab. 2). However, the existence of thioether cross-links in lanthipeptide No. 1 and No. 2 may cause steric hindering that interferes with proteinase K binding. This finding could explain why the nematicidal activity of CFS is partially lost after proteinase K treatment (Fig. 2b and 2c). In order to decipher the complete chemical structures of these lanthipeptides, their amino acid sequences were

used as input in RiPPMiner. An illustration of the chemical structures of the three predicted lanthipeptides is presented in Figure 4.

Tab. 2: Structural characterization of three putative lanthipeptides in *Bacillus firmus* I-1582. The putative lanthipeptides, prediction program that identified the specific lanthipeptide, predicted lanthipeptide class*, No. of amino acids*, No. of cleavage sites*, and No. of cross-links* are listed. A: antiSMASH 5.0, B: BAGEL4. *: predicted by RiPPMiner.

Putative lanthipeptides	Prediction program	Class	No. amino acids	No. cleavage sites	No. cross-links
No.1	A	I	36	11	5
No.2	A/B	II	25	13	3
No.3	B	II	21	11	0

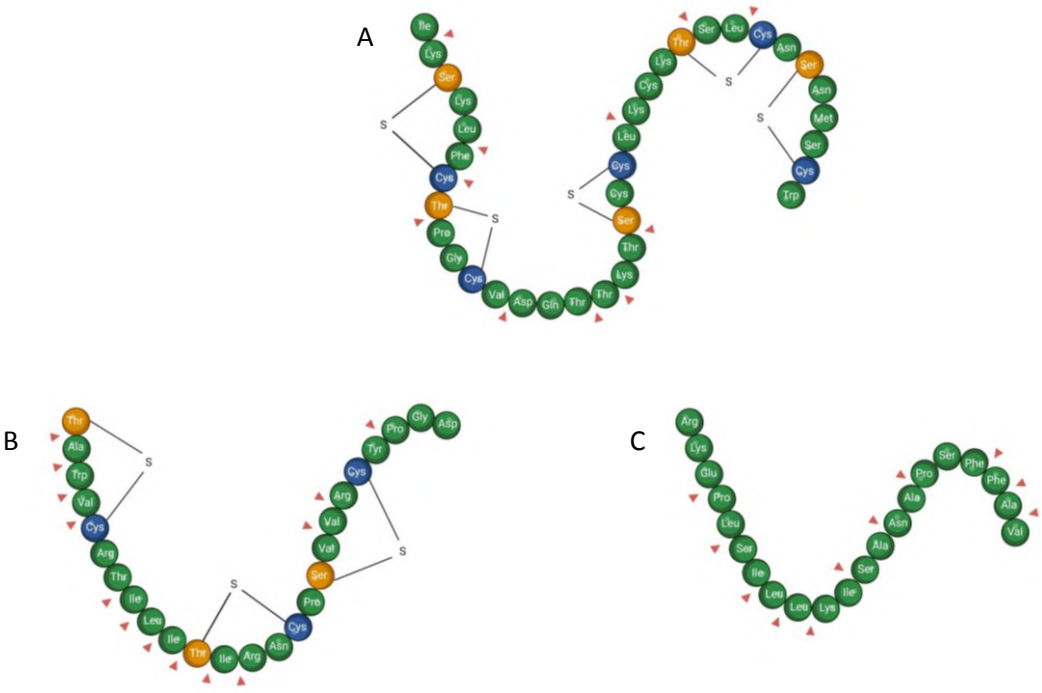

Fig. 4: Proposed chemical structure of three predicted lanthipeptides in *Bacillus firmus* I-1582. (A) Lanthipeptide No. 1; (B) Lanthipeptide No. 2; (C) Lanthipeptide No. 3. During post-translational modification, Ser and Thr are dehydrated into Dha and Dhb, respectively, while Cys attach the dehydrated residues to form a thioether cross-link. Ser and Thr are highlighted in yellow, while Cys are highlighted in blue. The red arrows indicate the proteinase K-specific cleavage sites.

Gene expression of the predicted lanthipeptides in *B. firmus* I-1582

To validate that the putative lanthipeptides are produced by *B. firmus* I-1582 and are present in the CFS utilized for the J2 mortality assay, an expression analysis was carried out. The gene expression levels were compared between bacterial cells cultured for 72 hours and for 12 hours. As demonstrated in Figure 5, the expression of all putative lanthipeptides is up-regulated in *B. firmus* I-1582. Bacterial cells cultured for 72 hours revealed a 38-, 3.2-, and 5.3-fold higher expression of No. 1, No. 2, and No. 3 compared to the 12 hours culture, respectively. These results further support the presence of these lanthipeptides in the 72 hour CFS and thus, their contribution to the demonstrated nematicidal activity of *B. firmus* I-1582 against *H. schachtii* (Supplementary Fig. 1).

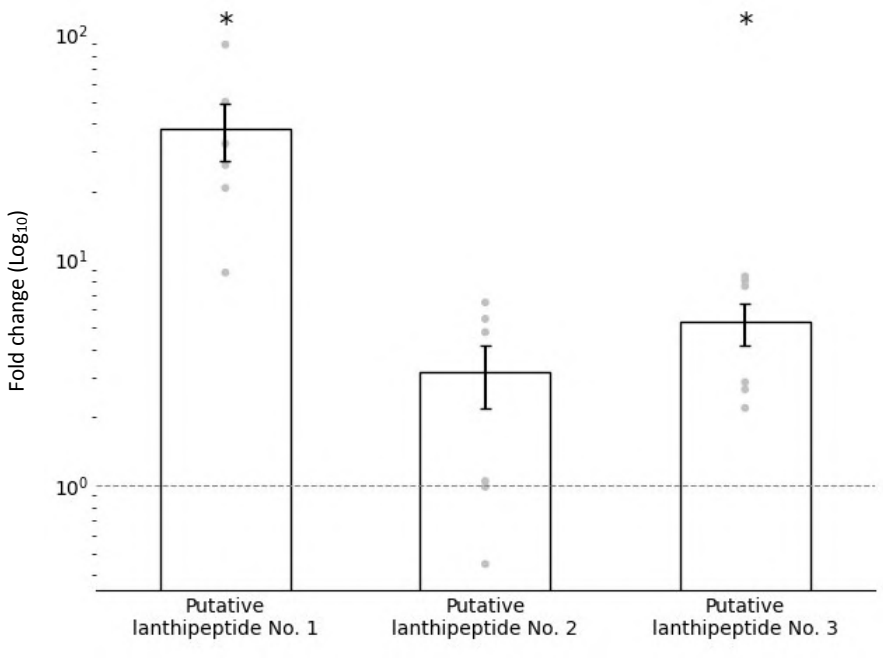

Fig. 5: Gene expression analysis of lanthipeptide No. 1, No. 2, and No. 3 *in Bacillus firmus* I-1582 cells cultured for 72 h. The dashed line indicates the expression level (= 1) of the putative lanthipeptides in *B. firmus* I-1582 cultured for 12 h. 16S rRNA served as an internal control. Values are displayed as mean ± standard error of two representative biological replicates (n = 6). Asterisks (*) indicate statistically significant difference compared to the control according to Dunnett's method ($p < 0.05$).

Discussion

B. firmus I-1582 was originally isolated from soil in Israel and is commercially applied as seed treatment or soil drenching for the bio-control of PPN (Wilson & Jackson, 2013). This strain and its formulated product have been well-studied under a series of laboratory, greenhouse and field conditions against several PPN including the sting nematode *Belonolaimus longicaudatus*, the root-knot nematodes *Meloidogyne incognita* and *Meloidogyne luci,* and the beet cyst nematode *H. schachtii* (Crow, 2014; Ghahremani et al., 2020; Susič et al., 2020; Huang et al., 2021). Still the molecular processes determining the bacterium's activity against PPN are not fully elucidated. Here we demonstrate that small molecules of *B. firmus* present in the CFS possess nematicidal activity against *H. schachtii* J2 in a temperature-dependent manner. In our previous study we could not observe *H. schachtii* parasitism at *Arabidopsis thaliana* to be inhibited in a CFS-supplemented agar system (Huang et al., 2021). The most obvious explanation is that the plant infection assay was conducted at 24 °C, a temperature at which no nematicidal activity of the CFS could be observed.

Experiments were performed by separating CFS fractions into MW above and below 3 kDa, with the active molecules found to be in the fraction < 3 kDa. By exposing fraction < 3 kDa to proteases, we observe a significant loss in nematicidal activity attesting that this effect can partially be attributed to proteinaceous molecules and partially to protease-stable molecules. Heating did not affect the molecules' activity. Towards identifying these active molecules, we sequenced the genome of *B. firmus* I-1582 and combined genome-mining tools with NCBI BLAST to investigate the presence of BGC which encode putative NP secreted by the bacterium. This in silico analysis identified one lanthipeptide BGC with three putative lanthipeptides, defined as No.1, No.2, and No.3, which have the theoretical MW of 3.9, 2.8, and 2.3 kDa, respectively. Special attention needs to be drawn to lanthipeptide No. 1. According to the user instruction of Amicon® Ultrafiltration Membrane, ultrafiltration membrane with a MWCO of 3 kDa is capable of concentrating target molecules with MW 2-3 times greater due to retention capabilities by various factors. Therefore, even though the MW of lanthipeptide No.1 is > 3 kDa, there is a high probability that it is still present in the fraction < 3 kDa. Subsequent gene expression analysis revealed that all three

predicted lanthipeptides, particularly peptide No. 1, are highly expressed in a 72-hour liquid culture of *B. firmus* I-1582. This provides evidence that all three putative lanthipeptides might contribute to the bacterium's nematicidal activity against *H. schachtii* J2.

Lanthipeptides, whose chemical stabilities are similar to ours, were discovered by Xin et al. (2015). The authors found three novel class II lanthipeptides, TinA1 (MW = 4,062.98 Da), TinA3 (MW = 4,048.96 Da), and TinA4 (MW = 4,063.02 Da) - identified in *Bacillus thuringiensis* BMB3201 - which exhibited broad-spectrum antimicrobial activities against several Gram-positive bacteria, and they observed that the HPLC-purified TinA4 retained most of its antimicrobial activity after thermal treatment, but not after protease digestion. Depending on the characteristics of the biosynthetic enzymes, lanthipeptides are classified into four classes (Arnison et al., 2013). Those found in the genus *Bacillus* spp. mainly belong to class I and class II. Most characterized class I and II lanthipeptides are known for their antibacterial activity and are also referred to as lantibiotics (Barbosa et al., 2015). In our study, *B. firmus* I-1582 putative lanthipeptide No. 1 belongs to class I, and No. 2 and No. 3 belong to class II. The biosynthesis of lanthipeptides first involves the formation of a linear precursor peptide from ribosomes. The precursor peptide consists of an N-terminal leader peptide, which is essential for enzyme recognition, and a C-terminal core peptide, which undergoes post-translational modifications (PTM). During PTM, serine (Ser) and threonine (Thr) residues can be dehydrated into 2,3-didehydroalanine (Dha) and 2,3-didehydrobutyrine (Dhb), respectively. Subsequently, lanthionine (Lan) and methyllanthionine (MeLan) thioether cross-links are formed through intramolecular Michael addition of cysteine (Cys) residues to the dehydrated residues Dha and Dhb, respecitively. In most cases, the leader peptide directs the microbial producer to secret the modified peptide in the late stages of lanthipeptide biosynthesis, after which the leader peptides is removed by proteolysis to generate the mature lanthipeptide. Sometimes, proteolysis precedes secretion (Repka et al., 2017). The thioether structures largely contribute to protecting the mature products from thermal and proteolytic degradation (Suda et al., 2010; Knerr & van der Donk, 2012; Montalbán-López et al., 2017). For the core peptides of the three putative lanthipeptides, multiple cleavage sites for proteinase K are predicted, suggesting that proteinase K is able to cut all three lanthipeptides to destroy their bioactivity. However, five and three thioether cross-links are predicted in lanthipeptide No. 1 and No. 2, respectively.

These ring structures may protect lanthipeptide No. 1 and No. 2 from binding to proteinase K, thus explaining why the nematicidal activity of the CFS is only partially lost after being treated with proteinase K.

While our *in vitro* test and *in silico* validation strongly suggest that lanthipeptides is likely the most important factor contributing to the bacterium's nematicidal activity, further investigations need to be continued in order to confirm our hypothesis. For example, lanthipeptides can be purified and characterised from *B. firmus* I-1582 by size-exclusion chromatography and mass spectrometry, and tested for the nematicidal activity. Alternatively, chemical synthesis could be an option to obtain lanthipeptides and their analogues, although it is difficult due to their complicated structures. In addition, mutant lines, including overexpression mutants and knockout mutants of *B. firmus* I-1582, should be tested for their bioactivity so that we can directly correlate it with the observed nematicidal activity. Recently, eleven *Brevibacillus* strains were tested for their nematicidal activity against the model nematode *Caenorhabditis elegans* and the root-knot nematode *Meloidogyne* spp. in the killing assay and the pot assay, respectively. Among them, *Brevibacillus* M2.1A displayed the highest killing effect against *C. elegans*, and the best control efficiency against *Meloidogyne* spp. parasitism at tomato plants. Surprisingly, BGC encoding class I lanthipeptides were detected in *Brevibacillus* M2.1A, whereas no lanthipeptide BGC were found in other *Brevibacillus* strains that were not as efficient as *Brevibacillus* M2.1A in controlling nematodes (Jähne et al., 2023).

Nowadays, peptide-based pest control agents have received considerable attention, due to the fact that large protein biologics, such as antibodies and enzymes, have difficulty penetrating the cuticle of pests in order to act on specific targets in their tissues, not to mention their limited stability in the field and the demand for a cold supply chain during transportation. Our study provides the first insight that lanthipeptides could to be virulence factors of *B. firmus* I-1582, thus contributing to the bacterium’s antagonistic activity against PPN. Particularly interesting is that we found its activity is temperature-dependent. We believe that our findings fundamentally advance an understanding of the novel peptides identified from *B. firmus*, and will help to improve this bacterium’s application efficacy as a potential BCA for sustainable nematode management.

Reference

Agrawal P, Khater S, Gupta M, Sain N, Mohanty D. RiPPMiner: a bioinformatics resource for deciphering chemical structures of RiPPs based on prediction of cleavage and cross-links. Nucleic Acids Research. 2017; 45 (1): 80-88. doi: 10.1093/nar/gkx408

Arnison PG, Bibb MJ, Bierbaum G, Bowers AA, Bugni TS, Bulaj G, Camarero JA, Campopiano DJ, Challis GL, Clardy J, Cotter PD, Craik DJ, Dawson M, Dittmann E, Donadio S, Dorrestein PC, Entian KD, Fischbach MA, Garavelli JS, Göransson U, Gruber CW, Haft DH, Hemscheidt TK, Hertweck C, Hill C, Horswill AR, Jaspars M, Kelly WL, Klinman JP, Kuipers OP, Link AJ, Liu W, Marahiel MA, Mitchell DA, Moll GN, Moore BS, Müller R, Nair SK, Nes IF, Norris GE, Olivera BM, Onaka H, Patchett ML, Piel J, Reaney MJ, Rebuffat S, Ross RP, Sahl HG, Schmidt EW, Selsted ME, Severinov K, Shen B, Sivonen K, Smith L, Stein T, Süssmuth RD, Tagg JR, Tang GL, Truman AW, Vederas JC, Walsh CT, Walton JD, Wenzel SC, Willey JM, van der Donk WA. Ribosomally synthesized and post-translationally modified peptide natural products: overview and recommendations for a universal nomenclature. Natural Product Reports. 2013; 30 (1): 108-160. doi: 10.1039/c2np20085f

Barbosa J, Caetano T, Mendo S. Class I and class II lanthipeptides produced by *Bacillus* spp. Journal of Natural Products. 2015; 78 (11): 2850-2866. doi: 10.1021/np500424y

Biggins JB, Ternei MA, Brady SF. Malleilactone, a polyketide synthase-derived virulence factor encoded by the cryptic secondary metabolome of *Burkholderia pseudomallei* group pathogens. Journal of the American Chemical Society. 2012; 134 (32): 13192-13195. doi: 10.1021/ja3052156

Blin K, Shaw S, Steinke K, Villebro R, Ziemert N, Lee SY, Medema MH, Weber T. antiSMASH 5.0: updates to the secondary metabolite genome mining pipeline. Nucleic Acids Research. 2019; 47 (1): 81-87. doi: 10.1093/nar/gkz310

Brötz H, Josten M, Wiedemann I, Schneider U, Götz F, Bierbaum G, Sahl HG. Role of lipid-bound peptidoglycan precursors in the formation of pores by nisin, epidermin and other lantibiotics. Molecular Microbiology. 1998; 30 (2): 317-327. doi: 10.1046/j.1365-2958.1998.01065.x

Clardy J, Walsh C. Lessons from natural molecules. Nature. 2004; 432 (7019): 829-837. doi: 10.1038/nature03194

Crow WT. Effects of a commercial formulation of *Bacillus firmus* I-1582 on golf course bermudagrass infested with *Belonolaimus longicaudatus*. Journal of Nematology. 2014; 46 (4): 331-335

Danecek P, Bonfield JK, Liddle J, Marshall J, Ohan V, Pollard MO, Whitwham A, Keane T, McCarthy SA, Davies RM, Li H. Twelve years of SAMtools and BCFtools. Gigascience. 2021; 10 (2): giab008. doi: 10.1093/gigascience/giab008

Darling AE, Mau B, Perna NT. progressiveMauve: multiple genome alignment with gene gain, loss and rearrangement. PLoS One. 2010; 5 (6): e11147. doi: 10.1371/journal.pone.0011147

Demain AL. New applications of microbial products. Science. 1983; 219 (4585): 709-714. doi: 10.1126/science.6337397

Firn R. Nature's chemicals: the natural products that shaped our world. New York: Oxford University Press. 2011. doi: 10.1093/aob/mcq208

Galyov EE, Brett PJ, DeShazer D. Molecular insights into *Burkholderia pseudomallei* and *Burkholderia mallei* pathogenesis. Annual Review of Microbiology. 2010; 64: 495-517. doi: 10.1146/annurev.micro.112408.134030

Gasteiger E, Hoogland C, Gattiker A, Duvaud S, Wilkins MR, Appel RD, Bairoch A. Protein identification and analysis tools on the ExPASy server. In: Walker JM, ed. The Proteomics Protocols Handbook. Humana Press. 2005; 571-607. doi: 10.1385/1-59259-890-0:571

Geng C, Nie X, Tang Z, Zhang Y, Lin J, Sun M, Peng D. A novel serine protease, Sep1, from *Bacillus firmus* DS-1 has nematicidal activity and degrades multiple intestinal-associated nematode proteins. Scientific Reports. 2016; 6 (25012). doi: 10.1038/srep25012

Ghahremani Z, Escudero N, Beltrán-Anadón D, Saus E, Cunquero M, Andilla J, Loza-Alvarez P, Gabaldón T, Sorribas FJ. *Bacillus firmus* strain I-1582, a nematode antagonist by itself and through the plant. Frontiers in Plant Science. 2020; 11 (796). doi: 10.3389/fpls.2020.00796

Guizelini D, Raittz RT, Cruz LM, Souza EM, Steffens MB, Pedrosa FO. GFinisher: a new strategy to refine and finish bacterial genome assemblies. Scientific Reports. 2016; 6 (34963). doi: 10.1038/srep34963

Hirsch A. Growth and nisin production of a strain of *Streptococcus lactis*. Journal of General Microbiology. 1951; 5 (1): 208-221. doi: 10.1099/00221287-5-1-208

Hsu ST, Breukink E, Tischenko E, Lutters MA, de Kruijff B, Kaptein R, Bonvin AM, van Nuland NA. The nisin-lipid II complex reveals a pyrophosphate cage that provides a blueprint for novel antibiotics. Nature Structural & Molecular Biology. 2004; 11 (10): 963-967. doi: 10.1038/nsmb830

Huang MM, Bulut A, Shresth B, Matera C, Grundler FMW, Schleker ASS. *Bacillus firmus* I-1582 promotes plant growth and impairs infection and development of the cyst nematode *Heterodera schachtii* over two generations. Scientific Reports. 2021; 11 (14114). doi: 10.1038/s41598-021-93567-0

Jähne J, Le Thi TT, Blumenscheit C, Schneider A, Pham TL, Le Thi PT, Blom J, Vater J, Schweder T, Lasch P, Borriss R. Novel plant-associated *Brevibacillus* and *Lysinibacillus* genomospecies harbor a rich biosynthetic potential of antimicrobial compounds. Microorganisms. 2023; 11 (1): 168. doi: 10.3390/microorganisms11010168

Katz L, Baltz RH. Natural product discovery: past, present, and future. Journal of Industrial Microbiology and Biotechnology. 2016; 43 (2-3): 155-176. doi: 10.1007/s10295-015-1723-5

Kloosterman AM, Cimermancic P, Elsayed SS, Du C, Hadjithomas M, Donia MS, Fischbach MA, van Wezel GP, Medema MH. Expansion of RiPP biosynthetic space through integration of pan-genomics and machine learning uncovers a novel class of lanthipeptides. PLoS Biology. 2020; 18 (12): e3001026. doi: 10.1371/journal.pbio.3001026

Knerr PJ, van der Donk WA. Discovery, biosynthesis, and engineering of lantipeptides. Annual Review of Biochemistry. 2012; 81: 479-505. doi: 10.1146/annurev-biochem-060110-113521

Li H. Aligning sequence reads, clone sequences and assembly contigs with BWA-MEM. arXiv: Genomics. 2013

Liu W, Xie Y, Ma J, Luo X, Nie P, Zuo Z, Lahrmann U, Zhao Q, Zheng Y, Zhao Y, Xue Y, Ren J. IBS: an illustrator for the presentation and visualization of biological sequences. Bioinformatics. 2015; 31 (20): 3359-3361. doi: 10.1093/bioinformatics/btv362

Manni M, Berkeley MR, Seppey M, Simão FA, Zdobnov EM. BUSCO update: novel and streamlined workflows along with broader and deeper phylogenetic coverage for scoring of eukaryotic, prokaryotic, and viral genomes. Molecular Biology and Evolution. 2021; 38 (10): 4647-4654. doi: 10.1093/molbev/msab199

Mendoza AR, Kiewnick S, Sikora, RA. *In vitro* activity of *Bacillus firmus* against the burrowing nematode *Radopholus similis*, the root-knot nematode *Meloidogyne incognita* and the stem nematode *Ditylenchus dipsaci*. Biocontrol Science and Technology. 2008; 18 (4): 377-389. doi: 10.1080/09583150801952143

Migunova VD, Sasanelli N. Bacteria as biocontrol tool against phytoparasitic nematodes. Plants (Basel). 2021; 10 (2), 389. doi: 10.3390/plants10020389

Montalbán-López M, van Heel AJ, Kuipers OP. Employing the promiscuity of lantibiotic biosynthetic machineries to produce novel antimicrobials. FEMS Microbiology Reviews. 2017; 41 (1): 5-18. doi: 10.1093/femsre/fuw034

Niu Q, Huang X, Zhang L, Lian L, Li Y, Li J, Yang J, Zhang K. Functional identification of the gene bace16 from nematophagous bacterium *Bacillus nematocida*. Applied Microbiology and Biotechnology. 2007; 75 (1), 141-148. doi: 10.1007/s00253-006-0794-7

Perez KJ, Viana JD, Lopes FC, Pereira JQ, Dos Santos DM, Oliveira JS, Velho RV, Crispim SM, Nicoli JR, Brandelli A, Nardi RM. *Bacillus* spp. Isolated from Puba as a Source of Biosurfactants and Antimicrobial Lipopeptides. Frontiers in Microbiology. 2017; 8 (61). doi: 10.3389/fmicb.2017.00061

Pham JV, Yilma MA, Feliz A, Majid MT, Maffetone N, Walker JR, Kim E, Cho HJ, Reynolds JM, Song MC, Park SR, Yoon YJ. A review of the microbial production of bioactive natural products and biologics. Frontiers in Microbiology. 2019; 10 (1404). doi: 10.3389/fmicb.2019.01404

Powell NT. Interaction of plant parasitic nematodes with other disease-causing agents. In: Zuckerman BM, Mai WF, Rohde RA, eds. Plant Parasitic Nematodes. Academic Press. 1971; p. 119-136. doi: 10.1016/B978-0-12-782202-0.50012-6

Repka LM, Chekan JR, Nair SK, van der Donk WA. Mechanistic understanding of lanthipeptide biosynthetic enzymes. Chemical Reviews. 2017; 117: 5457-5520. doi: 10.1021/acs.chemrev.6b00591

Rutledge PJ, Challis GL. Discovery of microbial natural products by activation of silent biosynthetic gene clusters. Nature Reviews Microbiology. 2015; 13: 509-523. doi: 10.1038/nrmicro3496

Sanchez S, Guzmán-Trampe S, Ávalos M, Ruiz B, Rodríguez-Sanoja R, Jiménez-Estrada M. Natural products in chemical biology. In: Civjan N, ed. Microbial Natural Products. John Wiley & Sons. 2012; p. 65-108. doi: 10.1002/9781118391815

Scherlach K, Hertweck C. Mining and unearthing hidden biosynthetic potential. Nature Communications. 2021; 12 (3864). doi: 10.1038/s41467-021-24133-5

Scherlach K, Hertweck C. Triggering cryptic natural product biosynthesis in microorganisms. Organic and Biomolecular Chemistry. 2009; 7 (9): 1753-1760. doi: 10.1039/b821578b

Schleker ASS, Rist M, Matera C, Damijonaitis A, Collienne U, Matsuoka K, Habash SS, Twelker K, Gutbrod O, Saalwächter C, Windau M, Matthiesen S, Stefanovska T, Scharwey M, Marx MT, Geibel S, Grundler FMW. Mode of action of fluopyram in plant-parasitic nematodes. Scientific Reports. 2023; 13 (13748). doi: 10.1038/s41598-023-40484-z

Suda S, Westerbeek A, O'Connor PM, Ross RP, Hill C, Cotter PD. Effect of bioengineering lacticin 3147 lanthionine bridges on specific activity and resistance to heat and proteases. Cell Chemical Biology. 2010; 17 (10): 1151-1160. doi: 10.1016/j.chembiol.2010.08.011

Susič N, Janežič S, Rupnik M, Stare BG. Whole genome sequencing and comparative genomics of two nematicidal *Bacillus* strains reveals a wide range of possible virulence factors. G3: Genes, Genomes, Genetics. 2020; 10 (3): 881-890. doi: 10.1534/g3.119.400716

Susič N, Žibrat U, Sinkovič L, Vončina A, Razinger J, Knapič M, Sedlar A, Širca S, Stare BG. From genome to field-observation of the multimodal nematicidal and plant growth-promoting effects of *Bacillus firmus* I-1582 on tomatoes using hyperspectral remote sensing. Plants (Basel). 2020; 9 (592). doi: 10.3390/plants9050592

Terefe M, Tefera T, Sakhuja PK. Effect of a formulation of *Bacillus firmus* on root-knot nematode *Meloidogyne incognita* infestation and the growth of tomato plants in the greenhouse and nursery. Journal of Invertebrate Pathology. 2009; 100 (2): 94-99. doi: 10.1016/j.jip.2008.11.004

Tian B, Yang J, Lian L, Wang C, Li N, Zhang KQ. Role of an extracellular neutral protease in infection against nematodes by *Brevibacillus laterosporus* strain G4. Applied Microbiology and Biotechnology. 2007; 74(2): 372-380. doi: 10.1007/s00253-006-0690-1

van Heel AJ, de Jong A, Song C, Viel JH, Kok J, Kuipers OP. BAGEL4: a user-friendly web server to thoroughly mine RiPPs and bacteriocins. Nucleic Acids Research. 2018; 46 (1): 278-281. doi: 10.1093/nar/gky383

Weller DM. Biological control of soilborne plant pathogens in the rhizosphere with bacteria. Annual Review of Phytopathology. 1988; 26 (1): 379-407. doi: 10.1146/annurev.py.26.090188.002115

Wiedemann I, Breukink E, van Kraaij C, Kuipers OP, Bierbaum G, de Kruijff B, Sahl HG. Specific binding of nisin to the peptidoglycan precursor lipid II combines pore formation and inhibition of cell wall biosynthesis for potent antibiotic activity. Journal of Biological Chemistry. 2001; 276 (3): 1772-1779. doi: 10.1074/jbc.M006770200

Wilson MJ, Jackson TA. Progress in the commercialisation of bionematicides. BioControl. 2013; 58: 715-722. doi: 10.1007/s10526-013-9511-5

Xiang N, Lawrence KS, Kloepper JW, Donald PA, McInroy JA. Biological control of *Heterodera glycines* by spore-forming plant growth-promoting rhizobacteria (PGPR) on soybean. PLoS One. 2017; 12 (7): e0181201. doi: 10.1371/journal.pone.0181201

Xin B, Zheng J, Xu Z, Li C, Ruan L, Peng D, Sun M. Three novel lantibiotics, ticins A1, A3, and A4, have extremely stable properties and are promising food biopreservatives. Applied and Environmental Microbiology. 2015; 81 (20): 6964-6972. doi:10.1128/AEM.01851-15

Zhang F, Peng D, Ye X, Yu Z, Hu Z, Ruan L, Sun M. *In vitro* uptake of 140 kDa *Bacillus thuringiensis* nematicidal crystal proteins by the second stage juvenile of *Meloidogyne hapla*. PLoS One. 2012; 7 (6): e38534. doi: 10.1371/journal.pone.0038534

Zhang MM, Qiao Y, Ang EL, Zhao H. Using natural products for drug discovery: the impact of the genomics era. Expert Opinion on Drug Discovery. 2017; 12 (5): 475-487. doi: 10.1080/17460441.2017.1303478

Zhao X, Kuipers OP. Identification and classification of known and putative antimicrobial compounds produced by a wide variety of Bacillales species. BMC Genomics. 2016; 17 (1). doi: 10.1186/s12864-016-3224-y

Zhao X, Kuipers OP. Nisin- and ripcin-derived hybrid lanthipeptides display selective antimicrobial activity against *Staphylococcus aureus*. ACS Synthetic Biology. 2021; 10 (7): 1703-1714. doi: 10.1021/acssynbio.1c00080

Supplementary material

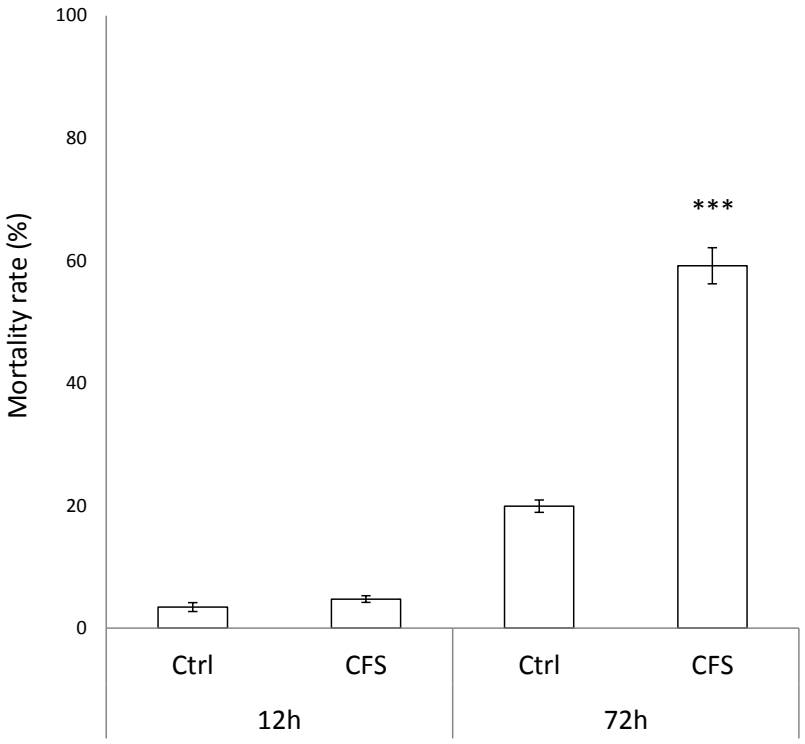

Sup. Fig. 1: *In vitro* nematicidal activity of *Bacillus firmus* I-1582 cell-free supernatant (CFS) collected from 12 h and 72 h liquid culture. *Heterodera schachtii* second stage juveniles (J2) were exposed to CFS, or tryptic soy broth (TSB) as negative control (Ctrl) at 37°C. Values are the mean ± standard error of two independent biological replicates (n = 6). Asterisks (*) indicate statistically significant differences compared to the control ($p < 0.05$).

Sup. Tab. 1: Primer sequences used in this study. Primers are shown in the 5’ to 3’ direction.

Gene symbol	Primer sequence (F)	Primer sequence (R)
16S	GAAGGCGACTCTTTGGTCTG	CCTTTGAGTTTCAGCCTTGC
Putative lanthipeptide No. 1	TGAAAGAGAATATGTTTGATCTGGA	TTGCTATTGCAAAGAGATGTTTTA
Putative lanthipeptide No. 2	GATTTTGAGCACCCGGTTT	CAATCTCCAGGATAGCATCTCAC
Putative lanthipeptide No. 3	TTTTTGCAGGAACAGTGGTG	GGGCATCTGCGGATATTTTA

Sup. Tab. 2: The cleavage sites of Proteinase K mapped onto the core peptide sequences.

	Proteinase K
Putative lanthipeptide No. 1	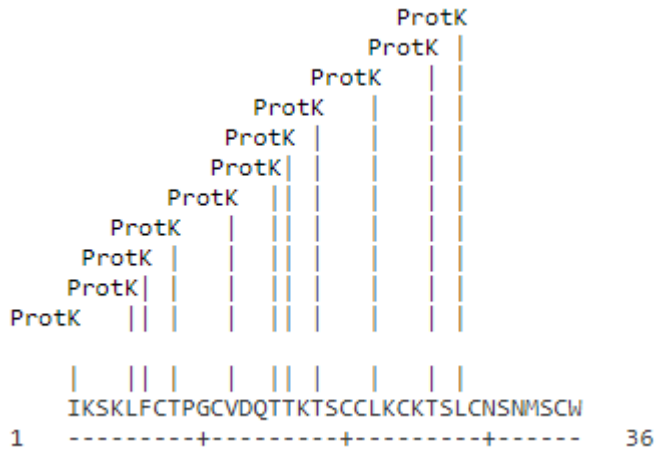
Putative lanthipeptide No. 2	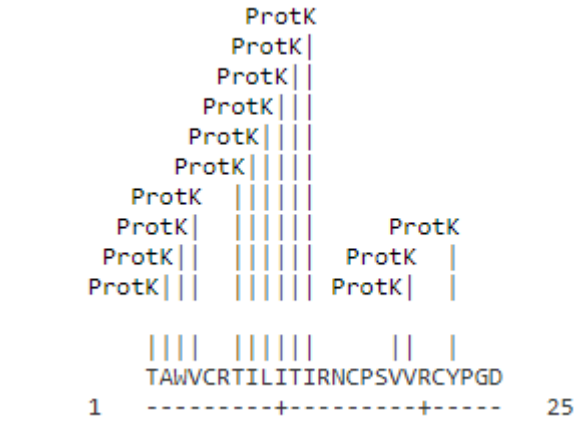
Putative lanthipeptide No. 3	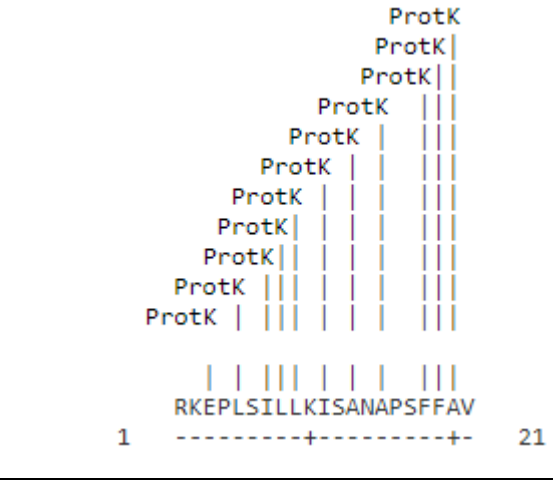

Chapter 4

frontiers | Frontiers in Microbiology

TYPE Original Research
PUBLISHED 02 May 2023
DOI 10.3389/fmicb.2023.1151882

OPEN ACCESS

EDITED BY
Monika Prakash Rai,
Amity University, India

REVIEWED BY
Pramod B. Shinde,
Central Salt and Marine Chemicals Research Institute (CSIR), India
Finian Leeper,
University of Cambridge, United Kingdom

*CORRESPONDENCE
J. Pietruszka
✉ j.pietruszka@fz-juelich.de
A. S. S. Schleker
✉ sylvia.schleker@uni-bonn.de
A. Loeschcke
✉ a.loeschcke@fz-juelich.de

†These authors have contributed equally to this work and share first authorship

‡These authors have contributed equally to this work and share last authorship

RECEIVED 26 January 2023
ACCEPTED 03 April 2023
PUBLISHED 02 May 2023

CITATION
Kossmann DF, Huang M, Weihmann R, Xiao X, Gätgens F, Weber TM, Brass HUC, Bitzenhofer NL, Ibrahim S, Bangert K, Rehling L, Mueller C, Tiso T, Blank LM, Drepper T, Jaeger K-E, Grundler FMW, Pietruszka J, Schleker ASS and Loeschcke A (2023) Production of tailored hydroxylated prodiginine showing combinatorial activity with rhamnolipids against plant-parasitic nematodes.
Front. Microbiol. 14:1151882.
doi: 10.3389/fmicb.2023.1151882

Production of tailored hydroxylated prodiginine showing combinatorial activity with rhamnolipids against plant-parasitic nematodes

D. F. Kossmann[1,2†], M. Huang[3†], R. Weihmann[4†], X. Xiao[3], F. Gätgens[4], T. M. Weber[2], H. U. C. Brass[2], N. L. Bitzenhofer[4], S. Ibrahim[4], K. Bangert[4], L. Rehling[3], C. Mueller[5], T. Tiso[5], L. M. Blank[5], T. Drepper[4], K.-E. Jaeger[1,4], F. M. W. Grundler[3], J. Pietruszka[1,2*‡], A. S. S. Schleker[3*‡] and A. Loeschcke[4*‡]

[1]Institute of Bio- and Geosciences (IBG-1): Biotechnology, Forschungszentrum Jülich GmbH, Jülich, Germany, [2]Institute of Bioorganic Chemistry, Forschungszentrum Jülich, Heinrich Heine University Düsseldorf, Jülich, Germany, [3]INRES, Molecular Phytomedicine, University of Bonn, Bonn, Germany, [4]Institute of Molecular Enzyme Technology, Forschungszentrum Jülich, Heinrich Heine University Düsseldorf, Jülich, Germany, [5]iAMB—Institute of Applied Microbiology, ABBt—Aachen Biology and Biotechnology, RWTH Aachen University, Aachen, Germany

Bacterial secondary metabolites exhibit diverse remarkable bioactivities and are thus the subject of study for different applications. Recently, the individual effectiveness of tripyrrolic prodiginines and rhamnolipids against the plant-parasitic nematode *Heterodera schachtii*, which causes tremendous losses in crop plants, was described. Notably, rhamnolipid production in engineered *Pseudomonas putida* strains has already reached industrial implementation. However, the non-natural hydroxyl-decorated prodiginines, which are of particular interest in this study due to a previously described particularly good plant compatibility and low toxicity, are not as readily accessible. In the present study, a new effective hybrid synthetic route was established. This included the engineering of a novel *P. putida* strain to provide enhanced levels of a bipyrrole precursor and an optimization of mutasynthesis, i.e., the conversion of chemically synthesized and supplemented monopyrroles to tripyrrolic compounds. Subsequent semisynthesis provided the hydroxylated prodiginine. The prodiginines caused reduced infectiousness of *H. schachtii* for *Arabidopsis thaliana* plants resulting from impaired motility and stylet thrusting, providing the first insights on the mode of action in this context. Furthermore, the combined application with rhamnolipids was assessed for the first time and found to be more effective against nematode parasitism than the individual compounds. To obtain, for instance, 50% nematode control, it was sufficient to apply 7.8 μM hydroxylated prodiginine together with 0.7 μg/ml (~1.1 μM) di-rhamnolipids, which corresponded to *ca.* ¼ of the individual EC_{50} values. In summary, a hybrid synthetic route toward a hydroxylated prodiginine was established and its effects and combinatorial activity with rhamnolipids on plant-parasitic nematode *H. schachtii* are presented, demonstrating potential application as antinematodal agents.

KEYWORDS

Prodiginines, plant-parasitic nematodes, plant protection, mutasynthesis and semisynthesis, *Pseudomonas putida*, combinatorial activity, rhamnolipids

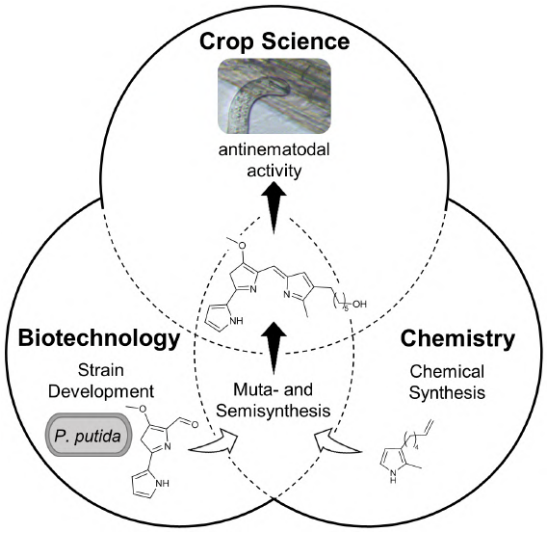

GRAPHICAL ABSTRACT

1. Introduction

Prodiginines are a group of bacterial secondary metabolites with diverse remarkable bioactivities, among which anticancer and antimicrobial effects have perhaps been described in most detail thus far (Fürstner, 2003; Stankovic et al., 2014; Hu et al., 2016; Sakai-Kawada et al., 2019; Yip et al., 2019; Berning et al., 2021; Li et al., 2022). Notably, prodiginine-producing bacteria such as *Streptomyces* and *Serratia* species also dwell in the rhizosphere, the dynamic micro-biosphere around the plant roots and site of manifold chemical interactions between the bacteria and plants (Berg, 2009; Lugtenberg and Kamilova, 2009; Meschke et al., 2012). Here, direct interactions can result in hormonal stimulation, increased stress tolerance and improved nutrient availability and uptake by plant roots. In addition, indirect beneficial effects for the plant can result from the suppression of pathogens. Although the ecophysiological role of prodiginines is still poorly understood, various bioactivities of prodigiosin (**1**) and related tripyrrolic analogs against several plant pathogens have already been reported (Someya et al., 2001; Meschke et al., 2012; Rahul et al., 2014; Roberts et al., 2021). Recently, their effectiveness against the plant-parasitic nematode (PPN) *Heterodera schachtii*, the causative agent of tremendous losses in crop plants, was described (Habash et al., 2020). Moreover, naturally-occurring bacterial secondary metabolites with surfactant properties, namely rhamnolipids, were recently reported to act against *H. schachtii* (Bredenbruch et al., 2023). It has further been shown that prodigiosin (**1**) possesses combinatorial antibacterial activities when applied together with biosurfactants, such as the lipopeptide serrawettin W1 and rhamnolipids (Hage-Hülsmann et al., 2018). It has been postulated that the pigment can only exert its full antimicrobial activity in combination with biosurfactants (Williamson et al., 2008; Roberts et al., 2021).

The aim of the present interdisciplinary study was to facilitate access to the relevant compounds and to investigate their combinatorial activities against *H. schachtii*. *Pseudomonas putida* has become a widely established biotechnological host for natural product biosynthesis (Nikel et al., 2016; Loeschcke and Thies, 2020; Weimer et al., 2020) including heterologous prodigiosin and rhamnolipid production (Domröse et al., 2015; Tiso et al., 2020; Cook et al., 2021). The rhamnolipid bioprocess has already been industrially implemented by Evonik Industries AG while research to improve accessing prodiginine derivatives is ongoing: recent studies showed heterologous expression of the *pig* gene cluster of *Serratia marcescens* via chromosomal integration, which established the biosynthesis of prodigiosin (**1**) (Domröse et al., 2015, 2019; Cook et al., 2021). Further, a mutasynthesis approach enabled the generation of new prodiginines (Klein et al., 2017, 2018). This procedure was based on the partial disruption of the native biosynthesis pathway and feeding of monopyrrole precursor analogs, which were incorporated into new tripyrrolic compounds. A limitation of this mutasynthesis approach was a relatively low product yield of 2–12% (Klein et al., 2017). Therefore, the development of a novel mutasynthesis *chassis* with enhanced bipyrrole production capacity and an optimization of mutasynthesis were identified as promising strategies to obtain target prodiginines more efficiently.

In previous work, a prodiginine bearing a terminal allylalcohol group (**2**) was reported to show remarkable plant growth promoting properties. In addition, it was not toxic for *Caenorhabditis elegans* at concentrations where prodigiosin (**1**) was lethal for this non-target organism (Habash et al., 2020). Based on these findings, the focus of the present study is the development of a feasible synthetic approach to hydroxylated prodiginines for investigations of anti-nematode activity. This study thus reports a mutasynthesis approach in a novel, efficient bipyrrole-producing *P. putida* strain and subsequent chemical conversion, i.e., semisynthesis, toward hydroxylated prodiginine **3** (Figure 1). The mode of action against *H. schachtii* as well as combinatorial activity with di-rhamnolipids (**4**) were investigated for the first time, demonstrating potential application as antinematodal agents.

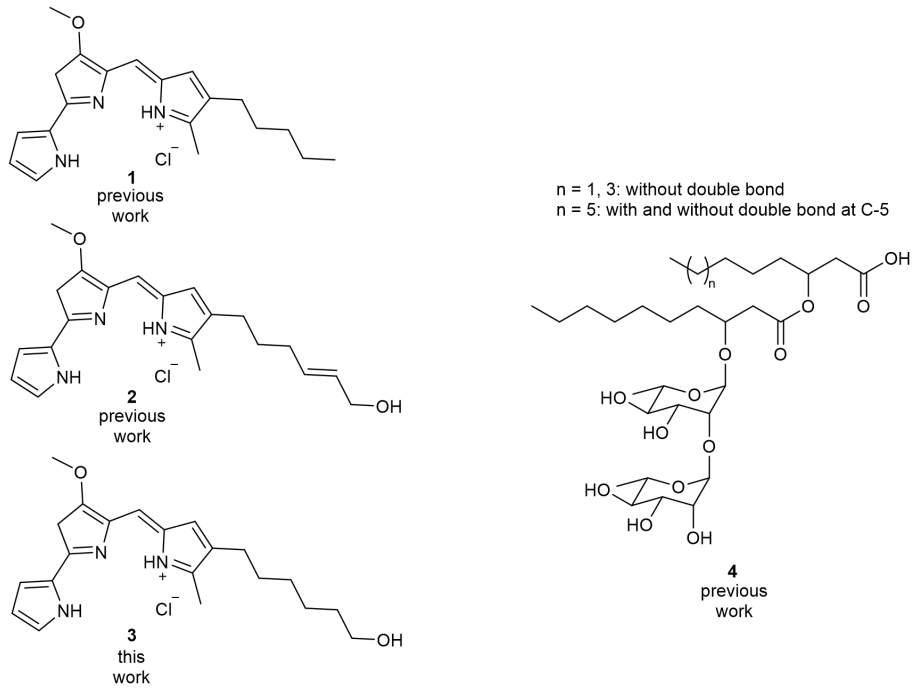

FIGURE 1
Bioactive compounds assessed in this study. The synthesis of prodigiosin **(1)** and hydroxylated derivative **(2)** has been established in previous studies. A synthesis route to hydroxylated prodiginine **(3)** is presented in this study, enabling the compound's application together with di-rhamnolipids **(4)**, which can be obtained via microbial biosynthesis as a mixture of congeners as indicated.

2. Results

2.1. Development of an enhanced *Pseudomonas putida chassis* for optimized mutasynthesis

In natural prodigiosin (**1**) biosynthesis, the monopyrrole MAP (2-methyl-3-amylpyrrole, **5**) and the bipyrrole MBC (4-methoxy-2,2′-bipyrrole-5-carbaldehyde, **6**) are condensed by a ligase (PigC in *S. marcescens*) to a tripyrrolic scaffold. The mutasynthesis approach has previously been established successfully in *P. putida* pig-r2 Δ*pigD* (Klein et al., 2017, 2018). The strain harbored the entire *S. marcescens pig* gene cluster—with the exception of the first MAP biosynthetic gene *pigD*, which was replaced by an antibiotic resistance gene. By feeding chemically synthesized monopyrroles to this MAP-deficient *P. putida* pig-r2 Δ*pigD* strain, the PigC-catalyzed condensation with MBC (**6**) led to novel tripyrrolic compounds in these previous studies.

Since mutasynthesis might be limited by biosynthetic provision of the bipyrrole precursor MBC (**6**), we aimed to establish a streamlined MBC-producing *chassis* preferentially lacking genetic and metabolic burdens. As a new strategy, a truncated *pig* gene cluster specifically designed to facilitate the biosynthesis of the bipyrrole **6** was integrated in the host. To this end, the artificial *pigAFGHIJKLMN* gene cluster (excluding the MAP (**5**) biosynthesis-encoding genes *pigBDE* and the ligase-encoding *pigC*, see Supplementary Figure S1) was assembled by PCR and yeast recombinational cloning into the yTREX vector following established protocols (Domröse et al., 2017; Weihmann et al., 2020). In this process, the promotor-less *lacZ* gene was inserted downstream of *pigN* (Figure 2A). The resulting vector was used for random transposon Tn5-based integration of the recombinant operon in the *P. putida* bacterial chromosome and LacZ was utilized as transcription reporter. Based on that, clones with strong gene expression were indicated by blue coloration as a result of X-gal conversion. Of these clones, 19 were selected and subjected to small scale cultivation, metabolite extraction and LC–MS analysis to verify bipyrrole product accumulation. Results were comparatively evaluated in relation to the previously established mutasynthesis *chassis P. putida* pig-r2 Δ*pigD* (Figure 2B). While four strains did not produce any detectable amounts of MBC (**6**), one clone (MBC17) produced a lower amount of MBC (**6**) than *P. putida* pig-r2 Δ*pigD*, and 14 accumulated the bipyrrole at higher levels (up to 8-fold increased). The best producer (MBC18) showed likewise elevated transcript levels (approx. 4-fold), indicating that a higher expression level could be reached in the new strain, which in turn contributed to higher bipyrrole synthesis. The enhanced MBC (**6**) level was verified for MBC18 in larger scale as applied in preparative mutasynthesis: Both strains, *P. putida* pig-r2 Δ*pigD* and MBC18, were cultivated in TB medium and polyurethane (PU) foam cubes were added as adsorbent for the hydrophobic compound, as previously established for prodigiosin (**1**) recovery (Domröse et al., 2015). Extracts from PU of the cultures with the newly constructed strain MBC18 contained about 12-fold more MBC (**6**) than those of the previously reported strain *P. putida* pig-r2 Δ*pigD* — a promising precondition for mutasynthesis.

The next step was to evaluate the capacity of the new strains for mutasynthesis with MBC17, MBC13, and MBC18 representing a low, an intermediate, and a high MBC level producer, respectively. The ligase PigC was thus introduced into these strains by plasmid-based expression from the IPTG-inducible P_{tac} promoter in pVLT33-pigC

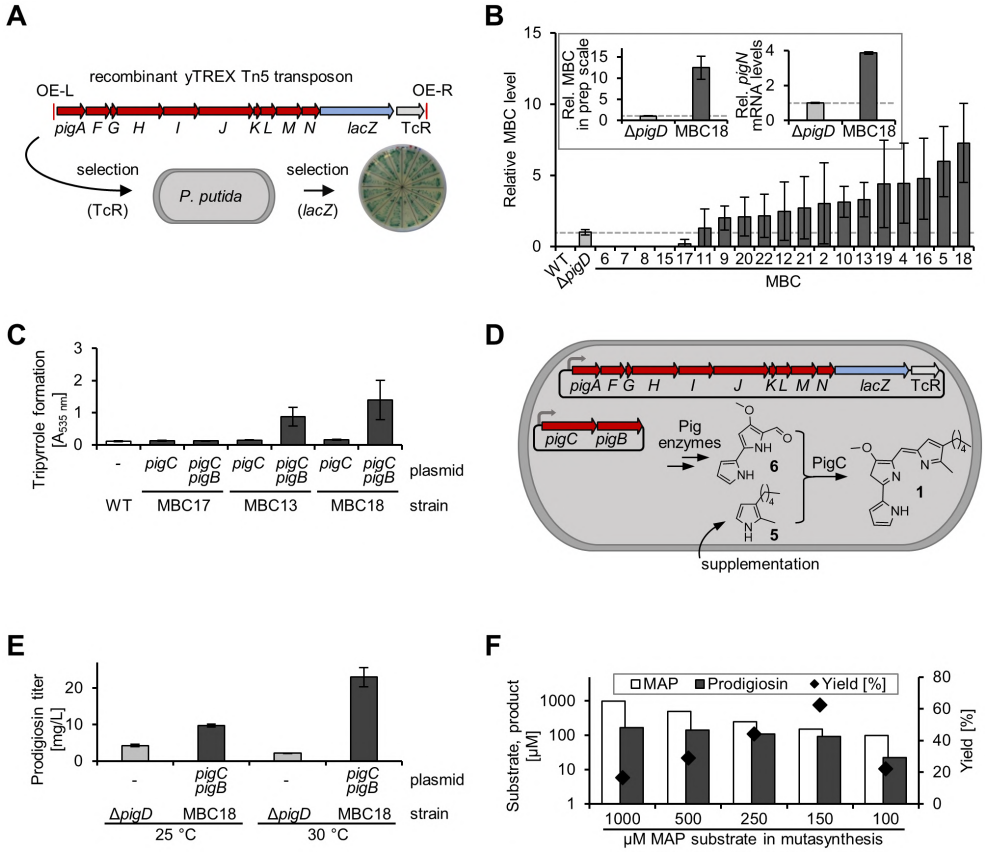

FIGURE 2
Construction of a *Pseudomonas putida* mutasynthesis *chassis*. **(A)** The artificial 4-methoxy-2,2′-bipyrrole-5-carbaldehyde (MBC) biosynthesis-encoding gene cluster was assembled by yeast-cloning and integrated in the bacterial chromosome via Tn5 transposition. After that, expressing clones were selected based on LacZ reporter activity. **(B)** Relative MBC production in small scale cultivation of engineered *P. putida* shown as x-fold increase relative to the signal of *P. putida* pig-r2 Δ*pigD*. Left Inset: Evaluation in preparative mutasynthesis setup (100 ml scale, MBC18 with pVLT33-pigC-pigB). Right inset: Relative *pigN* mRNA levels. **(C)** Dependence of the condensation of biosynthesized MBC (**6**) with supplemented MAP (**5**) on co-expression of PigB in *P. putida* stains MBC17, –13, –18 with plasmids pVLT33-pigC or pVLT33-pigC-pigB, respectively, in small scale cultivation. **(D)** Genetic setup of the new mutasynthesis *chassis* carrying the MBC (**6**) biosynthetic genes in the chromosome and expressing *pigC* and *pigB* from a plasmid. **(E)** Mutasynthesis performance of the newly established *chassis P. putida* MBC18/pVLT33-pigC-pigB in comparison with hitherto used *P. putida* pig-r2 Δ*pigD* in small scale cultivation at 25 or 30°C. The product was detected in extracts via spectrophotometry. Shown are mean values of independently replicated measurements (min. triplicates) with the respective standard deviation. **(F)** Optimization of preparative mutasynthesis in 5×100 ml scale with *P. putida* MBC18/pVLT33-pigC-pigB. The amount of substrate MAP (**5**) was varied from 1,000 µM to 100 µM to optimize conditions with respect to isolated prodigiosin (**1**) and corresponding yields (% mol of product relative to the substance amount of substrate).

(Brands et al., 2020). After small scale cultivation with supplementation of MAP (**5**, 1 mM), cells were extracted and prodigiosin-specific absorption was measured at 535 nm (Figure 2C). However, no noteworthy conversion of the fed monopyrrole to prodigiosin could be detected with either strain (MBC17, MBC13, MBC18/*pigC*).

Since it is known that in *in vitro* assays PigC does not require any additional proteins for functioning (Brass et al., 2019; Brands et al., 2020) it could be excluded that a generally necessary component was missing in the new strains. However, the previous *pigD* deletion mutant *P. putida* pig-r2 Δ*pigD* could facilitate conversion and it additionally contained functional PigB and PigE-encoding genes. This suggested an important role of either one or both of these proteins in the mutasynthesis setup (see Supplementary Figure S1). Based on their localization at the membrane and the proven importance of their membrane-anchoring domains, it may further be speculated that the last precursor-delivering enzymes PigN/F and PigB, as well as PigC could form a membrane-associated protein complex (Williamson et al., 2005; Chawrai et al., 2012; Couturier et al., 2019). This suggested that this complex consisting of PigC and PigN/F, but devoid of PigB might not be functional (see also Supplementary Figures S2, S3). PigB co-expression was therefore tested next by using plasmid pVLT33-pigC-pigB in the new strains (Figures 2C,D). While in the low-level precursor providing strain MBC17, co-expression of PigB did not lead to prodigiosin (**1**) formation, an increased signal was observed with MBC13 and highest levels were found in the high-level MBC-providing strain MBC18 (MBC17, MBC13, MBC18/*pigC-pigB*).

As a next step, mutasynthetic prodigiosin (**1**) production of the newly established *chassis P. putida* MBC18/pVLT33-pigC-pigB was assessed in comparison with hitherto used *P. putida* pig-r2 Δ*pigD*. To this end, small scale cultivation was used to test performance at 25°C as previously established (Klein et al., 2017, 2018) and at the optimal *P. putida* growth temperature 30°C (Figure 2E). At 25°C, 4.2 and 10 mg/L prodigiosin were obtained, while at 30°C, 2.3 and 21 mg/L were produced with *P. putida* pig-r2 Δ*pigD* and MBC18/pVLT33-pigC-pigB, respectively. These results therefore verified enhanced

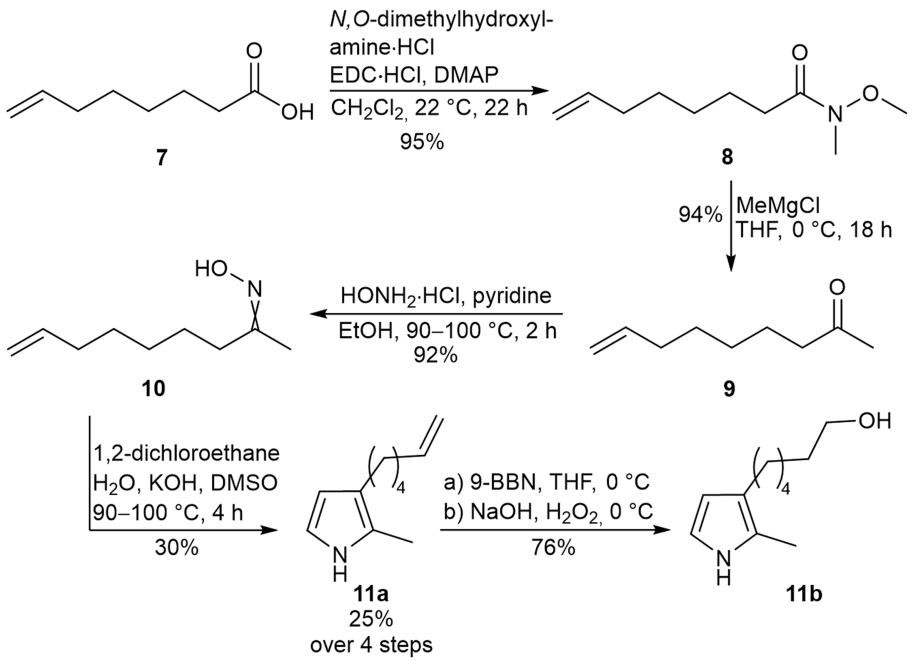

FIGURE 3
Synthesis route toward the 2,3-disubstituted pyrrole precursors **11a** and **11b**.

performance of the newly constructed *chassis*, especially at 30°C, so all following experiments were conducted at this temperature.

Since during small scale cultivation under the applied conditions with excess of MAP (1 mM, **5**), MBC (**6**) was consumed to below limits of quantification, an adjustment of MAP concentrations was tested next. Hence, different MAP (**5**) concentrations were supplemented to *P. putida* MBC18/pVLT33-pigC-pigB in order to potentially match the levels of both precursors in preparative scale experiments and optimize yields (Figure 2F). The best yield of 62% purified product was obtained with 150 µM MAP (**5**). Isolation by soxhlet extraction of PU and column chromatography on silica yielded 17 mg prodigiosin (**1**) from 500 ml mutasynthesis cultures. This outcome corresponding to 34 mg/l represented an improvement to previously reported 17 mg/l, obtained with the same pyrrole via comparable procedures (Klein et al., 2017). Remaining MBC (**6**) was below 2 µM in this experiment (Supplementary Figure S4). This procedure was therefore deemed as suitable for further steps toward accessing the hydroxylated target compound **3**.

2.2. Chemical synthesis of pyrroles, muta- and semisynthesis of hydroxylated prodiginine 3

In order to establish a synthesis route to a hydroxylated prodiginine tripyrrole, a pyrrole with terminal double bond was aimed as precursor to allow a late-stage semisynthetic functionalization. Previously reported prodiginine **2** was synthesized chemically in a condensation reaction of *Boc*-**6** and a pyrrole with allylalcohol function (Habash et al., 2020). With this approach, the functional group is already applied, but further modification and derivatization are less feasible. The here presented mutasynthesis approach is more flexible in terms of late-stage functionalization and allows to functionalize the obtained mutasynthesis product in a variety of ways, such as with a bromination or oxidation. In order to yield the hydroxylated prodiginine **3**, we applied a hydroboration as semisynthetic step.

Starting from carboxylic acid **7**, Weinreb-amide **8** and ketone **9** were obtained in two steps, consecutively. Afterwards, oxime **10** was synthesized to be used as starting material in the Trofimov pyrrole synthesis toward pyrrole **11a**, as previously described (Mikhaleva et al., 1981; Trofimov et al., 2015; Klein et al., 2018). The Trofimov pyrrole synthesis represents the yield-limiting step in this synthesis sequence (Figure 3). This could be explained by the strongly basic reaction conditions, which favor side-product formations as described previously (Ivanov et al., 2014). Observed side-products were a ketoxime diether and an *N*-alkylated pyrrole, which could be removed by flash column chromatography on silica. In a subsequent hydroboration with the organoborane 9-BBN (9-Borabicyclo[3.3.1]nonane), a hydroxylated pyrrole **11b** was obtained as precursor.

Both pyrroles were tested as mutasynthons, but only pyrrole **11a** was converted in *P. putida* MBC18/pVLT33-pigC-pigB (Figure 4A). The hydroxylated group likely prevents the pyrrole **11b** from crossing the cell membrane, since PigC-mediated condensation was observed in experiments with lysate (Figure 4B). Therefore, 150 µM **11a** was applied in a preparative mutasynthesis, yielding 30 mg/L of the corresponding tripyrrole **12** which corresponds to 54% yield.

The hydroxylated prodiginine **3** was synthesized in a final semisynthetic step by hydroboration of the obtained mutasynthesis product **12**, yielding targeted compound **3** in 65% yield (Figure 4C). Notably, for the hydroboration to be successful, the mutasynthesis product had to be purified via reversed phase column chromatography in advance. Overall, a hybrid synthesis route for a

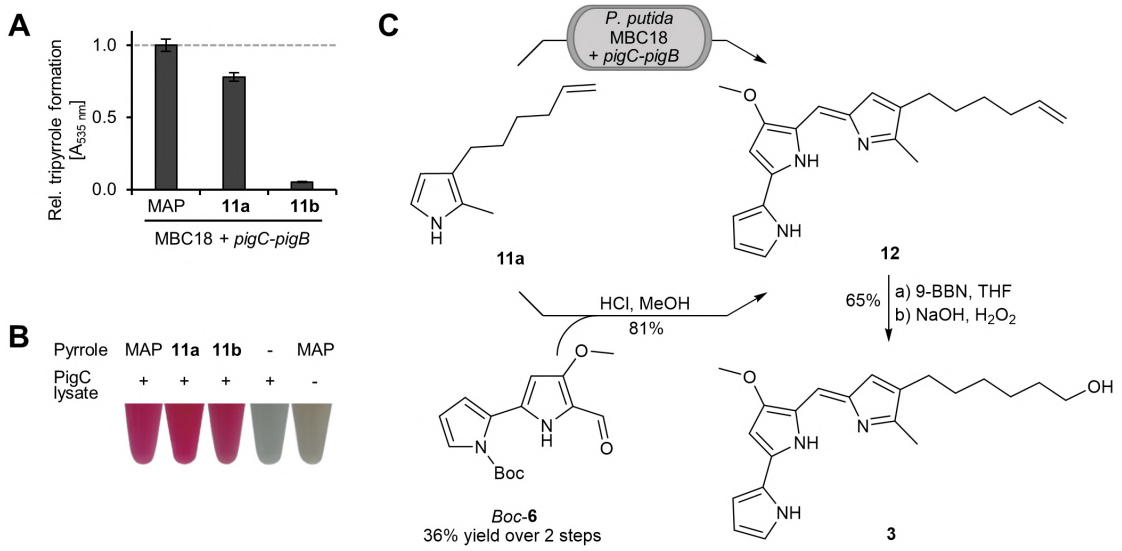

FIGURE 4
Synthetic route toward hydroxylated prodiginine 3. **(A)** Mutasynthetic tripyrrole formation upon feeding of **11a** and **11b**, respectively, in small scale cultivation of *P. putida* MBC18/pVLT33-pigC–pigB. The products were detected spectrophotometrically and quantified relative to the signal upon MAP (**5**) supplementation. Mean values of triplicate measurements with the respective standard deviation are shown. **(B)** Assessment *in vitro* of PigC substrate acceptance, shown as tripyrrole-typical coloration of reaction mixtures after incubation of lysate from PigC-expressing *E. coli* cells with MBC (**6**) and monopyrroles. **(C)** Synthesis scheme of hydroxylated prodiginine **3**. Pyrrole **11a** was supplemented to the MBC producing strain *P. putida* MBC18/pVLT33-pigC–pigB in preparative mutasynthesis to obtain the product **12**. As reference, the compound was also synthesized chemically in a condensation reaction with *Boc*-protected MBC (**6**). By the following semisynthetic hydroboration step, the final hydroxylated prodiginine **3** could be obtained.

hydroxylated prodiginine involving advantageous biosynthesis of the bipyrrole precursor **6** instead of laborious organic synthesis could be established.

2.3. Impact of prodiginines on the plant-parasitic nematode *Heterodera schachtii*

The main focus in this study was on hydroxylated prodiginine **3** for the above mentioned reasons. Additionally, the natural product prodigiosin (**1**) was used as reference in all subsequent assays. The individual effects of the hydroxylated prodiginine **3** and prodigiosin (**1**) against the PPN *H. schachtii* were determined first. To this end, the half maximal effective concentration (EC_{50}) for the reduction of nematode numbers on the model plant *Arabidopsis thaliana* was assessed. Prodiginines were found to inhibit nematode infestation by up to 80%. The EC_{50} (nematode infection) was 31.2 µM for hydroxylated prodiginine **3** and 15.1 µM for prodigiosin (**1**) (Figure 5). Although the synthesis of the previously presented prodiginine **2** is relatively laborious it appeared still interesting to validate its impact on *H. schachtii*. Prodiginine **2** and an alternative prodiginine with a side chain one carbon longer than prodiginine **3** (compound **13**, see Supplementary Information) did not exhibit stronger effects compared to prodiginine **3** (see Supplementary Figure S6) thus justifying our focus on hydroxylated prodiginine **3**.

A next aim was to pinpoint the nematode's life stage(s) and the time during host-pathogen interaction when the effect of prodiginines on the nematode becomes obvious. Therefore a time-resolved analysis of the nematodes' reaction to application of prodigiosin (**1**) and the hydroxylated prodiginine **3** was performed. To this end, fitness parameters of second-stage juveniles of *H. schachtii* (J2), nematode infection of *A. thaliana* and nematode development at the plant were investigated. These parameters were evaluated at different time points during exposure of the parasite to the above determined EC_{50} (nematode infection).

The motility of *H. schachtii* J2, which were exposed to prodigiosin (**1**) and the hydroxylated prodiginine **3** at their EC_{50} concentrations for 1 h, was significantly reduced by 32 and 39%, respectively, compared to the control (Figure 6A). An investigation of *H. schachtii* J2 stylet movement revealed a significant reduction in the frequency of thrusting at *A. thaliana* roots by 19 and 16% upon prodigiosin (**1**) and hydroxylated prodiginine **3** application, respectively (Figure 6B). This could be the reason that the number of nematodes that successfully penetrated the root epidermis (Figure 6C) and established a sedentary interaction with the plant was significantly reduced by prodiginines by 28 to 41% compared to the control (Figure 6D). Finally, the growth of *H. schachtii* females and males developing from J2 that successfully infected the plant despite prodiginine exposure was slightly reduced but not significantly impaired by prodiginines (Figure 6E).

The presented data provides for the first time specific hints to the mode of action of prodiginines and substantiates that prodiginines exert a direct antagonistic effect on *H. schachtii*. In contrast, the antinematodal effect of rhamnolipids has recently been shown to be indirect, i.e., triggering plant defense mechanisms (Bredenbruch et al., 2023). Based on these findings,

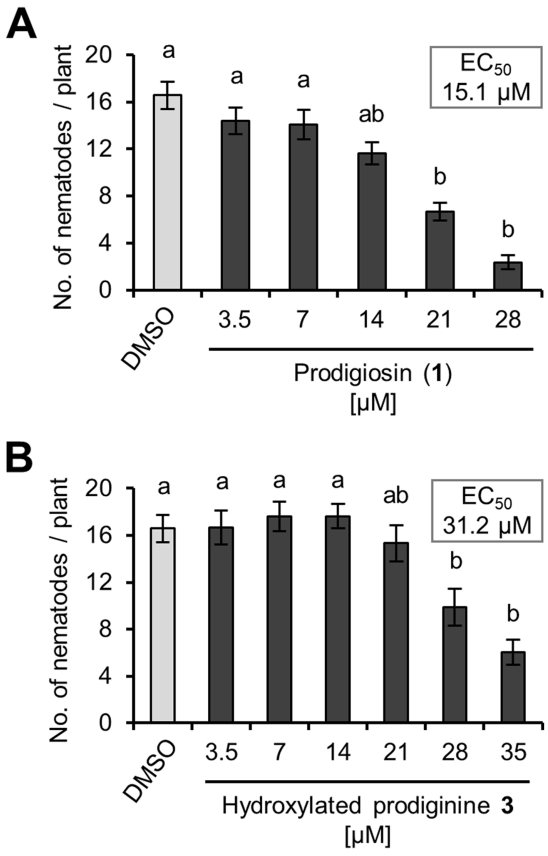

FIGURE 5
EC_{50} determination of prodiginines on the plant-parasitic nematode *Heterodera schachtii*. **(A)** Impact of prodigiosin (**1**) on nematodal plant infestation. **(B)** Impact of hydroxylated prodiginine **3** on nematodal plant infestation. The impact on *H. schachtii* was assessed as reduction of nematode numbers on *Arabidopsis thaliana*. EC_{50} values (effective concentration that causes a reduction of nematode infestation of *A. thaliana* by 50%) were calculated by using 'CompuSyn'. Results are expressed as the mean±standard error of three independent biological replicates ($n \geq 18$). Different letters indicate statistically significant differences among treatments according to Dunn's Method ($p<0.05$).

it is intriguing to assess the combined effects of prodiginines and rhamnolipids as a synergistic activity against nematodes may be hypothesized. For these investigations the previously evaluated and described mixture of di-rhamnolipid congeners (Bredenbruch et al., 2023) was chosen, which revealed an EC_{50} (nematode infection) of 2.8 µg/mL (corresponding to approximately ~ 4.3 µM; Supplementary Figure S7).

Investigations of the combined activities of prodiginines (**1** and **3**) and di-rhamnolipids (**4**) revealed that the combination of the two compounds was more effective against nematode parasitism than the individual compounds, i.e., the combined application reduced the required concentrations for the same effect (Figures 6F,G). To obtain, for instance, 50% nematode control, it was sufficient to apply ¼ the concentration of hydroxylated prodiginine **3** and di-rhamnolipids (**4**) together or prodigiosin (**1**) and di-rhamnolipids (**4**) together instead of the full dose of each compound individually (see Supplementary Figure S8 for dose response curves and combination index plots).

3. Discussion

3.1. Development of hybrid synthesis toward tailored hydroxylated prodiginine

The concept of mutasynthesis is highly attractive for synthetic chemists as a method for structural diversification of natural products by using genetically engineered microorganisms (Kirschning et al., 2007). By using nature's enzymatic biosynthetic machinery for the synthesis of precursor MBC (**6**) this study presents an environmentally friendly way by avoiding heavy metal catalyzed synthesis of *Boc*-**6** (Dairi et al., 2006; Domröse et al., 2015). Furthermore, this approach allows the incorporation of non-native building blocks into new derivatives due to enzyme promiscuity (Sun et al., 2015).

While in our previous studies, prodigiosin (**1**) biosynthesis resulted in titers, e.g., ranging from 60 to 150 mg/L (Domröse et al., 2015, 2017, 2019) depending on the applied conditions, mutasynthetic derivatives were only obtained with 0.6–3.1 mg/L (Klein et al., 2018) or maximally 19.8 mg/L (Klein et al., 2017). In general, this may reflect poor substrate entry into the cells, a low activity of PigC toward unnatural substrates, an insufficient MBC (**6**) supply, or a combination of these factors. In the present study, the MBC (**6**) supply was addressed by implementing expression of MBC (**6**) biosynthetic genes, which successfully led to reaching enhanced titers of 30–34 mg/L. Further improvements are conceivable with alternative ligase enzymes. The new strain setup of *P. putida* MBC18 allows their exchange more easily by use of alternative plasmids, whereas strain *P. putida* pig-r2 Δ*pigD* carried all *pig* genes in the chromosome. In this context, our studies uncovered, that coexpression of *pigB* is essential in this setup. It might be speculated that the enzymes PigN/F and PigB, that naturally deliver the pyrrole precursors, as well as PigC assemble to form a membrane-associated complex (Williamson et al., 2005; Chawrai et al., 2012; Couturier et al., 2019). This may hypothetically ensure fast product release via the membrane. Our findings suggest that an only partial assembly of this putative complex consisting of PigC and PigN/F, but devoid of PigB is not functional. Notably in this context, *Janthinobacterium lividum* appears to contain a *pigCB* fusion in its *pig* gene cluster (Schloss et al., 2010). However, further studies are required to elucidate these interactions.

Previous studies investigated the versatile substrate range of the condensing enzyme PigC (Klein et al., 2017, 2018; Brass et al., 2019). According to these findings, the present study focused on a mutasynthesis approach toward tailored hydroxylated prodiginines by feeding modified pyrroles to the new strain *P. putida* MBC18. In advance, the mutasynthesis experiment was optimized concerning the yields (Figure 2F). Notably, feeding a high amount of MAP (**5**) did not lead to a likewise high amount of prodigiosin (**1**) and thus resulted in relatively low yields up to 17%. Interestingly, by varying the MAP (**5**) concentration in a range of 100–1,000 µM, the prodigiosin (**1**) concentrations obtained (93–167 µM) were relatively constant and did not reflect the magnitude of the fed pyrrole concentration (Figure 2F). This observation could be explained by a substrate inhibition of involved enzymes. A PigC substrate inhibition by MAP (**5**) has been demonstrated in a previous study: conversion assays using different concentrations of MAP (**5**) at a fixed MBC (**6**) concentration suggested an ordered kinetic mechanism in which MBC (**6**) has to bind before MAP (**5**) (Chawrai et al., 2012). In the present study, 62% prodigiosin (**1**), obtained with an adjusted MAP (**5**) concentration, is the highest

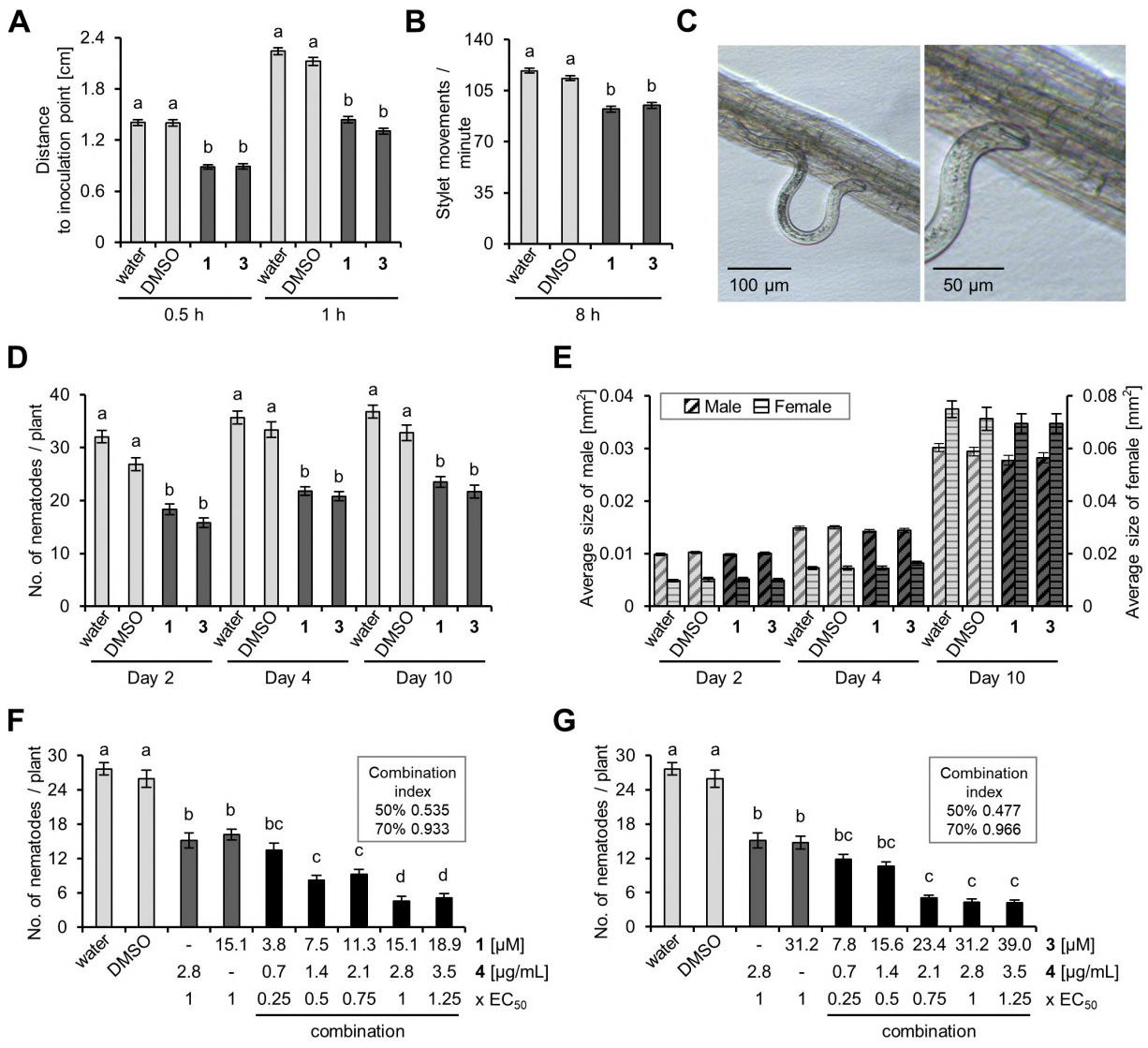

FIGURE 6
Prodiginine impact on *Heterodera schachtii* fitness parameters, plant parasitism, and combined activity with di-rhamnolipids. **(A)** *H. schachtii* J2 motility, assessed as distance to an inoculation point after incubation. **(B)** Stylet thrusting at *Arabidopsis thaliana* roots, assessed as movements/min. **(C)** *A. thaliana* root with an invading J2. **(D)** Nematode infection rate at *A. thaliana*, investigated at different time points after inoculation. **(E)** Nematode size development, evaluated during 10days after inoculation. **(F,G)** The combined effect of prodigiosin (**1**) and di-rhamnolipids (**4**) as well as hydroxylated prodiginine **3** and di-rhamnolipids (**4**), respectively, was assessed at 10days after inoculation. Combination indices were calculated using 'CompuSyn'. Results are expressed as the mean±standard error of at least three biological replicates [n≥614 **(A)**; *n*=40 **(B)**; *n*=56 (D); *n*≥70 **(E)**; *n*≥20 **(F)**; *n*≥22 **(G)**]. Different letters indicate statistically significant differences among treatments according to Dunn's Method ($p<0.05$). EC_{50} is the effective concentration that causes a reduction of nematode infestation of *A. thaliana* by 50%. Prodigiosin (**1**) and hydroxylated prodiginine **3** were used at their EC_{50} concentration in **A**, **B**, **D**.

yield achieved in a preparative scale. However, further investigation and optimization of the mutasynthesis approach may lead to even higher yields, for example by feeding the pyrrole over a period of time to overcome PigC substrate inhibition.

As mentioned above, a strength of mutasynthesis is the substrate promiscuity of the enzymes used. Results of an *in vitro* PigC assay showed acceptance for both pyrroles **11a** and **11b** (Figure 4B). However, using **11b** as mutasynthon in an *in vivo* approach did not result in formation of the targeted hydroxylated prodiginine **3**, rendering an alternative approach necessary. We assume that the hydroxyl group prevents the pyrrole **11b** from crossing the cell membrane. To overcome this issue, pyrrole **11a** was supplemented as mutasynthon to produce prodiginine **12** in a yield of 54%. The hydroxyl group was introduced in a semisynthetic step toward the targeted prodiginine **3**. Notably, the mutasynthesis product **12** had to be purified via reversed-phase column chromatography for the final hydroboration step to succeed. Alternative purification methods, such as aqueous washing steps (sat. NH_4Cl, sat. $NaHCO_3$, sat. Na_2SO_4, sat. NaCl or sat. LiCl) or normal phase column chromatography (silica or alox) led to an apparently inactivated prodiginine, which did not show any conversion to the hydroxylated prodiginine **3**, not even under high excess of the hydroboration agent 9-BBN. Quantitative ^{1}H-NMR spectroscopy showed, that the purity of the mutasynthesis product, which was isolated by normal phase column chromatography

increased from 60 ± 3% to 92 ± 5% after an additional reversed-phase column chromatography. This finding was crucial for the success of the hybrid synthesis toward hydroxylated prodiginine **3**, even if the impurities that led to an inactivation of isolated mutasynthesis products could not be identified and further investigations are necessary.

3.2. Prodiginine-induced reduction of the fitness and infectiousness of the plant-parasitic nematode *Heterodera schachtii*

Since PPN mostly inhabit the soil and primarily attack below-surface parts of plants, it is often challenging to control PPN. Microscopic life in the rhizosphere is particularly robust and naturally occurring microbial compounds have been studied and commercialized as potent bioactive ingredients against a diversity of soil-borne pathogens over the past decades (Handelsman and Stabb, 1996; Haas and Défago, 2005; Köhl et al., 2019). Our previous work revealed that prodiginines and rhamnolipids possess activity against the PPN *H. schachtii* (Habash et al., 2020; Bredenbruch et al., 2023). Rhamnolipids exert their activity by triggering plant defense responses effective against nematodes. Unlike that, this current study demonstrated that prodigiosin (**1**) and hydroxylated prodiginine **3** directly antagonize *H. schachtii* J2 by inhibiting motility and stylet thrusting (Figures 6A,B). The J2 is the infective larval stage of *H. schachtii*, which migrates within the soil towards the root. In the natural habitat, *H. schachtii* J2 migrate at the maximum speed when there is no lateral movement and each body part usually follows the movement of its front part (Wallace, 1958). The presence of the investigated prodiginines appears to hinder nematode forward movement.

Stylet thrusting of *H. schachtii* J2 is a prerequisite for destructively invading the host's root tissue and later—after reaching the vascular cylinder—carefully probing plant cells until a suitable cell is found, which becomes the initial syncytial cell (ISC). The frequency of this stylet movement is significantly reduced by prodiginines, as demonstrated in this study. The continuous vigorous stylet thrusting of J2 is an energy consuming process (Wyss and Zunke, 1986; Grundler et al., 1991; Wyss, 1992; Wyss and Grundler, 1992). Since it has been described that prodiginines can uncouple mitochondrial F-ATPases due to their H^+/Cl-symport activity (Konno et al., 1998), their direct effect on the cellular energy metabolism might be one explanation for the lower frequency of J2 stylet movements.

Once *H. schachtii* J2 accomplish the formation of permanent feeding sites, they become immobile and change from a migratory into a sedentary form (Wyss, 1992). Prodiginines were observed to interfere with nematode invasion and infection of *A. thaliana*. However, female and male development at the host plant is not influenced by prodiginines at 2 and 4 days after the inoculation, while it is slightly impaired after 10 days (Figures 6D,E). As stated in our previous study, a significant reduction of female size due to prodigiosin application can be observed after 13 days (Habash et al., 2020). Probably, the impact of prodiginines on the pathogen's development at the root becomes obvious only at later time points after infection. Future studies should investigate this aspect further and additionally determine whether prodiginine exposure interferes with reproduction.

While investigations on the molecular mode of action for the interaction of prodiginines with nematodes are missing, studies of their effects on bacteria document a disturbing impact on biological membranes and reactive oxygen species (ROS) generation (Darshan and Manonmani, 2015, 2016; Suryawanshi et al., 2017; Ravindran et al., 2020; Choi et al., 2021). Whether prodiginines cause disruption of PPN membranes and whether this contributes to the observed effects still needs to be elucidated.

Unlike "single compound - single target" approaches, multicomponent therapeutics enable interactions with multiple targets (Keith et al., 2005; Hopkins, 2007; Yildirim et al., 2007). The discovery of drug–drug combinations offers promising strategies for (1) the improvement of drug treatment efficacy, (2) the reduction of drug dosage to avoid toxicity, and (3) the minimization of drug resistance evolution (Jia et al., 2009; Cheng et al., 2019). Our results demonstrate that, when applying prodiginines and di-rhamnolipids combined, only ¼ of the concentration rather than the full dose of each single agent is required to achieve the same nematode control efficacy (50% reduction of nematode infestation; Figures 6F,G). This validates the two compounds to exert synergistic effects. Intriguingly, by increasing the doses for combinations, the combined effect is diminished and even appears antagonistic. Similar results were reported previously in the analyses of antibacterial effects, which were dependent on the ratio of prodigiosin and rhamnolipids (Hage-Hülsmann et al., 2018).

Synergistic effects between biosurfactants including rhamnolipids and various antibiotics have been described multiple times before (Boonlarppradab et al., 2008; Williamson et al., 2008; Sotirova et al., 2012; Magalhães and Nitschke, 2013; Das et al., 2014; Rossi et al., 2016). On the one hand, rhamnolipids, which exhibit surface-active properties, can increase the solubility of the drug and facilitate its access to target cells (Beal and Betts, 2000; Abdel-Mawgoud et al., 2010). On the other hand, rhamnolipids can perturb the packing of the cell membrane phospholipids by intercalating into the bilayer, which leads to increased permeability of the cell membrane (Dowhan, 1997; Ortiz et al., 2006). As a consequence, the interaction of combined applications facilitates more effective penetration through biological interfaces to better reach the site of action (Bhadoriya et al., 2013; Bnyan et al., 2018; Hage-Hülsmann et al., 2018).

However, the role of rhamnolipids in combined antinematodal activity goes far beyond that. Plants have developed sophisticated defense mechanisms that enhance resistance to their enemies. After perception of rhamnolipids, early events of cell signaling, including calcium influx, MAP kinase activation, ROS accumulation, and defense-related gene stimulation were detected in plants (Garcia-Brugger et al., 2006; Varnier et al., 2009). Besides, rhamnolipids also trigger the activation of a phytohormone-regulated immune signaling network and thus modulate late defense responses to a diversity of phytopathogens (Pieterse et al., 2012; Sanchez et al., 2012). A recent study confirmed that di-rhamnolipids put *A. thaliana* on alert so that the plant responds stronger to *H. schachtii* attack (Bredenbruch et al., 2023). The combined application of rhamnolipids and prodiginines may therefore effectuate molecular structures and processes on multiple levels in both, the plant and the pathogen, and may pose a promising starting point for the development of multicomponent antinematodal agents.

4. Materials and methods

4.1. Engineering and characterization of *Pseudomonas putida* strains, PigC activity assay

4.1.1. Bacterial strains and standard cultivation conditions

Cultivation of *P. putida* KT2440 (Nelson et al., 2002; Belda et al., 2016) was conducted at 30°C, if not stated otherwise, shaking (130 rpm) in Erlenmeyer shake flasks in LB medium (Carl Roth, Karlsruhe, Germany), or on LB agar plates (LB medium completed with 15 g/L Agar). Small scale production tests were conducted in TB medium (Carl Roth, Karlsruhe, Germany) in Flowerplates (m2p-labs GmbH, Baesweiler, Germany). Cultures of *P. putida* pig-r2 Δ*pigD* (Klein et al., 2017) were supplemented with 80 µg/mL streptomycin, MBC strains created in the present study with 50 µg/mL tetracycline, and MBC strains carrying pVLT33 derived plasmids with 25 µg/mL kanamycin. *Escherichia coli* strains S17-1 (Simon et al., 1983; used for conjugation), and DH5α (Hanahan, 1983; used for cloning) were cultivated at 37°C under constant agitation (120 rpm) in shake flasks in liquid LB medium or on LB agar plates.

4.1.2. Cloning of integrative yTREX vector with MBC biosynthetic genes and ligase expression plasmids

The synthetic MBC biosynthesis-encoding *pig* gene cluster was PCR-amplified in three parts for assembly into the yTREX vector (Domröse et al., 2017; Weihmann et al., 2020) which was linearized with endonuclease I-*Sce*I: *pigA* (primers AD142 + 171, 1,239 bp), *pigFGHI* (primers AD172 + 162, 4,867 bp) and *pigJKLMN* (primers AD163 + 164, 5,033 bp) using vector pPIG (Loeschcke et al., 2013) as template. In addition, *lacZ* was amplified as promotorless gene (primers AD124 + 125, 3,127 bp) using vector pRcExpII2-YF1-FixJ-PFixK2-LacZ (Weihmann et al., 2020) as template. All genes were amplified with the respective 5′-UTR sequences including the ribosome binding sites; primers added homology arms to each of the fragments. Assembly of the vector yTREX-MBC-lacZ, carrying the gene cassette *pigA-pigFGHIJKLMN-lacZ*, in *Saccharomyces cerevisiae* VL6-48 was conducted as previously described (Domröse et al., 2017; Weihmann et al., 2020). Plasmid pVLT33-pigC, carrying the *pigC* gene with an adapted codon usage for *P. putida* (Brands et al., 2020), was used for PigC expression. The *pigB* gene was amplified (primers RW144 + 145, 2090 bp) using yTREX-pig (Domröse et al., 2017) as template. The vector and PCR product were hydrolyzed with endonucleases *Hind*III und *Xba*I and ligated to obtain pVLT33-pigC-pigB. All plasmids and oligonucleotides are listed in Supplementary Table S1.

4.1.3. Generation of MBC producing *Pseudomonas putida* strains

To generate *P. putida* production strains, the plasmid yTREX-MBC-lacZ was transformed into *E. coli* S17-1 and further transferred to *P. putida* KT2440 via conjugation as previously described (Weihmann et al., 2020). Since yTREX constructs do not replicate in *P. putida*, positive selection for strains in which Tn5 transposition of the recombinant yTREX transposon occurred, could be conducted by using LB medium supplemented with tetracycline. In addition, 25 µg/mL irgasan was added to prevent *E. coli* growth. Among exconjugants, production strains were identified visually after 16 h of cultivation on agar plates (Weihmann et al., 2020): The selection medium after conjugation was additionally supplemented with 0.3 mM X-gal (stock solution: 50 mM in DMF), and expression strains were identified by blue color due to β-galactosidase activity.

4.1.4. Analysis of MBC biosynthesis in *Pseudomonas putida*

For verification of MBC biosynthesis in small scale cultivation, expression cultures of *P. putida* pig-r2 Δ*pigD* and MBC strains (denoted with 2, 4, 5, 6, 7, 8, 9, 10, 11, 12, 13, 15, 16, 17, 18, 20, 21 or 22) (n = 4, independent biological replicates) were cultivated in Flowerplates. To this end, 1 mL precultures in LB medium were used for inoculation of 1,1 mL main cultures in TB medium to an OD (650 nm) of 0.05. Flowerplates were covered with breathable air sheets (139.7 µm sterile Rayon films, VWR North America Cat.No. 60941-086) and incubated for 24 h (30°C, 1,400 rpm). After that, 700 µL samples were used for cell harvesting (15,000 rpm, 5 min). The pellet was resuspended in 300 µL methanol and subjected to sonication in a water bath (Sonorex RH 100 H) for 10 min. After centrifugation (15,000 rpm, 5 min), the supernatant was dried at 45°C under reduced pressure (in a Concentrator 5,301). For 2-phase extraction, 300 µL DCM und 300 µL MilliQ-water were added and mixed well, before centrifugation (15,000 rpm, 3 min). The organic lower layer was transferred in a fresh reaction tube and the extraction repeated. The resulting pooled DCM was again dried (45°C, Eppendorf Concentrator 5,301). Samples were resuspended in 200 µL methanol, centrifuged (15,000 rpm, 1 min) and finally subjected to LC–MS analysis or stored until that at 4°C. LC–MS analysis was conducted using an HP 1100 Series LC/MSD (Agilent Analytical Instruments) with an Atlantis T3 column (3 µm, 3*100 mm) from Waters. The eluents water (A) and methanol (B), both supplemented with 0.1% formic acid, were used for gradient chromatography at 0.6 mL/min flow rate: Starting at 90% A and 10% B, increasing to 60% B in 4 min, then in further 2 min to 100% B, which was maintained for 4 min. After that, starting conditions were implemented again (10% B) and held for 1 min. Sample volumes of 10 were injected and detection was accomplished with a G1315A DAD-detector and an G1946A mass spectrometer (API-ES, positive ion mode, single quadrupole detector, m/z-range 100–2000). After verification of specific signals corresponding to the ion $[M+H]^+$ of MBC (191 m/z), the UV/Vis signal (364 nm) of the corresponding peaks detected at 6.7 min were evaluated for relative quantification with reference to the values obtained with strain *P. putida* pig-r2 Δ*pigD*. For subsequent routine MBC analysis, HPLC-PDA analysis using an LC-10Ai (Shimadzu Deutschland GmbH, Duisburg, Germany) was also applied with an SPDM10Avp photodiode array detector (PDA), and an Accucore™ C18 HPLC column (2.6 µm, 4.6*50 mm) from Thermo Fisher Scientific (Walkham, United States). At a column oven temperature of 30°C, 10 µL samples were analyzed at 1 mL/min flow rate in a gradient elution using water (A) and acetonitrile (B), both with 0.1% formic acid: Starting at 95%A and 5% B for 0.5 min, increasing to 25% B at 0.9 min, to 55% at 9.5 min, and to 98% at 10 min, which was held for 1 min, before returning to 5% B at 11.5 min, which was maintained for 2 min. Chromatograms were recorded at 360 nm and detected MBC at 4.5 min (λ_{max} 363 nm). To analyze MBC in 100 mL cultures, 1 g polyurethane (PU) foam

cubes were added as described for mutasynthesis conditions, and extracted with 15 mL ethanol.

4.1.5. Quantification of *pig* gene transcript by RT-qPCR

Reverse transcription (RT) followed by quantitative PCR (qPCR) was employed to quantify mRNA levels of *pigN*. Precultures, grown in LB medium, were used to inoculate 1 mL TB main cultures of *P. putida* pig-r2 Δ*pigD* and MBC18 with pVLT33-pigC-pigB to an OD (650 nm) of 0.05 ($n = 3$, independent biological replicates). These were incubated shaking (1,200 rpm) at 30°C for 4 h, before induction of the latter with 0.5 mM IPTG (10 µL of a 50 mM stock solution in water). After additional 4 h incubation, 500 µL of each culture were harvested to extract total RNA with the NucleoSpin® RNA-Kit (Macherey-Nagel, Düren, Germany). DNAse treatment was conducted in three steps with DNase from Macherey-Nagel, Qiagen (Hilden, Germany) and Ambion (Thermo Fisher Scientific). The Maxima Reverse Transcriptase (Thermo Fisher Scientific) was used for reverse transcription of 2000 ng RNA in 20 µL volumes. The qPCR reaction mix contained 9.2 µL of the cDNA solution (diluted to correspond to 50 ng RNA), 0.4 µL containing 4 pmol of each primer (stocks: 10 pmol/µL), and 10 µL Maxima SYBR Green/ROX qPCR Master Mix (2x; Thermo Fisher Scientific). All qPCR reactions were carried out as technical quadruplicates in addition to the biological triplicates. Controls without reverse transcriptase and without template as well as monitoring of PCR product melting curves ensured signal specificity. Calibration with the pPIG plasmid allowed determination of *pigN* copy numbers in *P. putida* pig-r2 Δ*pigD* and MBC18, which were 177×10^4 ($\pm 4 \times 10^4$) and 683×10^4 ($\pm 12 \times 10^4$) per 100 ng total RNA, respectively. For direct comparison, the data was evaluated as expression levels relative to the signal of *P. putida* pig-r2 Δ*pigD*. To corroborate comparability, the transcript levels of *rpoD* were analyzed as internal control, which yielded similar results in both strains as expected [571×10^4 ($\pm 16 \times 10^4$) and 750×10^4 ($\pm 30 \times 10^4$) per 100 ng total RNA].

4.1.6. Mutasynthesis in small scale cultivation

Expression cultures of *P. putida* pig-r2 Δ*pigD* and strains MBC13, −17, −18 with plasmids pVLT33-pigC or pVLT33-pigC-pigB ($n = 3$, independent biological replicates) were cultivated in Flowerplates. Precultures in 1 mL LB medium were used for inoculation of 1 mL main cultures in TB medium to an OD (650 nm) of 0.05. Flowerplates were covered with breathable air sheets and incubated for 4 h (30°C, 1,200 rpm), before 1 mM MAP was supplemented to the cultures (20 µL of a 50 mM stock solution in DMSO) and gene expression in strains with plasmids was induced by addition of 0.5 mM IPTG (10 µL of a 50 mM stock solution in water). Cultivation was subsequently continued for 20 h at 30°C or 25°C. After that, cultures were harvested (12,000 rpm, 2 min). The pellets were pre-resolved with 20 µL milliQ-water and extracted with 500 µL acidified ethanol [4% (*v*/*v*) 1 N HCl in ethanol]. After centrifugation (2 min, 14,000 rpm), 150 µL samples were either diluted by a factor of 10 or directly subjected to spectrophotometric analysis in a microplate reader "Infinite M1000 pro" (Tecan Group LTD., Maennedorf, Switzerland) to measure characteristic absorption spectra from 400 to 700 nm. Plotting the absorption at 535 nm facilitated comparative evaluation. For quantification of prodigiosin formation via the previously published molar extinction coefficient (Domröse et al., 2015), the signal of the Tecan plate reader was calibrated with solutions of known concentration based on ε (535 nm) [$M^{-1}\ cm^{-1}$] = 139,800 (Domröse et al., 2015). Prodigiosin titers (expressed in mg/L) were determined by considering the molecular weight of the compound (323.432 g/mol) and the extracted culture volume.

4.1.7. PigC substrate acceptance assay

The *in vitro* assay with cell lysate of *E. coli* BL21 (DE3) pET28a(+)-*pigC* was performed as described previously (Klein et al., 2017; Brass et al., 2019). Accordingly, the heterologous expression of PigC was carried out using *E. coli* BL21 (DE3) pET28a(+)-*pigC* cells, which were stored at −20°C after cultivation and harvesting. Frozen cells (1 g) were thawed and resuspended in potassium phosphate buffer (KP_i buffer, 50 mM, pH 7.0; 5 mL). The cell suspension was disrupted using a SONOPULS Ultrasonic homogenizer (Bandelin, Berlin, Germany) for 2 × 5 min (five cycles, 40% power), to obtain lysed cells which were used for the PigC substrate acceptance assay. The assay solution contained 440 µL of cell lysate in KP_i buffer (50 mM, pH 7.0), 25 µL of a pyrrole **5**, **11a**, **11b** solution in DMSO (20 mM, end concentration: 1 mM), 25 µL of an MBC (**6**) solution in DMSO (20 mM, end concentration: 1 mM) and 10 µL of an ATP•Na_2 solution in water (62.5 mM, end concentration: 1.25 mM). The reaction mixture was shaken in a 1.5 mL tube at 300 rpm and 30°C for 4 h. The supernatant was removed after centrifugation (5 min, 21,100 rcf, 23°C) and the prodiginine pellet was resuspended in 300 µL acidic ethanol [4% (*v*/*v*) 1 N HCl in ethanol]. After centrifugation (5 min, 21,100 rcf, 23°C), the supernatant was transferred in a new 1.5 mL reaction tube and documented photographically.

4.2. Chemical precursor syntheses

4.2.1. General experimental procedures for chemical syntheses

All reactions were carried out under nitrogen atmosphere and magnetic stirring. Used glassware and magnetic stirring bars were dried previously at 110°C. All starting materials were purchased from commercial sources without further purification unless stated otherwise. Dichloromethane, diethyl ether, ethyl acetate (EtOAc) and petroleum ether (PE) were distilled prior to use. Tetrahydrofuran (THF) was used directly. Reactions were monitored by GC–MS, ^{1}H-NMR and thin layer chromatography (TLC; Polygram SIL G/UV254, Macherey-Nagel) using an acidic solution of *p*-anisaldehyde for staining or UV light at 245 nm for visualization. Purification of reaction products was carried out by flash chromatography on silica gel 60 (particle size 0.040–0.063 mm, 230–240 mesh, Macherey-Nagel). Analytics were carried out as described in the Supplementary Information, including Supplementary Tables S2, S3, and Supplementary Figure S5. The precursors 2-methyl-3-*N*-amylpyrrole (MAP, **5**), *tert*-butyloxycarbonyl-5′-formyl-4′-methoxy-1*H*,1′*H*-2,2′-bipyrrole (*boc*-MBC, *Boc*-**6**) and prodigiosin (**1**) as chemical references were synthesized as previously described (Dairi et al., 2006; Domröse et al., 2015).

4.2.2. *N*-methoxy-*N*-methyloct-7-enamide (8)

To a solution of 7-octenoic acid (2 mL, 13.0 mmol, 1.0 eq.) in dichloromethane (70 mL) was added *N*,O-dimethylhydroxylamine hydrochloride (1.19 g, 19.5 mmol, 1.50 eq.),

N-(3-dimethylaminopropyl)-*N*′ethylcarbodiimid hydrochloride (3.03 g, 19.5 mmol, 1.5 eq.) and 4-(dimethylamino)pyridine (2.38 g, 19.5 mmol, 1.5 eq.). After stirring for 22 h at 22°C, the reaction mixture was quenched with a saturated solution of NaCl and extracted with dichloromethane (3 × 50 mL). The combined organic layers were first washed with 1 N HCl, afterwards with saturated $NaHCO_3$ solution and dried over $MgSO_4$. After removal of the solvent under reduced pressure *N*-methoxy-*N*-methyloct-7-enamide (**8**, 2.29 g, 12.4 mmol, 95%) was obtained as a yellow oil and was used for the following experiment without further purification. R_f = 0.15 (PE/EtOAc 85:15); **^{1}H-NMR** (600 MHz, $CDCl_3$): δ [ppm] = 1.36 (m_c, 2H, 4-H), 1.41 (m_c, 2H, 5-H), 1.64 (m_c, 2H, 3-H), 2.05 (m_c, 2H, 6-H), 2.41 (t, $^3J_{2,3}$ = 7.7 Hz, 2H, 2-H), 3.18 (s, 3H, 1″-H), 3.68 (s, 3H, 1′-H), 4.93 (dd, $^{cis,3}J_{8a,7}$ = 10.2 Hz, $^2J_{8a,8b}$ = 1.2 Hz, 1H, 8-H_a), 4.99 (ddd, $^{trans,3}J_{8b,7}$ = 17.1 Hz, $^2J_{8b,8a}$ = 1.8 Hz, $^4J_{8b,6}$ = 1.8 Hz, 1H, 8-H_b), 5.80 (ddt, $^{trans,3}J_{7,8b}$ = 17.0 Hz, $^{cis,3}J_{7,8a}$ = 10.2 Hz, $^3J_{7,6}$ = 6.7 Hz, 1H, 7-H); **^{13}C-NMR** (151 MHz, $CDCl_3$): δ [ppm] = 24.6 (C-3), 28.8 (C-4), 29.1 (C-5), 32.0 (C-2), 32.3 (C-1″) 33.8 (C-6) 61.3 (C-1′), 114.5 (C-8), 139.1 (C-7); **IR** (ATR-film): $\tilde{\nu}$ [1/cm] = 3,074, 2,931, 2,855, 1,667, 1,463, 1,415, 1,384, 1,178, 998, 910, 732; **MS** (APCI, positive ion): *m*/*z* = 186 [$(M)^+$], 97, 83, 55.

4.2.3. Non-8-en-2-one (9)

N-methoxy-*N*-methyloct-7-enamide (**8**, 2.29 g, 12.4 mmol, 1.0 eq.) was dissolved in dry THF (100 mL) and methylmagnesium chloride (3 M in diethyl ether, 12.4 mL, 37.1 mmol, 3.0 eq.) was added within 15 min at 0°C. The reaction mixture was stirred for 1.5 h at 0°C and afterwards quenched by the addition of a saturated solution of NH_4Cl at 0°C and extracted with dichloromethane (3 × 60 mL). The combined organic layers were dried over $MgSO_4$ and the solvent was evaporated under reduced pressure to yield non-8-en-2-one (**9**, 1.63 g, 11.6 mmol, 94%) as a yellowish oil without further purification. R_f = 0.40 (PE/EtOAc 85:15); **^{1}H-NMR** (600 MHz, $CDCl_3$): δ [ppm] = 1.25–1.34 (m, 2H, 5-H), 1.35–1.43 (m, 2H, 6-H), 1.58 (tt, $^3J_{4,3}$ = 7.5 Hz, $^3J_{4,5}$ = 7.5 Hz, 2H, 4-H), 2.05 (m, 2H, 7-H), 2.13 (s, 3H, 1-H), 2.42 (t, $^3J_{3,4}$ = 7.5 Hz, 2H, 3-H), 4.93 (ddt, $^{cis,3}J_{9a,8}$ = 10.2 Hz, $^4J_{9a,7}$ = 2.3 Hz, $^2J_{9a,9b}$ = 1.2 Hz, 1H, 9-H_a), 4.99 (dd, $^{trans,3}J_{9b,8}$ = 17.1 Hz, $^2J_{9b,9a}$ = 1.7 Hz, 1H, 9-H_b), 5.79 (ddt, $^{trans,3}J_{8,9b}$ = 17.0 Hz, $^{cis,3}J_{8,9a}$ = 10.2 Hz, $^3J_{8,7}$ = 6.7 Hz, 1H, 8-H); **^{13}C-NMR** (151 MHz, $CDCl_3$): δ [ppm] = 23.8 (C-4), 28.7 (C-5), 28.8 (C-6), 30.0 (C-1), 33.7 (C-7), 43.9 (C-3), 114.6 (C-9), 139.0 (C-8), 209.4 (C-2); **IR** (ATR-film): $\tilde{\nu}$ [1/cm] = 2,928, 2,855, 1738, 1721, 1,443, 1,363, 1,217, 907; **MS** (APCI, positive ion): *m*/*z* = 123.

4.2.4. Dec-9-en-2-one oxime (10)

To a solution of the non-8-en-2-one (**9**, 1.73 g, 12.4 mmol, 1.0 eq.) in ethanol (6.2 mL) was added pyridine (0.78 g, 0.8 mL, 9.89 mmol, 0.8 eq.) and grounded hydroxylamine hydrochloride (1.5 eq.). The reaction mixture was refluxed for 2 h and afterwards extracted with dichloromethane (3 × 25 mL). The combined organic layers were washed with 1 N HCl (3 × 20 mL) and dried over $MgSO_4$. After removal of the solvent under reduced pressure, dec-9-en-2-one oxime (**10**, 1.76 g, 11.3 mmol, 92%) was obtained in a diastereomeric mixture of *E*:*Z* (1:3) without further purification. R_f = 0.34 (PE/EtOAc 80:20); **^{1}H-NMR** (600 MHz, $CDCl_3$): δ [ppm] = 1.28–1.36 (m, 2H, 5-H), 1.37–1.44 (m, 2H, 6-H), 1.51 (tt, $^3J_{4,3}$ = 7.5 Hz, $^3J_{4,5}$ = 7.5 Hz, 2H, 4-H), 1.87 (s, 3H, 1-H), 2.05 (dt, $^3J_{7,6}$ = 6.4 Hz, $^3J_{7,8}$ = 6.4 Hz, 2H, 7-H), 2.18 (t, $^3J_{3,4}$ = 7.5 Hz, 2H, 3-H), 4.94 (ddt, $^{cis,3}J_{9a,8}$ = 10.2 Hz, $^4J_{9a,7}$ = 2.4 Hz, $^2J_{9a,9b}$ = 1.3 Hz, 1H, 9-H_a), 5.00 (dd, $^{trans,3}J_{9b,8}$ = 17.1 Hz, $^2J_{9b,9a}$ = 1.5 Hz, 1H, 9-H_b), 5.80 (ddt, $^{trans,3}J_{8,9b}$ = 17.0 Hz, $^{cis,3}J_{8,9a}$ = 10.4 Hz, $^3J_{8,7}$ = 6.6 Hz, 1H, 8-H); **^{13}C-NMR** (151 MHz, $CDCl_3$): δ [ppm] = 13.4 (C-1), 26.2 (C-4), 28.7 (C-5), 28.8 (C-6), 33.7 (C-7), 35.8 (C-3), 114.4 (C-9), 139.1 (C-8), 159.1 (C-2); **IR** (ATR-film): $\tilde{\nu}$ [1/cm] = 3,074, 2,929, 2,855, 1,637, 1,461, 1,369, 910; **MS** (APCI, positive ion): *m*/*z* = 156 [$(M)^+$], 83; **HRMS** (ESI, positive ion): calculated for $C_9H_{18}NO$ $[(M+H)]^+$ = 156.1383, found = 156.1384.

4.2.5. 3-(hex-5-en-1-yl)-2-methyl-1*H*-pyrrole (11a)

A reaction mixture of dec-9-en-2-one oxime (**10**, 0.72 g, 4.64 mmol, 1.0 eq.), potassium hydroxide (1.30 g, 46.4 mmol, 5.0 eq.), water (62.7 mg, 62.3 µL, 3.48 mmol, 0.75 eq.) and DMSO (8.9 mL) was heated at 90–100°C (using previously degassed DMSO on molecular sieves (3.5 Å) could increase the yield). Over a period of 2 h, a solution of 1,2-dichloroethane (1.38 g, 1.10 mL, 13.9 mmol, 3.5 eq.) in DMSO (1 mL) was added dropwise. After 1 h of 1,2-dichloroethane addition a secondary amount of potassium hydroxide (5.0 eq.) was added. After an overall reaction time of 4 h at 90–100°C the reaction mixture was allowed to reach room temperature and subsequently ice water (20 mL) was added. The mixture was extracted with diethyl ether (3 × 20 mL) and the combined organic layers were dried over $MgSO_4$. After the solvent was evaporated under reduced pressure the crude product was purified by column chromatography on silica gel [PE:dichloromethane (60:40) + 1% trimethylamine (*v*/*v*)] to obtain 3-(hex-5-en-1-yl)-2-methyl-1*H*-pyrrole (**11a**, 228 mg, 1.40 mmol, 30%) as yellowish oil. R_f = 0.37 (PE/dichloromethane 60:40); **^{1}H-NMR** (600 MHz, $CDCl_3$): δ [ppm] = 1.44 (tt, $^3J_{3'',2''}$ = 7.5 Hz, $^3J_{3'',4''}$ = 7.5 Hz, 2H, 3″-H), 1.51–1.59 (m, 2H, 2″-H), 2.02–2.14 (m, 2H, 4″-H), 2.18 (s, 3H, 1′-H), 2.39 (t, $^3J_{1'',2''}$ = 7.6 Hz, 2H, 1″-H), 4.93 (dd, $^{cis,3}J_{6a'',5''}$ = 10.2 Hz, $^2J_{6a'',6b''}$ = 1.2 Hz, 1H, 6″-H_a), 5.00 (dd, $^{trans,3}J_{6b'',5''}$ = 17.1 Hz, $^2J_{6b'',6a''}$ = 1.7 Hz, 1H, 6″-H_b), 5.82 (ddt, $^{trans,3}J_{5'',6b''}$ = 16.9 Hz, $^{cis,3}J_{5'',6a''}$ = 10.2 Hz, $^3J_{5'',4''}$ = 6.7 Hz, 1H, 5″-H), 6.01 (dd, $^4J_{4,1}$ = 2.8 Hz, $^3J_{4,5}$ = 2.8 Hz, 1H, 4-H), 6.59 (dd, $^3J_{5,1}$ = 2.7 Hz, $^3J_{5,4}$ = 2.7 Hz, 1H, 5-H), 7.70 (brs, 1H, 1-NH); **^{13}C-NMR** (151 MHz, $CDCl_3$): δ [ppm] = 11.2 (C-1′), 25.9 (C-1″), 28.9 (C-3″), 31.0 (C-2″), 33.9 (C-4″), 109.0 (C-4), 114.3 (C-6″), 115.0 (C-5), 119.7 (C-3), 123.4 (C-2), 139.4 (C-5″); **IR** (ATR-film): $\tilde{\nu}$ [1/cm] = 3,385, 2,928, 2,855, 1741, 1,467, 1,363, 1,217, 907, 712; **MS** (APCI, positive ion): *m*/*z* = 164 [$(M)^+$]; 121, 108; **HRMS** (ESI, positive ion): calculated for $C_{11}H_{18}N$ $[(M+H)]^+$ = 164.1434, found = 164.1433.

4.2.6. 6-(2-methyl-1*H*-pyrrol-3-yl)hexan-1-ol (11b)

9-BBN (0.5 N in THF, 5.54 g, 3.10 mmol, 2.2 eq.) was added to a solution of 3-(hex-5-en-1-yl)-2-methyl-1*H*-pyrrole (**11a**, 230 mg, 1.41 mmol, 1.0 eq.) in dry THF (11.6 mL) over a period of 15 min at 0°C. After stirring for 1 h at 0°C, the reaction mixture was heated up at 70°C under reflux for 3 h. Subsequently an aqueous solution of 3 N NaOH (2.35 g, 2.35 mL, 7.05 mmol, 5.0 eq.) and 30% H_2O_2 (2.24 g, 2.00 mL, 19.7 mmol, 14.0 eq.) was added at 0°C. After 1 h at 0°C the reaction mixture was allowed to reach room temperature and was stirred for further 15 h at 22°C. Ice water (40 mL) was added and the mixture was extracted with dichloromethane (3 × 50 mL). The combined organic layer was dried over $MgSO_4$, the solvent was evaporated under reduced pressure and the crude product was purified by column chromatography on silica gel [PE:ethyl acetate (70:30 to 50:50) + 1% trimethylamine (*v*/*v*)] to isolate 6-(2-methyl-1*H*-pyrrol-3-yl)hexan-1-ol (**11b**, 193 mg, 1.06 mmol, 76%) as orange oil. R_f = 0.20 (PE/EtOAc 70:30); **^{1}H-NMR** (600 MHz, $CDCl_3$): δ [ppm] = 1.20 (brs, 1H, 1-OH), 1.34–1.42 (m, 4H, 3-H, 4-H), 1.51–1.61 (m, 4H, 2-H, 5-H), 2.18 (s, 3H, 1″-H), 2.39 (t, $^3J_{6,5}$ = 7.7 Hz, 2H, 6-H),

3.64 (t, $^{3}J_{1,2}$ = 7.1 Hz, 2H, 1-H), 6.00 (dd, $^{4}J_{4',1'}$ = 2.8 Hz, $^{3}J_{4',5'}$ = 2.8 Hz, 1H, 4′-H), 6.59 (dd, $^{3}J_{5',1'}$ = 2.7 Hz, $^{3}J_{5',4'}$ = 2.7 Hz, 1H, 5′-H), 7.72 (brs, 1H, 1′-NH); **^{13}C-NMR** (151 MHz, $CDCl_3$): δ [ppm] = 11.2 (C-1″), 25.8 (C-4), 26.0 (C-6), 29.4 (C-3), 31.4 (C-5), 33.0 (C-2), 62.7 (C-1), 109.0 (C-4′), 115.0 (C-5′), 119.7 (C-3′), 123.4 (C-2′); **IR** (ATR-film): $\tilde{\nu}$ [1/cm] = 3,373, 2,928, 2,855, 1735, 1,436, 1,363, 1,223, 1,059, 748; **MS** (APCI, positive ion): *m*/*z* = 182 [$(M)^+$], 164, 108; **HRMS** (ESI, positive ion): calculated for $C_{11}H_{20}NO$ [$(M+H)]^+$ = 182.1539, found = 182.1539.

4.3. Muta- and semisynthetic hydroxylated prodiginine production

4.3.1. General procedure for preparative scale mutasynthesis

A preculture of *P. putida* MBC18 with pVLT33-pigC-pigB in LB medium (25 µg/mL kanamycin) was incubated in a shake flask at 30°C and 130 rpm overnight. Five main cultures of 100 mL each in TB medium (25 µg/mL kanamycin) were inoculated to an OD_{650} of 0.05 and incubated in 1 l baffled flask with air-sheet seals for 4 h at 30°C and 130 rpm. The pyrrole precursor was dissolved in DMSO (5–50 mM stock, 10 mL). To each culture 2 mL of pyrrole stock solution was added (final concentration 0.1–1.0 mM). Induction was performed with 0.5 mM IPTG (50 mM stock in dH2O; 1 mL). After an additional hour at 30°C and 130 rpm, 1 g of polyurethane (PU) foam cubes (Softpur, Göllheim, Germany: Softpur foam, 25 kgm^{-3} density, 4 kPa compression hardness, each cube approximately 1 cm^3) were added to each culture and the cultures were incubated for further 23 h at 30°C and 130 rpm. After a total of 28 h of cultivation, the foam cubes were wrung out, washed with dH_2O, and then extracted with diethyl ether (250–500 mL) in a soxhlet extractor. After evaporation of the solvent, the crude product was dissolved in diethyl ether (20 mL), washed with water, and the aqueous layer was extracted with dichloromethane (3 × 15 mL). The combined organic layers were washed with saturated NaCl (20 mL) and dried over $MgSO_4$. After evaporation of the solvent, the crude product was purified by flash column chromatography on silica gel (CH_2Cl_2 + 1.0–1.5% NH_3 in MeOH). For subsequent hydroboration, the product was further purified by reversed-phase chromatography (column: ISAspher 100–5 C18 AQ, 5 µm, 150*20 mm from ISERA GmbH, Düren, Germany; column oven: 35°C; eluent: 60:40 acetonitrile:water + 0.1% formiate; flow rate 15 mL/min; injection of samples in 1 mL ethanol) to obtain the mutasynthesis product as red solid.

4.3.2. 4-Methoxy-5-[(5-methyl-4-hex-5-en-1-yl-2*H*-pyrrol-2-yliden)methyl]-1*H*,1′*H*-2,2′-bipyrrol (3)

According to the general procedure for preparative mutasynthesis and the use of pyrrole **11a** (12.2 mg, 75.0 µmol, 7.5 mM in DMSO, end concentration in 500 mL culture: 0.15 mm) as precursor prodiginine **12** (15.0 mg, 40.3 µmol, 54%) was obtained as red solid. R_f = 0.15 (dichloromethane); **^{1}H-NMR** (600 MHz, $CDCl_3$): δ [ppm] = 1.43 (tt, $^{3}J_{8'',7''}$ = 7.5 Hz, $^{3}J_{8'',9''}$ = 7.5 Hz, 2H, 8″-H), 1.53–1.59 (m, 2H, 7″-H), 2.08 (dt, $^{3}J_{9'',8''}$ = 7.2 Hz, $^{3}J_{9'',10''}$ = 7.2 Hz, 2H, 9″-H), 2.41 (t, $^{3}J_{6'',7''}$ = 7.6 Hz, 2H, 6″-H), 2.54 (s, 3H, 12″-H), 4.01 (s, 3H, 7-H), 4.95 (dd, $^{cis,3}J_{11a'',10''}$ = 10.2 Hz, $^{2}J_{11a'',11b''}$ = 2.2 Hz, 1H, 11″-H_a), 5.01 (dd, $^{trans,3}J_{11b'',10''}$ = 17.1 Hz, $^{2}J_{11b'',11a''}$ = 1.7 Hz, 1H, 11″-H_b), 5.80 (ddt, $^{trans,3}J_{10'',11b''}$ = 16.9 Hz, $^{cis,3}J_{10'',11a''}$ = 10.2 Hz, $^{3}J_{10'',9''}$ = 6.7 Hz, 1H, 10″-H), 6.08 (d, $^{4}J_{3,1}$ = 2.0 Hz, 1H, 3-H), 6.36 (dd, $^{3}J_{4',5'}$ = 3.7 Hz, $^{4}J_{4',1'}$ = 2.3 Hz, 4′-H), 6.68 (d, ^{3}J = 2.6 Hz), 6.92 (ddd, ^{3}J = 3.9 Hz, ^{3}J = 2.5 Hz, ^{3}J = 1.3 Hz), 6.96 (s, 1H), 7.24 (d, $^{4}J_{3'',1''}$ = 2.7 Hz, 1H, 3″-H), 12.58 (brs, 1H, 1′-NH), 12.75 (brs, 2H, 1-NH, 1″-NH); **^{13}C-NMR** (151 MHz, $CDCl_3$): δ [ppm] = 12.6 (C-12″), 25.3 (C-6″), 28.6 (C-8″), 29.7 (C-7″), 33.7 (C-9″), 58.9 (C-7), 93.0 (C-3), 111.9 (C-4′), 114.7 (C-10″), 116.1 (C-8), 117.2 (C-3′), 120.9 (C-5), 122.4 (C-2′), 125.3 (C-2″), 127.1 (C-5′), 128.3 (C-4″), 128.4 (C-3″), 138.8 (C-9″), 146.9 (C-5″), 147.9 (C-2), 165.9 (C-4); **IR** (ATR-Film): $\tilde{\nu}$ [1/cm] = 3,163, 3,099, 2,974, 2,928, 2,857, 1,630, 1,604, 1,544, 1,512, 1,414, 1,356, 1,261, 1,158, 1,137, 1,044, 993, 960, 838, 756; **MS** (APCI, positive-Ion): *m*/*z* = 336 [$(M)^+$], 266, 163; **HRMS** (ESI, positive ion): calculated for $C_{21}H_{26}N_3O$ [$(M+H)]^+$ = 336.2070, found = 336.2076.

4.3.3. Semisynthesis toward 6-(2-((4-methoxy-1*H*,1′*H*-(2,2′-bipyrrole)-5-yl) methylene)-5-methyl-2*H*-pyrrole-4-yl)hexan-1-ol (3)

9-BBN (0.5 n in THF, 94.2 mg, 0.05 mmol, 2.2 eq.) was added to a solution of 4-Methoxy-5-((5-methyl-4-hex-5-en-1-yl-2H-pyrrole-2-yliden)methyl)-1*H*,1′*H*-2,2′-bipyrrole (**12**, 9 mg, 0.02 mmol, 1.0 eq.) in dry THF (2 mL) over a period of 15 min at 0°C. After stirring for 1 h at 0°C, the reaction mixture was heated up at 70°C under reflux for 3 h. Subsequently an aqueous solution of 3 N NaOH (39.9 mg, 105 µL, 0.12 mmol, 5.0 eq.) and 30% H_2O_2 (38.0 mg, 34.1 µL, 0.34 mmol, 14.0 eq.) was added at 0°C. After 1 h at 0°C the reaction mixture was allowed to reach room temperature and was stirred for further 15 h at 22°C. Ice water (10 mL) was added and the mixture was extracted with dichloromethane (3 × 15 mL). The combined organic layer was dried over $MgSO_4$, the solvent was evaporated under reduced pressure and the crude product was purified by column chromatography on silica gel [dichloromethane + 0.5–4.0% trimethylamine (*v*/*v*)] to isolate 6-(2-((4-methoxy-1*H*,1′*H*-(2,2′-bipyrrole)-5-yl)methylene)-5-methyl-2*H*-pyrrole-4-yl)hexan-1-ol (**3**, 6.10 mg, 0.02 mmol, 65%) as red solid. R_f = 0.16 (PE/EtOAc 50:50); **^{1}H-NMR** (600 MHz, $CDCl_3$): δ [ppm] = 1.28 (brs, 1H, 12″-OH), 1.37 (m_c, 4H, 8″-H, 9″-H), 1.50–1.63 (m, 4H, 7″-H, 10″-H), 2.40 (t, $^{3}J_{6'',7''}$ = 7.6 Hz, 2H, 6″-H), 2.54 (s, 3 H, 13″-H), 3.64 (t, $^{3}J_{11'',10''}$ = 6.6 Hz, 2H, 11″-H), 4.00 (s, 3H, 7-H), 6.08 (d, $^{4}J_{3,1}$ = 1.9 Hz, 1H, 3-H), 6.35 (dd, $^{3}J_{4',5'}$ = 4.3 Hz, $^{4}J_{4',1'}$ = 2.0 Hz, 1H, 4′-H), 6.67 (d, $^{4}J_{3'',1''}$ = 2.6 Hz, 1H, 3″-H), 6.92 (ddd, $^{3}J_{3',4'}$ = 3.9 Hz, $^{4}J_{3',5'}$ = 2.5 Hz, $^{4}J_{3',1'}$ = 1.4 Hz, 1H, 3′-H), 6.94 (s, 1H, 8-H), 7.23 (dd, $^{3}J_{5',4'}$ = 2.7 Hz, $^{3}J_{5',1'}$ = 1.3 Hz, 1-H, 5′-H), 12.56 (brs, 1H, 1′-NH), 12.72 (brs, 2H, 1-NH, 1″-NH); **^{13}C-NMR** (151 MHz, $CDCl_3$): δ [ppm] = 12.6 (C-13″), 25.0 (C-6″), 25.7 (C-8″), 29.1 (C-9″), 30.2 (C-7″), 32.9 (C-10″), 58.9 (C-7), 63.1 (C-11″), 93.0 (C-3), 111.9 (C-4′), 116.3 (C-8), 117.3 (C-3′), 120.9 (C-5), 122.4 (C-2′), 125.3 (C-2″), 127.2 (C-5′), 128.3 (C-4″), 128.4 (C-3″), 147.0 (C-5″), 148.0 (C-2), 166.0 (C-4); **IR** (ATR-film): $\tilde{\nu}$ [1/cm] = 3,422, 3,172, 2,930, 2,861, 1,630, 1,602, 1,543, 1,511, 1,363, 1,261, 1,137, 960, 748; **MS** (APCI, positive ion): *m*/*z* = 354 [$(M)^+$], 279, 157; **HRMS** (ESI, positive ion): calculated for $C_{21}H_{28}N_3O_2$ [$(M+H)]^+$ = 354.2176, found = 354.2179.

4.4. Assessment of effects on the plant-parasitic nematode *Heterodera schachtii*

4.4.1. Plant material and nematode culture

Arabidopsis thaliana Columbia (Col-0) seeds were surface-sterilized by soaking in 0.7% sodium hypochlorite for 5 min and

submerging them in 70% (*v*/*v*) ethanol for 1 min. Subsequently, the seeds were rinsed with sterile distilled water 5 times, dried at room temperature for 4 h and stored at 4°C for further experiments. *H. schachtii* cysts were harvested from the roots of mustard (*Sinapsis alba*), which was grown aseptically on modified Knop agar medium, and submerged with sterile 3 mM $ZnCl_2$ in the Baermann funnel (Grundler et al., 1991). After 7 days, the freshly hatched second-stage juveniles (J2s) were collected for subsequent analysis. All preparation procedures were performed under aseptic conditions.

4.4.2. EC_{50} (nematode infection) determination of di-rhamnolipids and prodiginines

EC_{50} determination of selected compounds was performed in an *in vitro* agar system: Petri dishes (90 mm diameter) were filled with modified Knop medium (Sijmons et al., 1991; Matera et al., 2021) supplemented with prodiginines or di-rhamnolipids at different concentrations (Supplementary Table S4). Stock solutions of prodiginines in DMSO were applied to implement a final concentration of 0.5% DMSO. The di-rhamnolipids, which were obtained by microbial production as a congener mixture as previously described (Bredenbruch et al., 2023), were solved in water. Accordingly, modified Knop medium alone or supplemented with 0.5% (v/v) DMSO served as control. On the medium, 2 surface-sterilized *A. thaliana* seeds were germinated aseptically and incubated in a climate chamber under a red/blue light with a 16-h/8-h light/dark photoperiod at 24°C (Sijmons et al., 1991). At 12 days post seeding, each plant was inoculated with approximately 60 *H. schachtii* J2s. At 10 days post inoculation, the total number of males and females on each plant was counted under a Stereo Microscope (Leica, Germany). EC_{50} was determined by using software 'CompuSyn' (Chou and Martin, 2005). Three independent biological replicates of the experiment were performed. Each biological replicate included at least 6 technical replicates (plants) per variant.

4.4.3. Determination of the combinatorial effect of compounds on nematode infection

Assays to measure combinatorial effects were carried out in an analogous experimental set-up as the EC_{50} determination described above. The concentration of compounds alone or in combination is detailed in Supplementary Table S5. The compound combination effects (antagonistic, additive or synergistic) were evaluated according to the Combination Index Plot obtained by the software 'CompuSyn' (Chou and Martin, 2005). The experiments were performed independently in triplicate.

4.4.4. Time-resolved analyses of the compounds' impact on nematodes

The time-resolved analysis consisted of four assays investigating nematode motility, stylet thrusting, infection, and development. Petri dishes (90 mm diameter) were filled with modified Knop medium supplemented with prodigiosin (**1**) or hydroxylated prodiginine **3** at the determined EC_{50}, which is 15.1 and 31.2 µM, respectively. Modified Knop medium alone or supplemented with 0.5% (*v*/*v*) DMSO served as controls.

4.4.4.1. Nematode motility

Approximately 30 *H. schachtii* J2 were inoculated in the center of a Petri dish containing the test compound. The location of J2s was documented after 30 and 60 min and the distance to the inoculation point was measured by Image J (Schneider et al., 2012). The experiment was performed independently in quadruplicate.

4.4.4.2. Nematode stylet thrusting

Two surface-sterilized *A. thaliana* seeds were germinated aseptically on the medium containing the test compound. At 12 days post seeding, approximately 60 *H. schachtii* J2 were inoculated to each plant. At 6 h post inoculation, 10 J2, which successfully penetrated the root epidermis, were tracked under a Stereo Microscope (Leica, Germany) in order to count the number of stylet movements for 5 min. The experiment was performed independently in quadruplicate.

4.4.4.3. Nematode infection and development

Two surface-sterilized *A. thaliana* seeds were germinated aseptically on the medium containing the test compound. At 12 days post seeding, approximately 60 *H. schachtii* J2 were inoculated to each plant. At 2, 4 and 10 days post inoculation, the number of males and females was counted, and the size of male and female nematodes was measured under a LeicaS4E Stereo Microscope (Leica, Germany) equipped with Leica Application Suite (LAS) software. Four independent biological replicates with 14 plants per variant and biological replicate ($n = 56$) were conducted for the nematode infection assay. Three independent biological replicates with in total $n = 70$ technical replicates (nematodes) were performed for the development experiment.

4.4.5. Statistical analysis of bioactivity evaluating data

All data are expressed as mean ± standard error (SE). Statistical analysis was performed by using one-way analysis of variance (ANOVA; $p < 0.05$; SIGMAPLOT 12.5, Systat Software, Inc., San Jose, CA, United States).

Data availability statement

The original contributions presented in the study are included in the article/Supplementary material, further inquiries can be directed to the corresponding authors.

Author contributions

AL, AS, JP, FG, K-EJ, and TD conceived the research concept and designed the experiments. RW, FG, SI, NB, KB, DK, TW, and HB performed microbiological work as well as chemical syntheses and production of prodiginines. CM, TT, and LB provided rhamnolipids. MH, XX, and LR conducted investigations of antinematode activities. DK, RW, and MH drafted the manuscript with input from all the authors. All authors contributed to the article and approved the submitted version.

Funding

The work was supported by grants from the German Bioeconomy Science Center. The scientific activities of the Bioeconomy Science Center were financially supported by the Ministry of Culture and Science within the framework of the NRW Strategieprojekt BioSC (no. 313/323-400-00213). Parts of this work were funded by the state of NRW in the project RhamnoLizer. This

work was supported by the Open Access Publication Fund of the University of Bonn.

Acknowledgments

The authors thank Birgit Henßen for analytical support. We further gratefully acknowledge excellent technical support by Ute Schlee and Stefan Neumann.

Conflict of interest

The authors declare that the research was conducted in the absence of any commercial or financial relationships that could be construed as a potential conflict of interest.

Publisher's note

Supplementary material

The Supplementary material for this article can be found online at: https://www.frontiersin.org/articles/10.3389/fmicb.2023.1151882/full#supplementary-material

References

Abdel-Mawgoud, A. M., Lépine, F., and Déziel, E. (2010). Rhamnolipids: diversity of structures, microbial origins and roles. *Appl. Microbiol. Biotechnol.* 86, 1323–1336. doi: 10.1007/s00253-010-2498-2

Beal, R., and Betts, W. B. (2000). Role of rhamnolipid biosurfactants in the uptake and mineralization of hexadecane in *Pseudomonas aeruginosa*. *J. Appl. Microbiol.* 89, 158–168. doi: 10.1046/j.1365-2672.2000.01104.x

Belda, E., Van Heck, R. G. A., Lopez-sanchez, M. J., Cruveiller, S., Barbe, V., Fraser, C., et al. (2016). The revisited genome of *Pseudomonas putida* KT2440 enlightens its value as a robust metabolic chassis. *Environ. Microbiol.* 18, 3403–3424. doi: 10.1111/1462-2920.13230

Berg, G. (2009). Plant-microbe interactions promoting plant growth and health: perspectives for controlled use of microorganisms in agriculture. *Appl. Microbiol. Biotechnol.* 84, 11–18. doi: 10.1007/s00253-009-2092-7

Berning, L., Schlütermann, D., Friedrich, A., Berleth, N., Sun, Y., Wu, W., et al. (2021). Prodigiosin sensitizes sensitive and resistant urothelial carcinoma cells to cisplatin treatment. *Molecules* 26:1294. doi: 10.3390/molecules26051294

Bhadoriya, S. S., Madoriya, N., Shukla, K., and Parihar, M. (2013). Biosurfactants: a new pharmaceutical additive for solubility enhancement and pharmaceutical development. *Biochem. Pharmacol. Open Access* 2:113. doi: 10.4172/2167-0501.1000113

Bnyan, R., Khan, I., Ehtezazi, T., Saleem, I., Gordon, S., O'Neill, F., et al. (2018). Surfactant effects on lipid-based vesicle properties. *J. Pharm. Sci.* 107, 1237–1246. doi: 10.1016/j.xphs.2018.01.005

Boonlarppradab, C., Kauffman, C. A., Jensen, P. R., and Fenical, W. (2008). Marineosins a and B, cytotoxic spiroaminals from a marine- derived actinomycete. *Org. Biomol. Chem.* 10, 5505–5508. doi: 10.1021/ol8020644

Brands, S., Brass, H. U. C., Klein, A. S., Pietruszka, J., Ruff, A. J., and Schwaneberg, U. (2020). A colourimetric high-throughput screening system for directed evolution of prodigiosin ligase PigC. *Chem. Commun.* 56, 8631–8634. doi: 10.1039/d0cc02181d

Brass, H. U. C., Klein, A. S., Nyholt, S., Classen, T., and Pietruszka, J. (2019). Condensing enzymes from Pseudoalteromonadaceae for prodiginine synthesis. *Adv. Synth. Catal.* 361, 2659–2667. doi: 10.1002/adsc.201900183

Bredenbruch, S., Mueller, C., Atemnkeng, H., Schroeder, L., Tiso, T., Blank, L. M., et al. (2023). The biological activity of bacterial rhamnolipids is linked to their molecular structure. *bioRxiv* [Epub ahead of preprint], doi: 10.1101/2023.01.23.525263

Chawrai, S. R., Williamson, N. R., Mahendiran, T., Salmond, G. P. C., and Leeper, F. J. (2012). Characterisation of PigC and HapC, the prodigiosin synthetases from *Serratia* sp. and *Hahella chejuensis* with potential for biocatalytic production of anticancer agents. *Chem. Sci.* 3, 447–454. doi: 10.1039/c1sc00588j

Cheng, F., Kovács, I. A., and Barabási, A.-L. (2019). Network-based prediction of drug combinations. *Nat. Commun.* 10:1197. doi: 10.1038/s41467-019-09186-x

Choi, S. Y., Lim, S., Yoon, K., Lee, J. I., and Mitchell, R. J. (2021). Biotechnological activities and applications of bacterial pigments violacein and prodigiosin. *J. Biol. Eng.* 15:10. doi: 10.1186/s13036-021-00262-9

Chou, T., and Martin, N. (2005). *CompuSyn for Drug Combinations: PC Software and User's Guide: A Computer Program for Quantitation of Synergism and Antagonism in Drug Combinations, and the Determination of IC50 and ED50 and LD50 Values*. ComboSyn Inc., Paramus.

Cook, T. B., Jacobson, T. B., Venkataraman, M. V., Hofstetter, H., Amador-Noguez, D., Thomas, M. G., et al. (2021). Stepwise genetic engineering of pseudomonas putida enables robust heterologous production of prodigiosin and glidobactin a. *Metab. Eng.* 67, 112–124. doi: 10.1016/j.ymben.2021.06.004

Couturier, M., Bhalara, H. D., Chawrai, S. R., Monson, R., Williamson, N. R., Salmond, G. P. C., et al. (2019). Substrate flexibility of the flavin-dependent dihydropyrrole oxidases PigB and HapB involved in antibiotic prodigiosin biosynthesis. *Chembiochem* 21, 523–530. doi: 10.1002/cbic.201900424

Dairi, K., Tripathy, S., Attardo, G., and Lavallée, J.-F. (2006). Two-step synthesis of the bipyrrole precursor of prodigiosins. *Tetrahedron Lett.* 47, 2605–2606. doi: 10.1016/j.tetlet.2006.02.035

Darshan, N., and Manonmani, H. K. (2015). Prodigiosin and its potential applications. *J. Food Sci. Technol.* 52, 5393–5407. doi: 10.1007/s13197-015-1740-4

Darshan, N., and Manonmani, H. K. (2016). Prodigiosin inhibits motility and activates bacterial cell death revealing molecular biomarkers of programmed cell death. *AMB Express* 6:50. doi: 10.1186/s13568-016-0222-z

Das, P., Yang, X.-P., and Ma, L. Z. (2014). Analysis of biosurfactants from industrially viable pseudomonas strain isolated from crude oil suggests how rhamnolipids congeners affect emulsification property and antimicrobial activity. *Front. Microbiol.* 5:696. doi: 10.3389/fmicb.2014.00696

Domröse, A., Hage-Hülsmann, J., Thies, S., Weihmann, R., Kruse, L., Otto, M., et al. (2019). Pseudomonas putida rDNA is a favored site for the expression of biosynthetic genes. *Sci. Rep.* 9:7028. doi: 10.1038/s41598-019-43405-1

Domröse, A., Klein, A. S., Hage-Hülsmann, J., Thies, S., Svensson, V., Classen, T., et al. (2015). Efficient recombinant production of prodigiosin in pseudomonas putida. *Front. Microbiol.* 6:972. doi: 10.3389/fmicb.2015.00972

Domröse, A., Weihmann, R., Thies, S., Jaeger, K. E., Drepper, T., and Loeschcke, A. (2017). Rapid generation of recombinant pseudomonas putida secondary metabolite producers using yTREX. *Synth. Syst. Biotechnol.* 2, 310–319. doi: 10.1016/j.synbio.2017.11.001

Dowhan, W. (1997). "The role of phospholipids in cell function" in *Advances in Lipobiology*. ed. R. W. Gross (Amsterdam Niederlande: Elsevier), 79–107.

Fürstner, A. (2003). Chemistry and biology of roseophilin and the prodigiosin alkaloids: a survey of the last 2500 years. *Angew. Chemie - Int. Ed.* 42, 3582–3603. doi: 10.1002/anie.200300582

Garcia-Brugger, A., Lamotte, O., Vandelle, E., Bourque, S., Lecourieux, D., Poinssot, B., et al. (2006). Early signaling events induced by elicitors of plant defenses. *Mol. Plant-Microbe Interact.* 19, 711–724. doi: 10.1094/MPMI-19-0711

Grundler, F. M. W., Schnibbe, L., and Wyss, U. (1991). *In vitro* studies on the behaviour of second-stage juveniles of *Heterodera schachtii* (Nematoda: Heteroderidae) in response to host plant root exudates. *Parasitology* 103, 149–155. doi: 10.1017/S0031182000059394

Haas, D., and Défago, G. (2005). Biological control of soil-borne pathogens by fluorescent pseudomonads. *Nat. Rev. Microbiol.* 3, 307–319. doi: 10.1038/nrmicro1129

Habash, S. S., Brass, H. U. C., Klein, A. S., Klebl, D. P., Weber, T. M., Classen, T., et al. (2020). Novel prodiginine derivatives demonstrate bioactivities on plants, nematodes, and fungi. *Front. Plant Sci.* 11:579807. doi: 10.3389/fpls.2020.579807

Hage-Hülsmann, J., Grünberger, A., Thies, S., Santiago-Schübel, B., Klein, A. S., Pietruszka, J., et al. (2018). Natural biocide cocktails: combinatorial antibiotic effects of prodigiosin and biosurfactants. *PLoS One* 13:e0200940. doi: 10.1371/journal.pone.0200940

Hanahan, D. (1983). Studies on transformation of Escherichia coli with plasmids. *J. Mol. Biol.* 166, 557–580. doi: 10.1016/S0022-2836(83)80284-8

Handelsman, J., and Stabb, E. V. (1996). Biocontrol of soilborne plant pathogens. *Plant Cell* 8, 1855–1869. doi: 10.1105/tpc.8.10.1855

Hopkins, A. L. (2007). Network pharmacology. *Nat. Biotechnol.* 25, 1110–1111. doi: 10.1038/nbt1007-1110

Hu, D. X., Withall, D. M., Challis, G. L., and Thomson, R. J. (2016). Structure, chemical synthesis, and biosynthesis of Prodiginine natural products. *Chem. Rev.* 116, 7818–7853. doi: 10.1021/acs.chemrev.6b00024

Ivanov, A. V., Shcherbakova, V. S., Mikhaleva, A. I., and Trofimov, B. A. (2014). One-pot synthesis of pyrroles from ketones, hydroxylamine, and 1,2-dibromoethane in the system KOH-DMSO. *Russ. J. Org. Chem.* 50, 1775–1778. doi: 10.1134/S1070428014120100

Jia, J., Zhu, F., Ma, X., Cao, Z. W., Li, Y. X., and Chen, Y. Z. (2009). Mechanisms of drug combinations: interaction and network perspectives. *Nat. Rev. Drug Discov.* 8, 111–128. doi: 10.1038/nrd2683

Keith, C. T., Borisy, A. A., and Stockwell, B. R. (2005). Multicomponent therapeutics for networked systems. *Nat. Rev. Drug Discov.* 4, 71–78. doi: 10.1038/nrd1609

Kirschning, A., Taft, F., and Knobloch, T. (2007). Total synthesis approaches to natural product derivatives based on the combination of chemical synthesis and metabolic engineering. *Org. Biomol. Chem.* 5, 3245–3259. doi: 10.1039/b709549j

Klein, A. S., Brass, H. U. C., Klebl, D. P., Classen, T., Loeschcke, A., Drepper, T., et al. (2018). Preparation of cyclic Prodiginines by Mutasynthesis in pseudomonas putida KT2440. *Chembiochem* 19, 1545–1552. doi: 10.1002/cbic.201800154

Klein, A. S., Domröse, A., Bongen, P., Brass, H. U. C., Classen, T., Loeschcke, A., et al. (2017). New Prodigiosin derivatives obtained by Mutasynthesis in pseudomonas putida. *ACS Synth. Biol.* 6, 1757–1765. doi: 10.1021/acssynbio.7b00099

Köhl, J., Kolnaar, R., and Ravensberg, W. J. (2019). Mode of action of microbial biological control agents against plant diseases: relevance beyond efficacy. *Front. Plant Sci.* 10:845. doi: 10.3389/fpls.2019.00845

Konno, H., Matsuya, H., Okamoto, M., Sato, T., Tanaka, Y., Yokoyama, K., et al. (1998). Prodigiosins uncouple mitochondrial and bacterial F-ATPases: evidence for their H^+/cl^- symport activity. *J. Biochem.* 124, 547–556. doi: 10.1093/oxfordjournals.jbchem.a022147

Li, P., He, S., Zhang, X., Gao, Q., Liu, Y., and Liu, L. (2022). Structures, biosynthesis, and bioactivities of prodiginine natural products. *Appl. Microbiol. Biotechnol.* 106, 7721–7735. doi: 10.1007/s00253-022-12245-x

Loeschcke, A., Markert, A., Wilhelm, S., Wirtz, A., Rosenau, F., Jaeger, K.-E., et al. (2013). TREX: a universal tool for the transfer and expression of biosynthetic pathways in bacteria. *ACS Synth. Biol.* 2, 22–33. doi: 10.1021/sb3000657

Loeschcke, A., and Thies, S. (2020). Engineering of natural product biosynthesis in *Pseudomonas putida*. *Curr. Opin. Biotechnol.* 65, 213–224. doi: 10.1016/j.copbio.2020.03.007

Lugtenberg, B., and Kamilova, F. (2009). Plant-growth-promoting Rhizobacteria. *Annu. Rev. Microbiol.* 63, 541–556. doi: 10.1146/annurev.micro.62.081307.162918

Magalhães, L., and Nitschke, M. (2013). Antimicrobial activity of rhamnolipids against listeria monocytogenes and their synergistic interaction with nisin. *Food Control* 29, 138–142. doi: 10.1016/j.foodcont.2012.06.009

Matera, C., Grundler, F. M. W., and Schleker, A. S. S. (2021). Sublethal fluazaindolizine doses inhibit development of the cyst nematode *Heterodera schachtii* during sedentary parasitism. *Pest Manag. Sci.* 77, 3571–3580. doi: 10.1002/ps.6411

Meschke, H., Walter, S., and Schrempf, H. (2012). Characterization and localization of prodiginines from Streptomyces lividans suppressing *Verticillium dahliae* in the absence or presence of *Arabidopsis thaliana*. *Environ. Microbiol.* 14, 940–952. doi: 10.1111/j.1462-2920.2011.02665.x

Mikhaleva, A. I., Trofimov, B. A., Vasilev, A. N., Komarova, G. A., and Skorobogatova, V. I. (1981). Pyrroles from ketoximes and acetylene. Dihaloethanes in place of acetylene in reactions with cyclohexanone oxime. *Acad. Sci. USSR* 9, 1202–1204.

Nelson, K. E., Weinel, C., Paulsen, I. T., Dodson, R. J., Hilbert, H., Santos, V. A. P. M., et al. (2002). Complete genome sequence and comparative analysis of the metabolically versatile *Pseudomonas putida* KT2440. *Environ. Microbiol.* 4, 799–808. doi: 10.1046/j.1462-2920.2002.00366.x

Nikel, P. I., Chavarría, M., Danchin, A., and de Lorenzo, V. (2016). From dirt to industrial applications: pseudomonas putida as a synthetic biology chassis for hosting harsh biochemical reactions. *Curr. Opin. Chem. Biol.* 34, 20–29. doi: 10.1016/j.cbpa.2016.05.0111367-5931/#

Ortiz, A., Teruel, J. A., Espuny, M. J., Marqués, A., Manresa, Á., and Aranda, F. J. (2006). Effects of dirhamnolipid on the structural properties of phosphatidylcholine membranes. *Int. J. Pharm.* 325, 99–107. doi: 10.1016/j.ijpharm.2006.06.028

Pieterse, C. M. J., Van Der Does, D., Zamioudis, C., Leon-Reyes, A., and Van Wees, S. C. M. (2012). Hormonal modulation of plant immunity. *Annu. Rev. Cell Dev. Biol.* 28, 489–521. doi: 10.1146/annurev-cellbio-092910-154055

Rahul, S., Chandrashekhar, P., Hemant, B., Chandrakant, N., Laxmikant, S., and Satish, P. (2014). Nematicidal activity of microbial pigment from *Serratia marcescens*. *Nat. Prod. Res.* 28, 1399–1404. doi: 10.1080/14786419.2014.904310

Ravindran, A., Anishetty, S., and Pennathur, G. (2020). Molecular dynamics of the membrane interation and localisation of prodigiosin. *J. Mol. Graph. Model.* 98:107614. doi: 10.1016/j.jmgm.2020.107614

Roberts, D. P., Selmer, K., Lupitskyy, R., Rice, C., Buyer, J. S., Maul, J. E., et al. (2021). Seed treatment with prodigiosin controls damping-off of cucumber caused by Pythium ultimum. *AMB Express* 11:10. doi: 10.1186/s13568-020-01169-2

Rossi, C. C., Santos-Gandelman, J. F., Barros, E. M., Alvarez, V. M., Laport, M. S., and Giambiagi-deMarval, M. (2016). Staphylococcus haemolyticus as a potential producer of biosurfactants with antimicrobial, anti-adhesive and synergistic properties. *Lett. Appl. Microbiol.* 63, 215–221. doi: 10.1111/lam.12611

Sakai-Kawada, F. E., Ip, C. G., Hagiwara, K. A., and Awaya, J. D. (2019). Biosynthesis and bioactivity of prodiginine analogs in marine bacteria, Pseudoalteromonas: a mini review. *Front. Microbiol.* 10:1715. doi: 10.3389/fmicb.2019.01715

Sanchez, L., Courteaux, B., Hubert, J., Kauffmann, S., Renault, J. H., Clément, C., et al. (2012). Rhamnolipids elicit defense responses and induce disease resistance against biotrophic, hemibiotrophic, and necrotrophic pathogens that require different signaling pathways in Arabidopsis and highlight a central role for salicylic acid. *Plant Physiol.* 160, 1630–1641. doi: 10.1104/pp.112.201913

Schloss, P. D., Allen, H. K., Klimowicz, A. K., Mlot, C., Gross, J. A., Savengsuksa, S., et al. (2010). Psychrotrophic strain of *Janthinobacterium lividum* from a cold Alaskan soil produces prodigiosin. *DNA Cell Biol.* 29, 533–541. doi: 10.1089/dna.2010.1020

Schneider, C. A., Rasband, W. S., and Eliceiri, K. W. (2012). NIH image to ImageJ: 25 years of image analysis. *Nat. Methods* 9, 671–675. doi: 10.1038/nmeth.2089

Sijmons, P., Grundler, F., von Mende, N., Burrows, P. R., and Wyss, U. (1991). Arabidopsis thaliana as a new model host for plant-parasitic nematodes. *Plant J.* 1, 245–254. doi: 10.1111/j.1365-313X.1991.00245.x

Simon, R., Priefer, U., and Pühler, A. (1983). A broad host range mobilization system for *in vivo* genetic engineering: transposon mutagenesis in Gram negative bacteria. *Nat. Biotechnol.* 1, 784–791. doi: 10.1038/nbt1183-784

Someya, N., Nakajima, M., Hirayae, K., Hibi, T., and Akutsu, K. (2001). Synergistic antifungal activity of chitinolytic enzymes and prodigiosin produced by biocontrol bacterium, Serratia marcescens strain B2 against gray mold pathogen. *Botrytis cinerea. J. Gen. Plant Pathol.* 67, 312–317. doi: 10.1007/pl00013038

Sotirova, A., Avramova, T., Stoitsova, S., Lazarkevich, I., Lubenets, V., Karpenko, E., et al. (2012). The importance of rhamnolipid-biosurfactant-induced changes in bacterial membrane lipids of Bacillus subtilis for the antimicrobial activity of thiosulfonates. *Curr. Microbiol.* 65, 534–541. doi: 10.1007/s00284-012-0191-7

Stankovic, N., Senerovic, L., Ilic-Tomic, T., Vasiljevic, B., and Nikodinovic-Runic, J. (2014). Properties and applications of undecylprodigiosin and other bacterial prodigiosins. *Appl. Microbiol. Biotechnol.* 98, 3841–3858. doi: 10.1007/s00253-014-5590-1

Sun, H., Liu, Z., Zhao, H., and Ang, E. L. (2015). Recent advances in combinatorial biosynthesis for drug discovery. *Drug Des. Devel. Ther.* 9, 823–833. doi: 10.2147/DDDT.S63023

Suryawanshi, R. K., Patil, C. D., Koli, S. H., Hallsworth, J. E., and Patil, S. V. (2017). Antimicrobial activity of prodigiosin is attributable to plasma-membrane damage. *Nat. Prod. Res.* 31, 572–577. doi: 10.1080/14786419.2016.1195380

Tiso, T., Ihling, N., Kubicki, S., Biselli, A., Schonhoff, A., Bator, I., et al. (2020). Integration of genetic and process engineering for optimized rhamnolipid production using pseudomonas putida. *Front. Bioeng. Biotechnol.* 8:976. doi: 10.3389/fbioe.2020.00976

Trofimov, B. A., Mikhaleva, A. I., Ivanov, A. V., Shcherbakova, V. S., and Ushakov, I. A. (2015). Expedient one-pot synthesis of pyrroles from ketones, hydroxylamine, and 1,2-dichloroethane. *Tetrahedron* 71, 124–128. doi: 10.1016/j.tet.2014.11.031

Varnier, A. L., Sanchez, L., Vatsa, P., Boudesocque, L., Garcia-Brugger, A., Rabenoelina, F., et al. (2009). Bacterial rhamnolipids are novel MAMPs conferring resistance to *Botrytis cinerea* in grapevine. *Plant Cell Environ.* 32, 178–193. doi: 10.1111/j.1365-3040.2008.01911.x

Wallace, H. R. (1958). Movement of eelworms. The influence of pore size and moisture content of the soil on the migration of larvae of the beet eelworm. *Heterodera schachtii Schmidt. Ann. Appl. Biol.* 46, 74–85. doi: 10.1111/j.1744-7348.1958.tb02179.x

Weihmann, R., Domröse, A., Drepper, T., Jaeger, K. E., and Loeschcke, A. (2020). Protocols for yTREX/Tn5-based gene cluster expression in pseudomonas putida. *Microb. Biotechnol.* 13, 250–262. doi: 10.1111/1751-7915.13402

Weimer, A., Kohlstedt, M., Volke, D. C., Nikel, P. I., and Wittmann, C. (2020). Industrial biotechnology of *Pseudomonas putida*: advances and prospects. *Appl. Microbiol. Biotechnol.* 104, 7745–7766. doi: 10.1007/s00253-020-10811-9

Williamson, N. R., Fineran, P. C., Ogawa, W., Woodley, L. R., and Salmond, G. P. C. (2008). Integrated regulation involving quorum sensing, a two-component system, a GGDEF/EAL domain protein and a post-transcriptional regulator controls swarming and RhlA-dependent surfactant biosynthesis in Serratia. *Environ. Microbiol.* 10, 1202–1217. doi: 10.1111/j.1462-2920.2007.01536.x

Williamson, N. R., Simonsen, H. T., Ahmed, R. A. A., Goldet, G., Slater, H., Woodley, L., et al. (2005). Biosynthesis of the red antibiotic, prodigiosin, in Serratia: identification of a novel 2-methyl-3-n-amyl-pyrrole (MAP) assembly pathway, definition of the terminal condensing enzyme, and implications for undecylprodigiosin biosynthesis in Streptomyces. *Mol. Microbiol.* 56, 971–989. doi: 10.1111/j.1365-2958.2005.04602.x

Wyss, U. (1992). Observations on the feeding behavior of Heterodera schachtii throughout development, including events during moulting. *Fundam. Appl. Nematol.* 15, 75–89.

Wyss, U., and Grundler, F. M. W. (1992). Feeding behavior of sedentary plant parasitic nematodes. *Netherlands J. Plant Pathol.* 98, 165–173. doi: 10.1007/BF01974483

Wyss, U., and Zunke, U. (1986). Observations on the behaviour of second stage juveniles of Heterodera schachtii inside host roots. *Rev. Nématologie* 9, 153–165.

Yildirim, M. A., Goh, K.-I., Cusick, M. E., Barabási, A.-L., and Vidal, M. (2007). Drug-target network. *Nat. Biotechnol.* 25, 1119–1126. doi: 10.1038/nbt1338

Yip, C. H., Yarkoni, O., Ajioka, J., Wan, K. L., and Nathan, S. (2019). Recent advancements in high-level synthesis of the promising clinical drug, prodigiosin. *Appl. Microbiol. Biotechnol.* 103, 1667–1680. doi: 10.1007/s00253-018-09611-z

Chapter 5

Discussion

In the history of agriculture, the revolution in chemical pesticides including fungicides, insecticides, and nematicides occurred during the 20th century when the growing population required more potent pest control methods in terms of scale, speed, and effectiveness. Most of the chemicals were designed to exterminate pests in 3-4 days with up to 100 % killing efficiency. In addition, these ready-to-use products are easy to apply and can be targeted to a specific area with high precision. By eliminating various pests encountered in agricultural production, the application of chemical pesticides has enabled mass production of crops worldwide. However, it took decades before the devastating effects of pesticides were recognized. Controlling pests with chemicals can be extremely hazardous and cause health issues, such as allergy, asthma and cancer, if humans get into contact with them (Nicolopoulou-Stamati et al., 2016). The residues of pesticides may also affect the environment, contaminating surface- and ground-water, and causing toxic effects on plants and other non-target organisms (Pathak et al., 2022). Moreover, improper use of chemical control agents promotes the evolution of pesticide resistances. These are based on genetic changes, which are inheritable, thus facilitating the pest population to become more resistant to synthetic pesticides over time (Hawkins et al., 2019). As a consequence of all these concerns, the proposition being imposed is to develop novel strategies to increase crop yield and enhance crop quality while suppressing pest damage and reducing the adverse effects on humans, animals, and the natural environment.

The concept of integrated pest management (IPM) was first introduced in the 1950s (Stern et al., 1959). It recognizes that plants, pests, and the environment are interrelated within a system in which regular and systematic monitoring of crops for pests is essential to identify and quantify pest incidence and to make judicious decision on when and how to initiate control. The application of non-chemical tactics, such as biological control practices, should be taken into consideration prior to the use of chemical approaches. If synthetic pesticides are required, careful risk assessments should be conducted in advance based on specific pest densities and the potential consequences of controlling those pests in the environment (Barzman et al., 2015). Biological control strategies, as part of an IPM scheme, can be

applied individually or together with selective chemicals to reduce pesticide doses and the risk of developing pest resistance. The discovery of naturally occurring microbial control agents against pests typically involves several phases. It begins with *in vitro* and *in vivo* screening of a wide variety of microorganisms and continues with the investigation of control mechanisms, such as competition, antibiosis, and induced systemic resistance. Next, the production of large quantities of microbial biomass, as the following step, requires the study of microbial physiology and the usage of a biotechnological process. Moreover, to ensure that the microbial biomass remains viable and achieves high biocontrol activity, they need to be properly formulated and applied. The final phase, which is also usually the most difficult one, is the legal registration procedure, which can be both time and money consuming. In particular, it must be proven that these bio-based agents that are about to be launched into the market will not lead to any significant negative impacts on human health and environmental safety.

Plant-parasitic nematodes are among the most insidious pests parasitizing mainly belowground and occasionally aboveground plant parts. As an essential component of biotic constraints on crops, nematode infestation is often overlooked and misdiagnosed. Its damage to global crop yield loss, however, cannot be neglected. With increasing regulatory and socio-political demands for minimal environmental impact and residue-free crops, the innovation of the next-generation nematicides will focus on research in microbes and microbial natural products. The rhizosphere harbours diverse microorganisms and therefore serves as a hotspot for diverse activities, including root-root, root-microbe, and root-pest interactions. Among those, beneficial interactions between plants and their rhizosphere microbiomes have considerable implications for sustainable agriculture regarding the promotion of plant growth and the enhancement of plant resistance to pathogen invasion. Root exudates secreted by host plants shape the microbial community and modulate plant performance by altering the soil physicochemical environment around the root system, stimulating nutrient acquisition, attracting specific beneficial microorganisms, and triggering microbial activities that benefit the host plants. Enormous evidence demonstrates that some components present in root exudates act as substrates, chemotactic molecules and/or antimicrobial agents to mediate changes in microbial composition chemotaxis (Walker et al., 2003; Bais et al., 2006; Badri et al., 2013; Strehmel et al., 2014).

Chaparro et al. (2013) identified 57 out of 107 compounds in *A. thaliana* root exudates (ARE) and reported the composition changes over the course of plant development. These compounds can be broadly categorized into four groups: sugars, sugar alcohols, amino acids, and phenolics. The cumulative secretion levels of sugars and sugar alcohols were higher at early developmental stage and gradually decreased through plant growth. In contrast, the secretion levels of amino acids and phenolics increased over time. The secretion of high level of sugars, as carbon sources for microbial growth, might be responsible for our observation of the strongest chemotactic response of *B. firmus* I-1582 to ARE extracted from young seedlings (Huang et al., 2021 - Chapter 2). During aging, plants release a high proportion of phenolics with antimicrobial potentials and recruit particular microbial inhabitants of the rhizosphere that are beneficial to the host plants (Chaparro et al., 2014). Based on our microscopic observation, living *B. firmus* I-1582 colonized *A. thaliana* root and formed a layer along the root in the agar-based test system. Nematode infection assay demonstrated that roots inoculated with living bacterial cells encountered less infestation by *H. schachtii* compared with roots without bacteria inoculant. The early events after bacteria inoculation were further investigated by conducting nematode invasion assay. It turned out that the nematode penetration level exhibited a decreasing trend over time after *A. thaliana* roots were covered with living bacterial cells. All of the above let suggest that *A. thaliana* is able to attract *B. firmus* I-1582 and support their proliferation in its surroundings. Moreover, the presence of high load of bacteria along the root protects host plants from nematode invasion at early development stage.

In addition to protecting plants against the first generation of *H. schachtii* by creating a living biofilm, we also demonstrated that *B. firmus* I-1582 inhibits the reproduction of nematode progeny. According to our findings, virulence of the 2nd generation nematodes towards host plants was reduced after the exposure of the 1st generation females to living bacteria. However, since no bacteria are established along the roots, invasion by the 2nd generation juveniles cannot be inhibited by a bacterial biofilm. One possible explanation is that *B. firmus* I-1582 reduces fitness of the 2nd generation before they are ready to hatch. This, in turn, could be the result of either bacterial molecules inside the cyst with direct nematicidal activity or bacteria-induced plant defence mechanisms. Mendoza et al. (2008) suggested that *B. firmus* exerts antagonistic effect against nematodes through the production of

bioactive compounds during bacterial fermentation. The nematicidal compounds secreted by *Bacillus* strains are able to activate plant defence mechanisms by triggering induced systemic resistance (Cawoy et al., 2014). Indeed, our liquid lethality assay confirms the existence of bioactive molecules produced by *B. firmus* I-1582 and their nematicidal potentials on *H. schachtii* juveniles (Huang et al., unpublished - Chapter 3). Moreover, the chemical nature of these active molecules is found to be partially proteinaceous. In recent years, an abundance of natural products (NP), such as enzymes, antibiotics, bacteriocins, and insecticides, have been discovered from *Bacillus* strains and have proven valuable for pharmaceutical and agricultural applications (Schallmey et al., 2004). Unfortunately, many NP-producing bacteria are difficult to cultivate under standard laboratory conditions, and even if the cultivation is successful, the concentration of the desired NP in their original microbial hosts is typically too low to be detectable. However, the application of genome-based approaches has made these recourses more accessible. Genome mining combined with bioinformatics has been employed to explore putative NP encoded by cryptic biosynthetic gene clusters (BGC). Our dry- and wet-lab data suggests that one BGC encoding three putative lanthipeptides is present in *B. firmus* I-1582 genome and highly expressed in *B. firmus* I-1582 cells.

As mentioned above, microbial NP can be sometimes difficult to obtain from natural producers due to their low abundance. Hence, utilizing engineered microorganisms becomes an up-and-coming strategy to facilitate the synthesis of target compounds and their derivatives in large quantities. In particular, with its rapid and robust growth, high biomass production, low by-product secretion, remarkable tolerance to oxidative stress, and high adaptability to harsh heterologous microenvironments, the Gram-negative bacterium *Pseudomonas putida* has become a well-established heterologous host for the biosynthesis of high-value NP (Weimer et al., 2020). Lately, engineered *Pseudomonas putida* has been developed as an ideal platform for the production of novel prodigiosin and a group of prodiginine derivatives (Loeschcke and Thies, 2020). Prodiginines have attracted a great attention due to their anti-cancer, anti-microbial, and anti-parasitic activities (Li et al., 2022). Stylet thrusting of *H. schachtii* J2, which ensures nematode invasion of host's root tissue and establishment of permanent feeding site in vascular cylinder, is an energy-consuming process (Wyss and Zunke, 1986; Grundler et al., 1991; Wyss, 1992; Wyss and Grundler,

1992). As demonstrated in our study, the frequency of stylet movement was significantly reduced by prodiginines (Huang et al., 2023 - Chapter 4). Prodigiosin has been reported to uncouple F-ATPases through promotion of H^+/Cl^- symport and hinder energy transduction across vesicular membranes in *Escherichia coli*, which may have a direct effect on cellular energy metabolism, which offers an explanation for the lower frequency of J2 stylet movement (Konno et al., 1998). As a consequence of decreased stylet thrusting, nematode infestation is significantly reduced in the presence of prodiginines.

Since the bioprocess of rhamnolipids has already been industrially implemented, interests in their commercial application as biosurfactants in drug research has steadily increased over the last few decades. On the one hand, rhamnolipids can increase the solubility of low-solubility drug substances and enhance drug transport to target cells (Beal and Betts, 2000; Abdel-Mawgoud et al., 2010). On the other hand, rhamnolipids can disrupt the packing of phospholipids in cell membrane by intercalating into the phosphatidylcholine bilayer, which leads to increased permeability of cell membrane (Dowhan, 1997; Ortiz et al., 2006). However, it goes far beyond that when it comes to combined anti-parasitic activity of rhamnolipids. A more recent study reveals that di-rhamnolipids put plants on alert, and thus make them more responsive to parasite attack (Bredenbruch et al., 2023). The discovery of multicomponent drugs, containing two or more active ingredients, offers multiple advantages, such as high efficacy and low toxicity, less individual dosage, and slow drug resistance (Jia et al., 2009; Cheng et al., 2019). To quantify the interaction between prodiginines and di-rhamnolipids, the Chou-Talalay method is utilized in our study (Chou and Talalay, 1984). According to our finding, the synergistic effect occurred at low doses of the combined application. By increasing the doses of combination, the effect level switched from synergism to antagonism. Besides, when applying prodiginines and di-rhamnolipids combined, only ¼ of the concentration of each single compound were required to achieve the same nematode control efficacy as the full dose of a single application (Huang et al., 2023 - Chapter 4). Therefore, rhamnolipids can be used as a potential drug synergist with other agents to facilitate more potent access to the site of action through biological interface and to implement higher level of biocontrol efficacy on PPN.

Conclusion and Outlook

This study comprehensively investigates the impact of *B. firmus* I-1582 and the bacterial secondary metabolites, prodiginines and rhamnolipids, as microbial-based control agents on the economically important plant-parasitic nematode *H. schachtii*, as well as the underlying mechanism. In a nutshell:

- *B. firmus* I-1582 successfully colonizes host roots and inhibits infection and development of *H. schachtii* over two generations in an agar-based gnotobiotic system.
- Small molecules produced by *B. firmus* I-1582 exert a strict temperature-dependent antagonistic activity against nematodes. We assume that lanthipeptides play a role here.
- The combined application of prodiginines and rhamnolipids enhances efficacy, and reduces compound usage, thus offering a promising strategy for improving nematode management practices.

Looking ahead, there are several avenues for further exploration and application:

- An evaluation of the nematicidal properties of purified lanthipeptides is necessary. More concretely, one must be able to isolate lanthipeptides from their natural host or to produce them by engineered microbial hosts. Alternatively, deletion of biosynthetic gene clusters encoding lanthipeptides in *B. firmus* I-1582 is an additional approach to further investigate the function of these molecules in detail.
- There is a gap between the research findings and practical implementations. To fill the gap, we note that soil-based experiments can shed light on the interaction of these microbial-based agents, nematodes and crops, and their effectiveness in controlling nematodes in soil systems. In addition, blending the proposed control strategies into existing integrated nematode management practices across different cropping systems can also provide valuable insight on performance under diverse conditions.

Conclusively, the utilization of bio-based control agents offers a sustainable solution for nematode management. However, various factors, including concentration, temperature, and pH should be considered in agri- and horticultural applications. Variability of environmental factors may lead to inconsistency in the efficacy and longevity of biocontrol products. Nonetheless, our study contributes valuable insights to the dynamic interplay among these factors and the performance of bio-based products, paving the way for more informed and optimized strategies for nematode management in agri- and horticultural settings.

References

Abdel-Mawgoud AM, Lépine F, Déziel E. 2010. Rhamnolipids: diversity of structures, microbial origins and roles. Applied Microbiology and Biotechnology. 86, 1323-1336.

Badri DV, Chaparro JM, Zhang R, Shen Q, Vivanco JM. 2013. Application of natural blends of phytochemicals derived from the root exudates of *Arabidopsis* to the soil reveal that phenolic-related compounds predominantly modulate the soil microbiome. The Journal of Biological Chemistry. 288, 4502-4512.

Barzman M, Bàrberi P, Birch ANE, Boonekamp P, Dachbrodt-Saaydeh S, Graf B, Hommel B, Jensen JE, Kiss J, Kudsk P, Lamichhane JR, Messéan A, Moonen AC, Ratnadass A, Ricci P, Sarah JL, Sattin M. 2015. Eight principles of integrated pest management. Agronomy for Sustainable Development. 35, 1199-1215.

Cawoy H, Mariutto M, Henry G, Fisher C, Vasilyeva N, Thonart P, Dommes J, Ongena M. 2014. Plant defense stimulation by natural isolates of *Bacillus* depends on efficient surfactin production. Molecular Plant-Microbe Interactions. 27, 87-100.

Chaparro JM, Badri DV, Vivanco JM. 2014. Rhizosphere microbiome assemblage is affected by plant development. The ISME Journal. 8, 790-803.

Cheng F, Kovács IA, Barabási AL. 2019. Network-based prediction of drug combinations. Nature Communications. 10, 1197.

Chou TC, Talalay P. 1984. Quantitative analysis of dose-effect relationships: the combined effects of multiple drugs or enzyme inhibitors. Advances in Enzyme Regulation. 22, 27-55.

Dowhan W. 1997. The role of phospholipids in cell function. In: Gross RW, ed. Advances in Lipobiology. Elsevier, 79-107.

Hawkins NJ, Bass C, Dixon A, Neve P. 2019. The evolutionary origins of pesticide resistance. Biological reviews of the Cambridge Philosophical Society. 94, 135-155.

Huang M, Bulut A, Shrestha B, Matera C, Grundler FMW, Schleker ASS. 2021. *Bacillus firmus* I-1582 promotes plant growth and impairs infection and development of the cyst nematode *Heterodera schachtii* over two generations. Scientific reports. 11, 14114.

Jia J, Zhu F, Ma X, Cao Z, Cao ZW, Li Y, Li YX, Chen YZ. 2009. Mechanisms of drug combinations: interaction and network perspectives. Nature Reviews Drug Discovery. 8, 111-128.

Konno H, Matsuya H, Okamoto M, Sato T, Tanaka Y, Yokoyama K, Kataoka T, Nagai K, Wasserman HH, Ohkuma S. 1998. Prodigiosins uncouple mitochondrial and bacterial F-ATPases: evidence for their H^+/Cl^- symport activity. Journal of Biochemistry. 124, 547-56.

Li P, He S, Zhang X, Gao Q, Liu Y, Liu L. 2022. Structures, biosynthesis, and bioactivities of prodiginine natural products. Applied Microbiology and Biotechnology. 106, 7721-7735.

Loeschcke A, Thies S. 2020. Engineering of natural product biosynthesis in *Pseudomonas putida*. Current Opinion in Biotechnology. 65, 213-224.

Nicolopoulou-Stamati P, Maipas S, Kotampasi C, Stamatis P, Hens L. 2016. Chemical pesticides and human health: the urgent need for a new concept in agriculture. Frontiers in Public Health. 4, 148.

Pathak VM, Verma VK, Rawat BS, Kaur B, Babu N, Sharma A, Dewali S, Yadav M, Kumari R, Singh S, Mohapatra A, Pandey V, Rana N, Cunill JM. 2022. Current status of pesticide effects on environment, human health and it's eco-friendly management as bioremediation: a comprehensive review. Frontiers in Microbiology. 13, 962619.

Schallmey M, Singh A, Ward OP. 2004. Developments in the use of *Bacillus* species for industrial production. Canadian Journal of Microbiology. 50, 1-17.

Stern VM, Smith RF, van den Bosh R, Hagen KS. 1959. The integration of chemical and biological control of the spotted alfalfa aphid: the integrated control conceopt. Hilgardia. 29, 81-101.

Walker TS, Bais HP, Grotewold E, Vivanco JM. 2003. Root exudation and rhizosphere biology. Plant Physiology. 132, 44-51.

Weimer A, Kohlstedt M, Volke DC, Nikel PI, Wittmann C. 2020. Industrial biotechnology of *Pseudomonas putida*: advances and prospects. Applied Microbiology and Biotechnology. 104, 7745-7766.

Wyss U. 1992. Observations on the feeding behavior of *Heterodera schachtii* throughout development, including events during moulting. Fundamental and Applied Nematology. 15, 75-89.